THE REMOVAL OF PHOSPHORIC COMPOUNDS FROM SURFACE WATER NEAR A FARMLAND USING MAIZE TASSEL IMMOBILIZED IN POLYVINYL ALCOHOL

BY

AGIE, Jennifer Osato
MEng/SEET/2016/6126

DEPARTMENT OF CHEMICAL ENGINEERING
FEDERAL UNIVERSITY OF TECHNOLOGY, MINNA

NOVEMBER, 2019

ABSTRACT

In this study, proximate analysis and characterization techniques were carried out on maize tassel fibres in order to check its feasibility as a bio-sorbent for bio-sorption process before the immobilization with Polyvinyl Alcohol (PVA). The moisture content, ash content, apparent density, particle size and crude protein of maize tassel fibre were determined to show that the bio-material was exceptional for its use in column adsorption. The surface chemistry of the bio-material shows the presence of carboxylic groups and lactonic groups present in the material using Fourier Transform-Infrared spectroscopy (Nicolet 560 spectrophotometer) and Boehmn titration showed the number of acidic sites present in the material. The Brunauer–Emmett–Teller (BET) isotherm (Novastation D version 11.03) was used to find the surface area, pore volume and pore size diameter. The tassel was added to the poly vinyl alcohol at a temperature of 80 ºC with the aid of a magnetic stirrer in the ratio of 2:1 after which it was cooled and extruded with the aid of a syringe to form beads. Column adsorption studies were carried out to investigate the performance of the column by varying flow rates, bed heights and initial concentration on the breakthrough curve to get the breakthrough time and the exhaustion time of the adsorbent bed was used up. The column efficiency was evaluated using Clark model and Thomas model. The proximate analysis revealed moisture content, ash content, apparent density, particle size and crude protein to be 4.51 %, 2.134 %, 0.41 g/ml, 300 μm and 4.06 % respectively for maize tassel fibre. The FT-IR and Boehmn titration showed the number of acidic sites present in the material to be 0.9 mmol/g but the presence of phenolic groups is minimally present in the maize tassel fibre. The Brunauer–Emmett–Teller (BET) isotherm was used to find the surface area, pore volume and pore size diameter to be 652.3 m^2/g, 0.4056 cm^3/g and 2.144 nm respectively .The Thomas Model was found to predict the breakthrough better than Clark model for the phosphoric compounds with R^2 value of 97.5 % for bed heights and flow rates.

TABLE OF CONTENTS

Content	Page
COVER PAGE	i
TITLE PAGE	ii
DECLARATION	iii
CERTIFICATION	iv
DEDICATION	v
ACKNOWLEDGEMENTS	vi
ABSTRACT	viii
TABLE OF CONTENTS	ix
LIST OF TABLES	xv
LIST OF FIGURES	xvii
ABBREVIATION, GLOSSARIES AND SYMBOLS	xix
CHAPTER ONE	1
1.0 **INTRODUCTION**	1
1.1 Background to the Study	1
1.2 Statement of the Research Problem	3
1.3 Justification of the Study	4
1.4 Aim and Objectives of the Study	5
1.5 Scope of the Study	6

CHAPTER TWO 7

2.0 LITERATURE REVIEW 7

2.1 Water Quality 7

2.2 Phosphorus 8

2.2.1 Phosphorus cycle 9

2.3 Methods of removal of phosphorus 11

2.4 Modes of Adsorption 15

2.4.1 Evaluation of the column performance 17

2.4.1.1 Clark model 20

2.4.1.2 Thomas model 21

2.5 Adsorbent 21

2.5.1 The use of metal oxide and hydroxide as an adsorbent 22

2.5.2 The use of Industrial waste as an adsorbent 22

2.5.3 Chemically Modified Clay Adsorption 23

2.5.4 Adsorption using agricultural waste Materials 24

2.6 Maize 26

2.6.1 Modification of maize tassel 28

2.6.2 Support materials for the immobilization of bio-sorbents 30

2.7 Polyvinyl Alcohol 30

CHAPTER THREE 34

3.0 MATERIALS AND METHODOLOGY 34

3.1 Materials and Chemicals 34

3.2 METHODOLOGY 35

3.2.1 Collection and Preparation of maize tassel powder 35

3.2.2 Characterization of the maize tassel fibre 35

3.2.2.1 Determination of moisture content 36

3.2.2.2 Determination of ash content 36

3.2.2.3 Determination of bulk density/ apparent density 36

3.2.2.4 Determination of iodine Number 37

3.2.2.5 Determination of point zero charge 38

3.2.2.6 Determination of crude protein 38

3.2.2.7 Determination of oxygen containing functional groups 39

3.2.2.8 Determination of surface functional groups 40

3.2.2.9 Determination of surface area and pore volume 40

3.2.2.10 Surface morphology determination 41

3.2.2.11 Phosphate determination 41

3.2.3 Preparation of maize tassel-PVA beads 41

3.3 Collection and characterization of the surface water 42

3.3.1 pH 42

3.3.2 Dissolved oxygen 42

3.3.3 Chemical oxygen demand 42

3.3.4 Biochemical oxygen demand 43

3.4 Column Adsorption Studies 43

3.4.1 Effect of bed height 43

3.4.2 Effect of initial concentration 44

3.4.3 Effect of inlet flow rates 44

3.5 Modelling of fixed bed column breakthrough 44

CHAPTER FOUR 45

4.0 RESULTS AND DISCUSSION 45

4.1 Proximate Analysis of Maize Tassel 45

4.1.1 Surface characterization of maize tassel 46

4.1.2 Surface chemistry characterization of the maize tassel fibre 49

4.1.3 Surface chemistry characterization of the maize tassel fibre immobilized in PVA 51

4.1.4 Surface chemistry characterization of the maize tassel fibre immobilized in PVA after adsorption of phosphoric compounds 52

4.1.5 Surface morphology determination of the maize tassel immobilized in PVA before and after Adsorption 53

4.2 Characterization of the Surface Water 54

4.3 Effect of Bed Study 54

4.3.1 Effect of bed height 54

4.3.2 Effect of flow rate 56

4.3.3 Effect of initial concentration 58

4.4 Evaluation of Column Performance 61

4.5 Analysis of Fixed Bed Models 65

4.5.1 Clark model 65

4.5.1.1 Effect of bed height on Clark model 65

4.5.1.2 Effect of flow rate using Clark model 67

4.5.1.3 Effect of initial concentration on Clark model 68

4.5.2 Thomas model 69

4.5.2.1 Effect of bed height on Thomas model 69

4.5.2.2 Effect of flow rate using Thomas model 70

4.5.2.3 Effect of initial concentration 71

4.6 Comparison of the Experimental Data and the Applied Models 72

CHAPTER FIVE 73

5.0 CONCLUSION AND RECOMMENDATIONS 73

5.1 Conclusion 73

5.2 Recommendation 74

REFERENCES 75

APPENDIX 83

LIST OF TABLES

Table		Page
2.1	Conventional methods for the removal of phosphoric compounds	12
2.2	Different methods of adsorption with its merits and demerits	16
2.3	Authors and their findings on the modification of maize tassel	28
2.4	List of authors and their findings	32
3.1	Summarizes the list of materials and chemicals used	34
3.2	List of Equipment/Apparatus used	34
4.1	Surface characterization of maize tassel	45
4.2	Adsorption parameters obtained by the application of the bet model to adsorption isotherms of maize tassel	47
4.3	The oxygen functional groups of maize tassel	49
4.4	The bonds present in maize tassel fibre	50
4.5	The Bonds Present in Maize Tassel Immobilized in PVA	51
4.6	Table showing the values gotten from the surface water	54
4.7	Column data parameter obtained on sorption characteristics of maize tassel immobilized in PVA at varying bed height	61
4.8	Column data parameter obtained on sorption characteristics of maize tassel immobilized in PVA at varying flow rates	62

4.9 Column data parameter obtained on sorption characteristics of maize tassel immobilized in PVA at varying initial concentration 64

4.10 Clark model constants at different bed heights of 2-6 cm and flow rate of 8 ml/min and initial concentration of phosphoric compounds 65

4.11 Clark model constants at different flow rate of 4-12 ml/min and bed height of 4 cm and initial concentration of phosphoric compounds 67

4.12 Clark model constants at different initial concentration of phosphoric compounds with flow rate of 8 ml/min and bed height of 4 cm 68

4.13 Thomas parameters at different bed heights of 2-6 cm, Flow rate 8ml/min and Initial concentration of the phosphoric compounds 69

4.14 Thomas parameters at different flow rates of 4-8ml/min, bed height of 4 cm and Initial concentration of the phosphoric compounds 70

4.15 Thomas parameters at different initial concentration of phosphoric compounds with flow rates of 8ml/min and bed height of 4 cm 71

LIST OF FIGURES

Figure	Page
2.1Schematic diagram of phosphorus cycle	11
2.2 Graphical representation of a breakthrough curve	18
4.1 A plot of the change in final ph and initial ph against the initial ph for maize tassel	48
4.2 FT-IR spectrum of maize tassel	50
4.3 FT-IR result for maize tassel fibre immobilized with PVA	51
4.4 FT-IR result of phosphoric compounds loaded in maize tassel immobilized with PVA	52
4.5 SEM micrograph of maize tassel immobilized in PVA before (a) and after (b) adsorption	53
4.6 Breakthrough curve showing the removal of phosphoric compounds at a bed height of 2 cm	54
4.7 Breakthrough curve showing the removal of phosphoric compounds at a bed height of 4 cm	55
4.8 Breakthrough curve showing the removal of phosphoric compounds at a bed height of 6 cm	55

4.9 Breakthrough curve showing the removal of phosphoric compounds at a flow rate of 4 ml/min 57

4.10 Breakthrough curve showing the removal of phosphoric compounds at a flow rate of 8 ml/min 57

4.11 Breakthrough curve showing the removal of phosphoric compounds at a flow rate of 12 ml/min 58

4.12 Breakthrough curve showing the removal of phosphoric compounds at initial phosphoric concentration of 2, 6.13 and 11.23 mg/L 59

4.13 Breakthrough curve showing the removal of phosphoric compounds at initial phosphoric concentration of 1.5, 4.8 and 8.9 mg/L 59

4.14 Breakthrough curve showing the removal of phosphoric compounds at initial phosphoric concentration of 1, 3.15 and 5.83 mg/L 60

ABBREVIATION, GLOSSARIES AND SYMBOLS

%	Percentage
BET	Brunauer, Emmett and Teller
C_o	Initial Concentration
EDX	Energy Dispersion X-ray Spectroscopy
FTIR	Fourier –Transform Infrared Spectroscopy
g	Gram
mg	Milligram
Ortho	Orthophosphates
Phos	Phosphorus
Pyro	Pyrophosphates
SEM	Scanning Electron Microscope
T	Temperature (^oC, K),
t	Time (hr)

CHAPTER ONE

1.0 INTRODUCTION

1.1 Background to the Study

Water is one of the basic needs for all living species alongside with food and air. There are pollutants present in water bodies and among them phosphoric compounds are one of them which causes eutrophication (premature aging of the water body) that leads to the ruins and death of aquatic plants, animals and other living microorganisms. However, one of the major causes of severe water pollution are; Agriculture, industrial development and urbanization (Nguyen, 2015).

Phosphoric compounds occur naturally at low levels in water, plants and animals. It also occurs unnaturally in fertilizers (used in agriculture), cleaning agents (used in industries), wastewater (from household sewage) and bodies of biological organisms.
The elevated concentration of phosphates in water body leads to the changes in pH and in water oxygen levels that can be unfavourable to aquatic life. Phosphoric compounds are the major nutrients responsible for eutrophication. Eutrophication occurs as a result of the rapid growth of algae or cyanobacteria bloom due to excess of nutrients in water which acts as a blanket that covers the top of water and inhibits sunlight from reaching aquatic plants. This leads to their death and decline in water oxygen levels (Viswanathan *et al.,* 2014).

The release of industrial and municipal effluents onto land and surface water bodies has polluted water resources such as surface and groundwater, making the management of water resources more complex thereby becoming a threat to the health of human and its population that affects the liver, kidney and heart (Hashem, 2007).

The EPA criterion for acceptable phosphoric concentration in water is 0.1 mg/L or less. The estimated cost of phosphorus removal to achieve a permissible limit of 0.1 mg/L is $44.5 billion in the United States. This only demonstrates the necessity for an effective and inexpensive way to treat phosphorus contaminated waters (Viswanathan *et al.,* 2014).

Various studies have been carried out to improve procedures and technologies for the removal of phosphoric compounds from water body. These techniques are as follows, physical, chemical and biological methods. From the wide classifications mentioned above, adsorption is the technique that provides the best removal efficiency of phosphoric compounds (Gautam *et al.*, 2014).

Current studies have shown to remove toxic substances from aqueous solutions or from water bodies are the use of adsorbents of biological origin, including alginate, dead and living biomass, chitosan, lignin, and others. Agricultural waste products such as maize tassel (Zvinowanda *et al.*, 2008), rice husks (Krishnani *et al.,* 2007), corn cobs (Kahn and Wahab, 2006) and polymerized orange peels (Guo *et al.,* 2009) have been reported for their removal of toxic substances from aqueous solutions.

The use of raw plant material in water treatment has a major impediment of its susceptibility to bacterial attack that react with the water impurities, which will result to the formation of algae and bacteria that will end up destroying the biomass (Mamba *et al*., 2012).

The powdered maize tassel is soft and when used alone it clogs the column thus preventing free flow of water. In order to apply this waste material effectively in column experiments, it is essential to immobilize onto an inert substance which can provide support without the maize tassel losing its capacity to remove toxic substances.

Immobilization of such material will create material with mechanical strength and rigidity (Sekhula *et al.,* 2016).

Polyvinyl alcohol (PVA) is a type of synthetic polymer that is easily available, cheap, and possesses tremendous resistance properties; it is a water-soluble material containing large amounts of hydroxide groups. It has inert ability which makes it a good immobilizer (Chu and Hashim, 2006).

This study will focus on the immobilization of maize tassel-PVA for the removal of phosphoric compounds from water body and studying the bed height, varying the initial concentration of the effluent and flow rate for column adsorption.

1.2 Statement of the Research Problem

The pollution of surface water from fish pond can be accredited to runoff from agricultural fields. The pollutants released into the pond can be harmful to aquatic life.

Phosphoric compounds are nutrients that are vital to plant, animal and human growth but needed at low level for survival. However, at high level in nature it can cause algal bloom causing Eutrophication which leads to the depletion of oxygen level in water body there by affecting aquatic life.

There is a trend for substituting pure adsorbents with natural by-products for the development of cost-effective adsorbents. Maize is one of the major staple crops in many developing countries, once the useful nutrient rich portions of maize plants have been harvested, the remaining portion of the plant is usually discarded as waste.

However, it has been reported that during bio-sorption processes there is a problem of leaching of organic matter from the bio-sorbent which leads to change of colour and taste of the final treated water. Metal ions present in the biomaterial can also be leached

into the water when raw biomaterial is used, causing adverse effects on the bio-sorption process. In order to tackle the above challenge, chemical modification is deemed to offer possible solutions.

1.3 Justification of the Study

Maize is a major food crop that is grown in Nigeria in diverse ecological zones and is one of the second most grown crop in Nigeria in terms of area harvested (5.8 million Ha) and second largest in Africa after South Africa with an estimate of 10.79 million MT produced in 2014 (Food and Agriculture Organization Corporate Statistical Database (FAOSTAT), 2014).

In recent years, maize production in Nigeria varied significantly from 7.1 million tonnes in 2006 to 10.4 million tonnes in 2017 (International Institute of Tropical Agriculture (IITA), 2017).

Agricultural wastes are by-products, presently unused or underused for animal feed. These wastes have the following qualities; high cellulose content which is good for adsorption capacity, it is in abundance, eco-friendly, renewable make agricultural solid waste viable option for waste water remediation (Zvinowanda *et al.*, 2008).

Mostly, the materials used for natural biomass materials generally display very low affinity for phosphorus and hereby have relative low sorption capacities. For the enhancement of phosphorus bio-sorption capacity, pre-treatment and modification of the bio-surfaces is required. Therefore, an inexpensive and with limited environmental impact for biomass pre-treatment agent is desirable (Markou *et al.*, 2016).

Column experiments provide data which can be applied for industrial purposes. It is used to itemize the factors which are vital to aid design industrial scale fixed bed adsorption column (Yagub *et al.,* 2015)

However, the use of dead biomass in powdered form has some problems, such as difficulty in the separation of biomass after bio-sorption, mass loss after regeneration and low strength and small particle size, which make it difficult to use in column applications. To solve these problems, dead biomass can be immobilized in a bio-polymeric or polymeric matrix used as a supporting material (Odysseas, 2016). So a good support material used for immobilization should be rigid and chemically inert which is why Poly Vinyl alcohol was used.

1.4 Aim and Objectives of the Study

The aim of this work is to use Maize tassel immobilized in poly vinyl alcohol matrix to form beads (PVA beads) to remove phosphoric compounds from surface water. The aim can be achieved through the following objectives;

- Preparation and production of maize tassel immobilized in polyvinyl alcohol to form matrix beads.
- Characterization of the bio-sorbent using FT-IR, SEM-EDX and BET was carried out on maize tassel-PVA beads before and after adsorption.
- Collection and characterization of the surface water from fish pond.
- Evaluation of the following adsorption parameters; flow rate, bed height and initial concentration of the influent.
- Evaluation of the column efficiency using empirical models which are the kinetic isotherms using Clark and Thomas.

1.5 Scope of the Study

The scope of this work includes the preparation of maize tassel immobilized in poly vinyl alcohol matrix to form beads and effluent was collected from a fish pond to know the concentration of phosphoric compounds present. The adsorption process was evaluated using column sorption process and the efficiency was evaluated using Clark and Thomas empirical models.

CHAPTER TWO

2.0 LITERATURE REVIEW

2.1 Water Quality

Water is one of the basic necessities for human beings alongside with food and air. However, one of the causes of severe water pollution industrial development, lagged agriculture and urbanization. Looking at today's water quality management, eutrophication is a major concern which is caused by the excessive phosphorus and nitrogen in water body. Aquatic plants thrive in a eutrophic environment; which contains a diversity of potent toxins and its blooms can cause increased water turbidity, anoxia and death of living organisms. This could lead to serious environmental and risk to human health. One of the most important challenges to water quality managers is to control eutrophication and reduce its harm to humans. One of the major limiting factors for eutrophication is phosphorus, so it is more efficient to control the concentration of phosphorus rather than nitrogen (Qu *et al.,* 2016).

Good quality water is vital for agricultural, industrial and domestic purposes. Although, various pollutants from these sources are discharged daily to pollute freshwater bodies hereby leading to adverse effects on the ecosystem (Ghulam *et al.,* 2018).

The presence of the following water pollutants copper, zinc, manganese, lead, boron and phosphorus are needed in low concentrations to support and maintain functions in aquatic ecosystem. Phosphorus plays a crucial role in eutrophication of surface waters. The elevated concentrations of phosphorus in rivers have been associated to increasing rates of growth in plants, change in specie composition and increase of planktonic, epiphytic and epibenthic algae which will result to shading of higher plants. Phosphorus occurs in a wide variety of forms in natural waters, in both dissolved and particulate

phases, and in inorganic and organic forms, including biomass. These forms are highly interactive with each other and with the aquatic ecosystem (Jarvie *et al.,* 2002)

2.2 Phosphorus

Phosphorus (P) is a non-metal and the 15th element of the periodic table and found in the 5th group or ―nitrogen family‖ and is one of the most essential materials for everyday life, altering each and every organism on Earth. Phosphorus can be found in two different physical forms namely; white (or yellow) phosphorus and red phosphorus which have diverse physical and chemical characteristics. White phosphorus, usually in the form P_4, has significantly high reactivity due to its tetrahedral structure causing ring strain while red phosphorus is present as polymeric chains that shows more stability. Red phosphorus can be converted into white phosphorus by heating it in the absence of oxygen at a temperature of 300 ºC or under direct exposure to sunlight. It is never found free in its elemental form in nature due to its high reactivity (Capodaglio *et al.,* 2018).

Phosphorus (P) is an essential nutrient to human, animal and plant growth. It is one of the most common substances found in nature and it is mostly found in water, food and our bodies. In its pure form, it is very poisonous to both man and animals (Worsfold *et al.,* 2016).

Phosphorus is a macronutrient vital for the growth of plants and other biological organisms. It is one of the most important building substances of DNA and RNA (in the form of phosphate ion PO_4^{3-}), plays vital roles in transfer of energy through living cells as a component of adenosine triphosphate (complex carbohydrates) and phospholipids (formation of cell membranes). A substantial amount of phosphorus can be found in human bodies, mainly in bones and teeth, as calcium hydroxyapatite $Ca_{10}(PO_4)_6(OH)_2$ (Capodaglio *et al.,* 2018).

The presence of phosphorus in fresh water bodies limits the growth of algae. The forms of phosphorus that exists in aqueous solutions and waste waters are orthophosphate, polyphosphate and organic phosphate (Nguyen, 2015).

2.2.1 Phosphorus cycle

Over the last 150 years, the human effect on the global phosphorus cycle has been significant. Phosphorus is initially solubilized from apatite minerals, by chemical weathering during soil development. Physical weathering also plays a vital role by producing fine materials with extremely high surface area /mass ratios, which improves chemical weathering in continental environments (floodplains, delta systems) (Filippeli, 2010).

The major difference of the phosphorus cycle related to other element cycles is that there is absence of gaseous compounds which is found only in soil and aquatic environments. Phosphorus is considered as the limiting nutrient because it is not readily available in the atmosphere. The decomposition of biomass by bacterial activities converts organic phosphorus to inorganic phosphorus which is then released back to the environment (Nguyen, 2015).

The most important weathering source for phosphorus in soils is apatite minerals. These minerals can be weathered as a result of reaction with dissolved carbon dioxide:

$Ca_5(PO_4)_3OH + 4CO_2 + 3H_2O \longrightarrow 5Ca^{2+} + 3HPO_4^{2-} + 4HCO_3^-$ (2.1) The release of phosphorus from mineral grains in soils undergoes several processes. Firstly, the reduced pH produced from respiration-related CO_2 in the area of both degrading organic matter and root hairs dissolves P-bearing minerals (mainly apatites) and phosphorus is being released to root pore spaces. Secondly, the organic acids

released by the roots of plants can dissolve apatite minerals and release phosphorus to soil pore spaces. Phosphorus is strongly immobile in soils and these results to its slow rate of diffusion from dissolved form in pore spaces and limits its supply to rootlet surfaces. Furthermore, the phosphorus available in soils is in organic matter, which is directly not accessible for plant nutrition. Plants have developed two specific tactics to increase the supply of phosphorus to roots which are phosphatase (an enzyme that can release bioavailable inorganic phosphorus from organic matter) often excreted by plants and soil microbes, and the symbiotic fungi *Mycorrhizae* can coat plant rootlets, excreting phosphatase and organic acids to release phosphorus and providing an active uptake site for rapid diffusion of phosphorus from soil pore spaces to root surfaces.

Phosphorus in soils is present in variety of forms, and its distribution between these forms changes dramatically with time and soil development. The forms can be grouped into refractory (not readily bio-available) and labile (readily bio-available). The refractory forms include phosphorus in apatite minerals and phosphorus co-precipitated with and/or adsorbed onto iron and manganese oxy-hydroxides (termed ―occluded‖ P). The reducible oxy-hydroxides have large binding capacities for phosphate, due to their immense surface area and numerous delocalized positively charged sites. The labile forms include phosphorus in soil pore spaces (as dissolved phosphate ion) and adsorbed onto soil particle surfaces (termed ―non-occluded‖ P), as well as P incorporated in soil organic matter. On a newly-exposed lithic surface, nearly all of the phosphorus is present as phosphorus in apatite. With time and soil development phosphorus is increasingly released from this form and incorporated in the others. Over time, the total amount of phosphorus available in the soil profile decreases, as soil phosphorus is lost through surface and sub-surface runoff. Eventually, the soil reaches a terminal steady state, when soil P is heavily recycled and any phosphorus lost through runoff is slowly

replaced by new phosphorus weathered from apatite minerals at the base of the soil column (Filippeli, 2009).

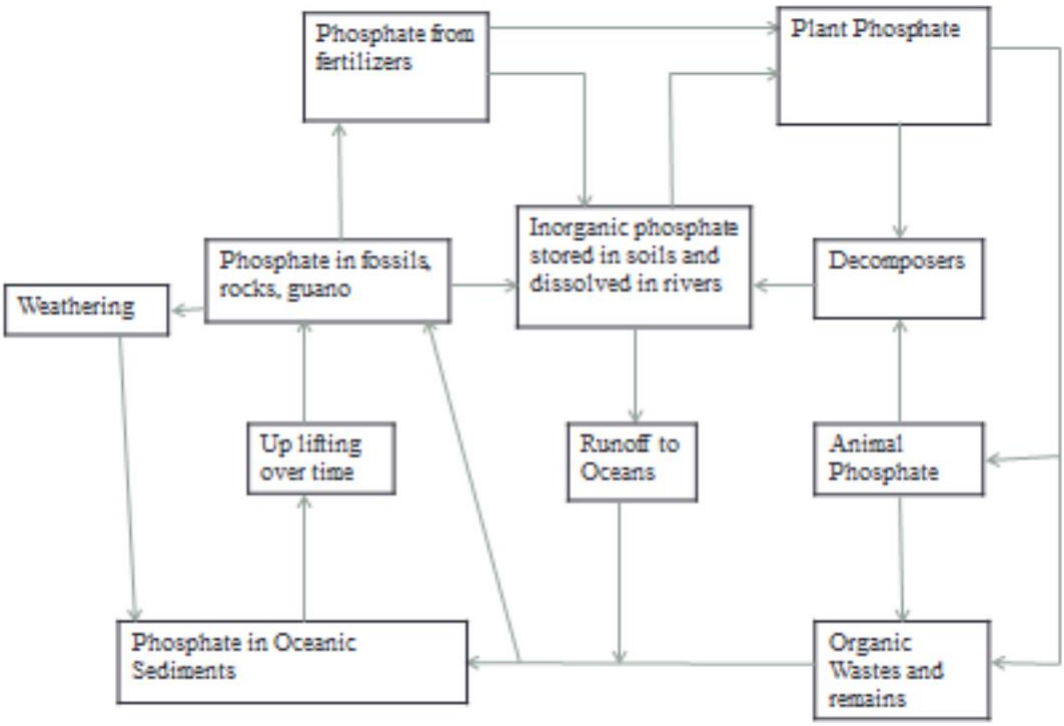

Figure 2.1: Schematic diagram of phosphorus cycle (Source: Filippeli, 2009**)**

2.3 Methods of removal of phosphorus

With the ever-increasing use of water for municipal and industrial purposes, it has become more important to appraise water quality on a continuous basis. Water treatment process selection is a complex task involving the consideration of many factors which include, available space for the construction of treatment facilities, reliability of process equipment, waste disposal constraints, desired finished water quality and capital and operating costs (Bhatnagar and Sillanpaa, 2010).

There are a variety of methods currently available for the removal of phosphorus from wastewater and the current major treatment methods lie in adsorption, chemical precipitation, enhanced biological phosphorus removal and constructed wetlands. The Table 2.1 shows the various methods for the removal of phosphoric compounds with the merits and demerits of each method;

Table 2.1: Conventional methods for the removal of phosphoric compounds

Methods	Demerits	Reference
Chemical precipitation	• During the removal of phosphorus, a large amount of sludge is produced • Calculations of the dosages of the chemicals are difficult due to the changing levels of alkalinity of the media. • Safety of the operator is concerned when handling the chemicals • The necessity to transport large amounts of chemicals to the wastewater treatment facilities	Gautam *et al.,* (2014)
Enhanced biological phosphorus removal	➢ It has low reliability and stability. ➢ The efficiency of the phosphate removal can be attributed to high rainfall, nutrient limitation and excessive nitrate input in the anaerobic reactor. ➢ Decreased efficiency of phosphorus removal is caused by microbial competition between polyphosphate accumulating organisms (PAOs) and glycogen (non-polyphosphate) accumulating organisms (GAOs)	Gautam *et al.,* (2014)

Table 2.2: Contd.

Crystallization	• Increased salinity • Complex process	Nguyen, (2015)
Constructed Wetlands	• Susceptibility to climate • Amassing of heavy metals and hazardous pollutants	Nguyen, (2015)

(Source: as in the Table 2.1)

Adsorption is the accumulation or enrichment of chemical substances onto a surface or interface where the adsorbing phase is called the adsorbent and the material being adsorbed is called the adsorbate. The adsorbent is required to have an extremely large surface area on which the adhesion of contaminants can occur. It occurs between two phases, such as: gas-liquid, gas-solid, liquid-liquid, or liquid-solid interface. Adsorption has been proven as an effective removal method for numerous types of pollutants in water treatment, where ions or molecules are removed from liquids by adsorption onto solid surfaces. It is a process that can be simplified below

a) Solute is transferred from the liquid to adsorbent's boundary layer.

b) External diffusion occurs, whereby the solute is transferred to the surface of the adsorbent through the boundary layer.

c) The solute is diffused from the surface to active sites, termed intra-particle diffusion.

d) Sorption of the adsorbate to the solid phase, by several forces described below.

The solubility of a dissolved substance is essential in determining the intensity of adsorption process. The second driving force is the electrical attraction of the solute to the solid. This type occurs as a result of chemical interaction or van der Waals attraction with the adsorbent. The adsorption induced by van der Waals force is defined as

physisorption, and the other type of adsorption is termed as chemisorption. In adsorption processes, these two types interact together and it is quite difficult to differentiate between the two (Nguyen, 2015).

Adsorption provides an attractive alternative for contaminated effluent treatment, in case the adsorbent is inexpensive without pre-treatment. This is an effective equilibrium separation process, superior to other techniques, simple and flexible design, operation and adaptability to alteration environment. This process has given quite simple and economical and produces less sludge and it can be easily disposed due to its high efficiency, relatively economical operation it can be used for the removal and recycling of phosphate resources. Thermodynamic studies carried out shows that the adsorption is endothermic and spontaneous in nature. However, the adsorption capacities of carbon depends on the different sources of raw materials, the history of its preparation and treatment conditions such as pyrolysis temperature and activation time, surface chemistry, surface charge, pore structure, porous texture, high surface area, chemical nature, inner surface of adsorbent, adsorption mechanisms depending on several interactions such as electrostatic and non-electrostatic (hydrophobic) interactions, sorption properties and kinetics (Gautam *et al.,* 2014).

Activated carbon (AC) has a high adsorbing capacity and has various applications in industries to; clean industrial wastewater, agricultural effluents, in medicine and discolour sugar. What makes AC such a good adsorbent is its porous structure that depicts its surface area. The presence of carbon in any material can produce activated carbon and also depending on different aspects such as economy and characteristics of the material it might be suitable or not for manufacturing of AC. In the process of manufacturing AC there are two methods of activation which are, physical and chemical. When activating chemically the carbonization and activation happens

simultaneously. For carbonization the carbonaceous material is heated in the absence of oxygen at a temperature of 1100 ºC, also called pyrolysis. In this process most of the oxygen, hydrogen and volatiles are eliminated, leaving the carbon groups structured so that pores are present giving the adsorbing characteristic of the carbon. After the raw material has been carbonized it needs to be activated to enhance the pore structures thereby increasing the adsorbing qualities further by enlarging the pores and burning off tars. For physical activation, the raw material is first impregnated with the activating reagent, which degrades the cellulosic material which enables the precursor to carbonize at lower temperatures. Chemical activation is preferred over physical activation because of the lower temperatures and shorter time needed in activating the material. After the impregnation, in absence of air, the impregnated material is then heated in a rotary kiln between 400 and 800 ºC. After the activation the material is cooled, washed and dried. The most commonly used activating agents are phosphoric acid, zinc chloride and sulphuric acid. The pore size in the carbon is set by the impregnation ratio; the larger the impregnation ratio the larger the pore diameter becomes (Birbas, 2011).

The adsorption of phosphorus allows the possibility on the material of phosphorus desorption and regeneration of the recovered phosphate from wastewater. A wide array of materials can be used as a sorbent for this adsorption process which includes, metal oxides and hydroxides, furnace slag, fly ash and chemically modified clays.

2.4 Modes of Adsorption

Batch, continuous moving bed, continuous fixed bed (up flow or down flow), continuous fluidize bed and pulsed bed are several modes by which the contact between adsorbate and adsorbent is mainly occurred in the adsorption system. They all have their benefits and drawbacks and are listed below in Table 2.2

Table 2.2: Different methods of adsorption with its merits and demerits

Modes	Merits	Demerits
Batch	• Easy, cheap and quick. • To analyze the feasibility of adsorbent- adsorbate	• Used for small quantity of wastewater • The concentration of the pollutant is low. • It cannot be used practically in an industry
Continuous fixed bed	• Easy and cheap • Large quantity of waste water • It can treat high concentration of the pollutants • It can be practically used in industries.	• Adsorbent erosion • A quantitative approach is needed before the design and optimization the bed.
Continuous moving bed	• Large quantity of waste water • It can treat high concentration of the pollutants • It can be practically used in industries. • Frequent change of the adsorbent	• Complicated and expensive • Large amount of adsorbent is required • Continuous regeneration and storage of the adsorbent is required
Continuous fluidized bed	• Large quantity of waste water • It can treat high concentration of the pollutants • It can be practically used in industries • It allows rapid mixing of adsorbent—adsorbate • The flow of the adsorbate is continuous and automated with easy handling and controlled operation.	• Complicated and expensive

(Source: Patel, 2019)

Table 2.2 shows that fixed bed column is a better choice and industrially feasible for removal of various contaminations from synthetic as well as real wastewater. The performance of fixed-bed column is studied by breakthrough curves (a representation of the pollutant-effluent concentration versus time profile in a fixed-bed column). The mechanism of this adsorption is based on different phenomena, like axial dispersion, film diffusion resistance, intra-particle diffusion resistance (both pore and surface diffusion) and sorption equilibrium with the sorbent (Patel, 2019).

2.4.1 Evaluation of the column performance

The performance of a fixed-bed column is described through the theory of breakthrough curve (effluent time concentration). The time and shape for breakthrough curve are very important features responsible for the process and the dynamic response of an adsorption column. The loading behaviour of phosphoric compounds to be adsorbed from waste water in a fixed-bed is expressed in terms of C_t /C_0 as a function of time or volume of the effluent for a given bed height, giving a breakthrough curve (Han *et al.*, 2009).

The abrupt slope of the breakthrough curve shows the efficient utilization of the adsorbent in the column. Mass transfer zone is the surface of the bed where adsorption occurs. As the fluid flows through the column, the mass transfer zone varies from 0 % of the inlet concentration (corresponding to solute free sorbent) to 100 % of the inlet concentration (corresponding to the total saturation. Saturation time, t_s, is established when the concentration in the effluent is higher than 90–95 % of the inlet concentration and the service time is the breakthrough time, tr, is established when the effluent concentration reaches normally the disposal allowable limits of the phosphoric compounds (Yahya, 2015).

A breakthrough plot is usually expressed in terms of adsorbed pollutant concentration (C_{ad}). Where C_{ad}= inlet pollutant concentration

C_0 = outlet pollutant concentration

C_t or normalized concentration is defined as the ratio of effluent phosphorus concentration (Ct) to the inlet phosphorus concentration (C_0) i.e. (C_t/C_0) as a function of time, t or volume of effluent for a given bed height. Time equivalent to total or stoichiometric capacity is given below in equation (2.1);

$$\int \quad (\quad _) \tag{2.1}$$

While time equivalent to usable capacity is given in equation (2.2);

$$\int \quad (\quad _) \tag{2.2}$$

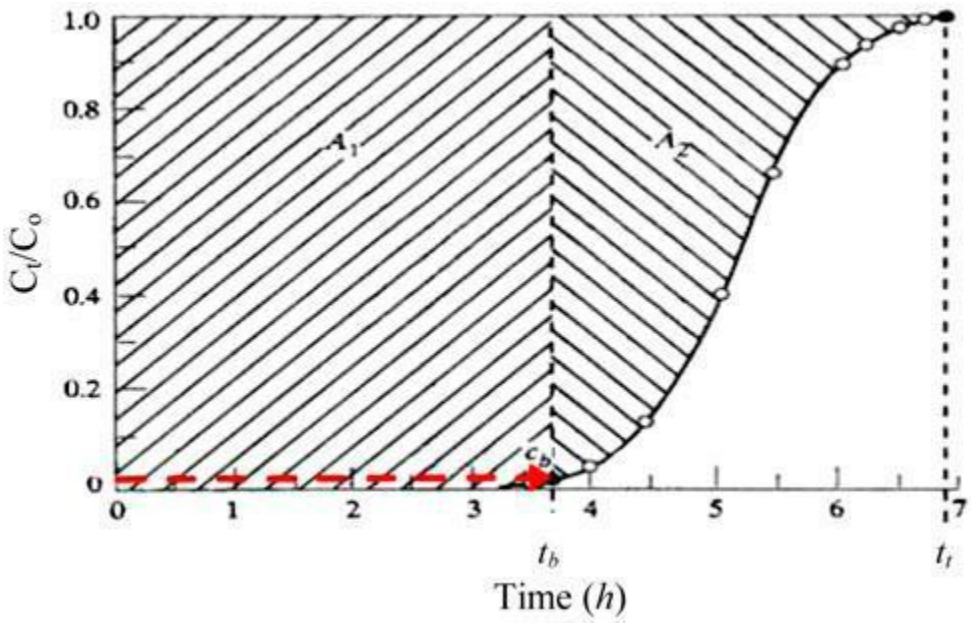

Figure 2.2: Graphical representation of a breakthrough curve (Source**:** Yagub *et al.*, (2015)

Usable capacity of bed up to the breakthrough point time, t_b and A_2 area calculation gives unused bed height (t_u). Area under the curve ∫ (—) gives t_t of (total time), whereas area under curve ∫ (—) gives, t_u value t_u/t_t is the fraction of the total bed capacity or length utilized up to break point. Area under the curve can be determined either graphically or by numerical integration but in this work, it would be determined graphically. The unused bed length (HUNB) or Mass Transfer Zone (MTZ) can be calculated with the equation (2.3) below;

— — (2.3)

Where H_T = Total bed height and t_b= breakpoint time

$$MTZ = H_{UNB} \quad (2.4)$$

The used bed length H_B (up to the break point) can be calculated with the equation (2.5) below;

(—) (2.5)

Whenever the BTC is expressed, the following parameters calculations from equation 2.1 to 2.5 are applicable. The total effluent volume can be estimated in the equation below;

$$V_{eff} = Qt_{total} \quad (2.6)$$

Where Q is the volumetric flow rate (mL/min) and t_{total} is the total flow time (min). The area under the BTC (A) is obtained by integrating the adsorbed concentration C_t/C_0 (mg/L) vs. t (min). The plot can be used to find the total adsorbed phosphorus quantity (maximum column capacity). The total adsorbed phosphorus quantity (q_{total}) in the column for a given feed concentration and flow rate is determined by the equation below;

—— —— ∫ (—) (2.7)

The total amount of phosphorus sent to column (m_{total}) is given by the equation (2.8);

——— (2.8)

The total percentage removal of phosphorus can also be found from the ratio of total adsorbed quantity (q_{total}) to the total amount sent to column (m_{total}) from the equation below;

—— (2.9)

Successful design of a column adsorption process requires prediction of the concentration-time profile or breakthrough curve for the effluent (Han *et al.,* 2009).

In order to calculate the breakthrough data for the removal of phosphoric compounds from surface water for an effective design of the adsorption process, the following breakthrough curve models were used;

2.4.1.1 Clark model

This model defines a new simulation of breakthrough curves based on the use of a mass-transfer concept in combination with the Freundlich isotherm.

— (———) ¯ (2.10)

From a plot of C_t/C_0 against t at a given bed height and flow rate using nonlinear regressive analysis, the values of A and r can be obtained (Han *et al.,* 2009).

Equation 2.10 can be linearized in the equation (2.11);

[(¯)]

2.4.1.2 Thomas model

This model follows the Langmuir kinetics of adsorption and desorption is extensively used to evaluate the performance of a column and predict its breakthrough curves and its established solely on the negligibility of axial dispersion. The drawback of this model is it's centred on second order kinetics and hence doesn't restrict the sorption by a chemical reaction and is controlled by mass transfer at the surface. The model is represented by the equation below;

(2.12)

Where K_{th} is the Thomas rate constant (mL min^{-1} mg^{-1}), q_o is the equilibrium phosphoric compounds uptake per g of the adsorbent (mg/ g). X is the amount of adsorbent in the column (g), Co is the influent phosphoric compounds concentration (mg/L), C_t is the concentration of effluent at time t (mg/L), and v is flow rate (ml/min). C_t /C_o are the ratio of effluent and influent phosphoric compounds concentrations. Thomas constant Q_o and K_{th} can be obtained through graph plotted between Ln [(Co/Ct)-1] against t (Singh *et al.*, 2015).

2.5 Adsorbent

2.5.1 The use of metal oxide and hydroxide as an adsorbent

The process by which phosphorus removal occurs through adsorption using metal oxide and hydroxide is a result of the exchange of ligands. This mechanism works best at neutral or acidic pH due to decreased competition of hydroxide ions.

Arias *et al.*, (2006), reported the use of a material consisting of iron and aluminium hydroxide coating quartz particles for adsorption of phosphorus from wastewater. These coated quartz particles were obtained through iron and aluminium hydroxide precipitation onto quartz followed by increasing the pH and washing with distilled

water. The new coated particles contained 4.5 % iron and 4.5 % aluminium. Through batch experiments with phosphorus solutions, researchers determined that the adsorption of phosphorus increased with decreasing crystallinity of the iron oxide coated quartz particles. However, this change was less apparent in the aluminium hydroxide coated particles. Another important observation from this study was that adsorption was significantly higher in the aluminium hydroxide coated quartz particles than the iron oxide coated particles. This was explained by the interactions between the metal oxides and the phosphorus. The iron oxide interaction with phosphorus was mainly electrostatic while aluminium hydroxide interacts with phosphorus through both electrostatic forces and formation of hydrogen bonds with the orthophosphate anion.

2.5.2 The use of Industrial waste as an adsorbent

Furnace slag is a by-product of steel industry and has a small amount of silicates and amorphous glasses in it. It has the ability to remove phosphorus from wastewater and it possesses a low sorption capacity. The study that was carried out and published in 2008, revealed that water-cooled blast furnace slag and natural wollastonite were used to remove phosphates from waste water although less efficiently. ATR-FTIR characterization of the furnace slag after adsorption process did not show a clearly defined peak caused by the presence of adsorbed phosphate anions but this was most likely due to overlap with some adjacent silicate peaks (Nehrenheim and Gustafsson, 2008).

Blast furnace slag was also used by Oguz 2004, to remove phosphate from aqueous solutions. The mechanisms of phosphate removal were explained on the basis of the results of X-ray spectroscopy, measurements of zeta potential of particles, specific surface area, and images of scanning electron microscopy (SEM) of the particles before and after adsorption. It was proposed that the removal of phosphate predominantly

occurred by a precipitation mechanism and weak physical interactions between the surface of adsorbent and the metallic salts of phosphate. Heated samples of acid-treated slag and mixtures of slag with kaolinite and $Al(OH)_3$ were examined by Jha *et al.*, (2008) to determine their uptake capacities for NH_4^+ and PO_4^{3-} from aqueous solutions. The highest PO_4^{3-} uptake capacity was obtained with the slag $Al(OH)_3$ mixture heated at 900 ºC whereas the highest uptake of NH_4^+ was found in the slag $Al(OH)_3$ mixture heated at 800 ºC. It was shown that heating slag composites prior to incorporation into wastewater treatment filters resulted in an increased degree of NH_4^+ and PO_4^{3-} uptake.

Zeolites synthesized from fly ash were used to determine its efficiency in the removal of phosphorus from waste waters and it possesses a high cation exchange capacity. When compared with raw fly ash, zeolite synthesized from fly ash has a higher immobilization capacity of phosphate ions (Viswanathan *et al.*, 2014).

2.5.3 Chemically modified clay adsorption

Clays are generally layered alumina-silicate materials that can be used in phosphorus adsorption in waste water treatment due to its high availability and natural origins. Currently, the types of clay used in phosphorus adsorption are; vesuvianite, montmorillonite and bentonite that possess a high negative surface charge balanced by the presence of alkali earth cations (sodium and calcium ions). The presence of these cations determines and increases the interlayer spacing in clay materials by substituting these cations with larger inorganic hydroxyl-metal poly-cations. Research studies have been carried out using bentonite as the source of clay in adsorbent materials. The evaluation of the sorption capacity for both organic compounds and phosphates using bentonite added with both organic and inorganic cations was produced and it shows that bentonite containing both the organic and inorganic cations had higher phosphate

removal efficiency than bentonite containing only the hydroxyl-aluminium species (Viswanathan *et al.,* 2014).

The benefit of using vesuvianite as an adsorbent material is due to its low density nature which enables it to float on the surface of water. During adsorption processes, the adsorbents used mostly are heavy and the regeneration of phosphorus becomes difficult due to the adsorbent sinking to the bottom of the water body. Vesuvianite was modified using lanthanum and was used for the removal of phosphorus and it showed high sorption capacity compared to using vesuvianite (Li *et al.,* 2009).

2.5.4 Adsorption using agricultural waste Materials

Agricultural waste materials possess unique properties which are; it's economical, eco-friendly (because of its unique chemical composition), availability in abundance, its renewability in nature and low cost are while it has been considered and used for the treatment of wastewater. The major part of agricultural waste materials that is responsible for sorption capacity on various pollutants is the cellulose while the rest of the components present are; hemicellulose, lignin, lipids, proteins, simple sugars, water, hydrocarbons, and starch, comprising of variety of functional groups. It is a rich source used for the production of activated carbon due to its reasonable hardness and low ash content. These agricultural waste materials have been used either in their natural form or after undergoing some physical or chemical modification (Demirbas, 2008).

Over the years, various agricultural wastes have been studied as an adsorbent and they include; shells and/or stones of fruits like nuts (Fadhil and Deyab 2008), peanut hull (Zhu *et al.,* 2009), almonds (Christopher and Wayne 2002) and apricots stones (Soleimani and Kaghazchi 2008); and wastes gotten as a result from the production of cereals such as rice (Wang and Lin 2008) and maize (Mwangi *et al*., 2011; Zvinowanda

et al., 2008; Moyo *et al*., 2014; Moyo and Okonkwo 2013). Research studies have been carried out on the gains of using different agricultural wastes as materials for adsorption process used for waste water remediation.

A study was implemented by Inoue *et al.*, (2007) on the adsorption study of orange waste loaded with lanthanum (III), cerium (III), and iron (III) ions for phosphorus removal. The conversion of the pectin in orange waste was converted to pectic acid through saponification process with the use of calcium hydroxide and made into a gel and loaded with the aforementioned ions. It was reported that the loading capacity of iron (III) ions was greater than lanthanium (III) and cerium (III) ions with maximum adsorption capacity values of phosphate ions for lanthanum (III) loaded orange waste gel and the cerium (III) loaded orange waste gel was determined to be 11.17 and 10.71 mg P/g respectively. The optimum pH for which the maximum adsorption capacity of the two gels took place between the ranges of pH 5 and pH 10 with the maximum at pH 10 and at these pH values the main phosphate species in solutions were $(HPO_4)^{2-}$ and $(H_2PO_4)^{-}$. Also for the iron (III) loaded gel, the maximum adsorption capacity was reported to be at a low pH between 3 and 5, which is usual of iron containing adsorptive materials.

Eggshell waste is one of the agricultural wastes that was studied and used for adsorption of phosphorus from aqueous solution and reported by Kose and Kivanc (2011). The maximum phosphate removal occurred within a pH range of 2–10 which showed that initial pH of the aqueous solution had little effect on the phosphate removal. It was also determined that a positively charged surface site of the adsorbent material favoured phosphate anion adsorption due to electrostatic attraction, as was seen in several other studies. The adsorption capacity was determined to be 23.02 mg/g composite which is higher than all the previously mentioned absorbent materials.

The use of activated carbon fibre loaded with lanthanum oxide as reported by Nazarian, (2017) was used to remove phosphates from water and the effects of the variables; lanthanum/activated carbon fibre, impregnation time, activation time and activation temperature were studied using response surface methodology. The removal of phosphates by the adsorbent prepared under optimal conditions was up to 97.6 % with the initial phosphate concentration of 30 mgP/L was done efficiently and the results of Fourier transform infrared (FT-IR) spectroscopy related to the adsorption process shows the probable mechanism of phosphate ions onto the adsorbent was not only done by the exchange of ligands but as a result of Lewis acid-base interaction due to La-O bonding.

2.6 Maize

Maize tassel (known as the male flower) is found at topmost part of the plant which produces pollen grains transferred by current of air to fertilize the female flowers called the silk. One maize tassel fibre can produce in excess an average of 25 million pollen grains to fertilize the ear of the corn which are useful between 1- 4 hr which would detach and end up covering a distance of 300 m, while the cob produces not less than 1000 filled seeds. During seed production, one line of the tassel fibre that produces pollen grains is sufficient to fertilize 2–3 lines of the female flower in the following proportion of 1:4 or 1:6 (male: female). Thus, maize tassel as a natural occurring matter can be utilized to yield monetary worth of products due to the presence of bioactive compounds (Duangpapeng *et al.*, 2018).

The growth cycle of maize is about three to four weeks after fertilization. During the process of fertilization the maize tassel plays an important role. This implies that beyond fertilization the tassel has no use to the farmer. The farmer cuts it off after fertilization to ease the part that will yield viable kernels (Mamba *et al.*, 2012).

The maize used in this work is known as (Zea mays) which is one of the essential edible grains globally. The by-products of maize plant which are tassels, cobs, husks, silks and ears have high percentage of starch and bioactive compounds utilized for the production of feed for humans and animals and to manufacture bio-ethanol. Research studies have been carried out to show the utilization of maize by-products such as; the growth of effective and consistent removal methods to retrieve phytochemicals and the evaluation of the components of the phytochemicals that is used for the treatment of illness. The health benefits of the phytochemicals include cardiovascular protein effects, anti-aging, anti-apoptosis, anti-atherosclerosis, anti-inflammation and anti-carcinogen which act as antioxidants that are useful to the health of humans (Duangpapeng *et al.*, 2018).

Cellulose, hemicellulose, and lignin are the key components of any lingo-cellulosic resource and the amounts of each of the components on any fibre depend on the time it was plucked (age), source and the process of extraction. Cellulose is one of the major constituents of a maize tassel which is highly renewable, with a linear polymer of b-D-glucose. The production rate of cellulose annually is 1.5 trillion tons from maize tassel, its source is unlimited, eco-friendly and bio-compatible (Klemm *et al.*, 2005).

Due to the following qualities maize tassel possess, it has been used by researchers in the search to solve problems. It is a plant based renewable source of adsorbent, it is biodegradable and it has suitable application in reducing hazardous materials. The composition of cellulose, lignin and hemicellulose present in maize tassel fibres are 41, 18 and 29 % respectively (Maepa *et al.*, 2015).

Cellulose surface hydroxyl groups are present in the tassel which is responsible for the bond with positively charged metal ions which implies that it can be useful for bio-sorption process (Zvinowanda *et al.*, 2008; Olorundare *et al.*, 2014).

Bio-sorption is the removal of contaminants from wastes or industrial effluents by living or non-living organisms. These organisms possess various functional groups that attract these contaminants and serve as a great efficiency for their removal (Farooq *et al.*, 2010)

2.6.1 Modification of maize tassel

The table below shows the different authors and their findings on the modification of maize tassel.

Table 2.3: Authors and their findings on the modification of maize tassel.

Author and year	Findings	Gap
Agyei *et al.*, 2016 (Utilization of chemically activated maize tassel for remediation of eutrophic phosphorus)	Batch experiments were carried out to study the removal of phosphate from simulated samples.	Further research work should be carried on varying temperature and agitation speed to check their adsorption effect.
Sekhula *et al.*, 2012 (Fixed bed Column Adsorption of Cu (II) onto Maize Tassel-PVA Beads)	The Thomas, Adams and Bohart and Yoon-Nelson models were studied to evaluate the column adsorption performance.	Characterization of the adsorbent should have been carried out like; BET, FTIR
Zvinowanda *et al.*,2008 (Physicochemical Characterization of Maize Tassel as an Adsorbent; Surface Texture, Microstructure and	The following analysis was carried on maize tassel; BET, SEM and DTA/DSC.	FTIR Analysis would have been carried out on the adsorbent

Thermal Stability		
Maepa *et al.,* 2015 (Extraction and Characterization of Natural Cellulose Fibers from Maize Tassel)	The maize tassel fibers were treated with NaOH and were characterized.	BET and SEM should have been carried out.
Moyo *et al.,* 2013 (Adsorption Batch Studies on the Removal of Pb(II) Using Maize Tassel Based Activated Carbon)	The adsorbent was used for the adsorption of Pb(II) ions from aqueous solutions.	Fixed bed study and real effluents were not used.
Olorundare *et al .,* 2013 (Steam activation, characterization and adsorption studies of activated carbon from maize tassels)	Batch experiments were carried out in the range 50-300 mg/l of methylene blue concentration at 30 ºC, for effect of pH, adsorbent dosage and contact time.	BET and TGA of the tassel fibre would have been carried out.
Mwangi *et al.,* 2011 (A comparative study of modified and unmodified maize tassels for removal of selected trace metals in contaminated water)	There is presence of high amount of soluble organic substances that can dissolve in aqueous media present in tassels, contributing to secondary pollution during water treatment process.	BET (to determine the surface area and pore volume) and SEM (to determine the pore size and micro porosity of the tassel fibre) would have been carried out.
Zvinowanda *et al.,* 2008	Batch experiments were	The application of the

(Biosorption of Toxic Metals: the potential use of Maize Tassel for the Removal of Pb (II) From Aqueous Solutions)	carried out, and the effects of the following parameters were studied; contact time, pH, temperature and concentration on the extent of Pb (II) removal.	adsorbent to the removal of heavy metals, trace metals and other elements from wastewater and river water will show the potential of maize tassel as a useful and cost-effective adsorbent.

(Source: as in the Table 2.3)

2.6.2 Support materials for the immobilization of bio-sorbents

Agricultural wastes have received a lot of attention and it also has its drawbacks either as a results of their fragility, non-uniform shape or leaching tendency; thus making them un-suitable for large-scale processes. These can however be solved through entrapment in a polymeric matrices. The technique is based on the use of another substance to hold the active micro-particles together. The following are the list of supporting matrices for the modification of bio-sorbents which are; Alginate, Polysulfone, polyacrylamide, silica gel, gutaraldehyde and polyvinyl alcohol (Yahya, 2015).

2.7 Polyvinyl Alcohol

Polyvinyl alcohol is a colourless, tasteless, odourless, harmless, bio-compatible, thermo stable, granular or powdered synthetic polymer which has the following properties; large dielectric strength, excellent charge storage ability and optical properties. The availability of PVA commercially in diverse categories is due to its viscosity and degree of hydrolysis. Other consumers of PVA include the textile industry, paper making, coatings, adhesives, medicines, optics, and 3D printing. The major PVA producers are Europe, Japan, USA, and China. In 2016, worldwide production of plastics and PVA

was about 335 million metric tons and 1124 kilo metric tons, respectively. In order to modify the properties of PVA, abundant hydroxyl groups play an important role. The semi-crystalline nature of PVA is due to hydrogen bonding between PVA chains. PVA exists in different morphologies for variety of applications including pharmaceutical, biomedical and others. For instance, PVA gel beads may be used in water filtration systems. Due to the hydrophilic nature of PVA, cross-linkers are used to synthesize hydrogels for a number of applications. The biomedical uses of PVA include embolization particles, eye drops, contact lenses, meniscus, artificial cartilage and adhesion barrier. It was first synthesized in 1924 by Hermann and Haehnel by saponifying poly(vinyl ester) with sodium hydroxide solution resulting in a PVA solution. The physicochemical and mechanical attributes of PVA are governed by the number of hydroxyl groups present in the PVA polymer. PVA is synthesized not by polymerization of its structural monomer (i.e., vinyl alcohol) due to its unstable nature. For commercial production of PVA, the basic raw material for the polymerization of PVA is vinyl acetate (as monomer). The controlled partial alkaline hydrolysis (saponification) of vinyl acetate is performed where the ester group of vinyl acetate is partially replaced with hydroxyl group in an environment of aqueous sodium hydroxide (Aslam *et al.*, 2018).

PVA has been used as an embedded matrix with bio sorbents or enzymes for the adsorption of contaminants from wastewaters and the following were the findings reported by authors.

Table 2.4: List of authors and their findings

Author and year	Findings	Gap
Jang and Lee 2016 (Enhanced adsorption of cesium on PVA-alginate encapsulated Prussian blue-graphene oxide hydrogel beads in a fixed-bed column system)	A study for the removal of Cesium from aqueous was performed using PVA-alginate encapsulated Prussian blue-graphene oxide (PB-GO) hydrogel beads as a novel adsorbent in a continuous fixed-bed column.	Proximate analysis were not carried out on the composite
Chu and Hashim 2007 (Copper biosorption on immobilized seaweed biomass: Column breakthrough characteristics)	Laboratory-scale column tests were carried out to ascertain the breakthrough curves with varying flow rates and feed concentrations	Recycling of the bio-sorbent could lead to the development of a feasible metal remediation technology.
Oladipo and Gazi 2014 (Fixed-bed column sorption of borate onto pomegranate seed powder-PVA beads: A response surface	The removal of boron from aqueous system using pomegranate seed powder (PS) functionalized with polyvinyl alcohol (PVA)	A SEM-EDX micrograph would have been performed.

methodology approach)	was studied.	
Li *et al.*, 2010 (Selective removal for Pb^{2+} in aqueous environment by using novel macroreticular PVA beads)	Batch experiments were carried out using macroreticular poly(vinyl alcohol) (MR-PVA) beads as an adsorbent to adsorb Pb(II)	Proximate analysis, SEM-EDX, FT-IR, BET would have been carried out on the beads.
Unuabonah *et al.*, 2010 (Modeling of fixed-bed column studies for the adsorption of cadmium onto novel polymer–clay composite adsorbent)	Kaolinite clay was treated with polyvinyl alcohol to produce a novel water-stable composite called polymer–clay composite adsorbent.	The novel polymer–clay composite adsorbent has great potentials as a low-cost adsorbent for the recovery of heavy metals.
Zhang *et al.*, 2010 (Characterization and adsorption mechanism of Zn^{2+} removal by PVA/EDTA resin in polluted water)	Batch adsorption experiments were conducted using an adsorbent PVA/EDTA resin to adsorb Zn(II) ions from single component system	Detailed studies will be needed to further assess the PVA/EDTA resins through column experiment and application to industrial effluents.

(Source: as in the Table 2.4)

CHAPTER THREE

3.0 MATERIALS AND METHODOLOGY

3.1 Materials and Chemicals

Table 3.1: Summarizes the list of materials and chemicals used

S/N	Chemicals	Manufacturer	Purity
1	Polyvinyl Alcohol	Aldrich	99 %
2	Distilled Water		
3	Hydrochloric Acid	Avondale	99 %
4	Sodium Hydroxide Pellets	Avondale	99 %
5	Methanol	Avondale	99 %

Table 3.2: List of Equipment/Apparatus used

S/N	EQUIPMENT	MODEL	MANUFACTURER	SOURCE
1	Weighing Balance	MP300	Citizen	WAFT
2	pH Meter	PH 25	REX	WAFT
3	Magnetic Stirrer	Model 400	Gallenkamp, England	WAFT
4	Oven	N505F	Genlab England	WAFT
5	Furnace	-	-	WAFT
6	Crucible	-	-	WAFT

7	Sieve			WAFT
8	Vernier Calliper			WAFT
9	Filter paper	-	-	WAFT
10	Magnetic stirrer	-	Labtech	WAFT
11	Measuring cylinder	Jatech	Pyrex England	WAFT
12	Beaker	-	Pyrex England	WAFT
13	Funnel	-	-	WAFT
14	Pipette	-	Pyrex England	WAFT

*WAFT: Water and Fisheries Technology Department

3.2 METHODOLOGY

3.2.1 Collection and Preparation of maize tassel powder

Maize tassel collected from a farmland in Chikakore Byazhin, Kubwa Abuja, was first air dried for two days in a fume cupboard and then thoroughly rinsed with 500 ml of distilled water. The material was then left to air dry to remove water. Finally, the tassel was dried in an oven at 105 °C for 3 h to expel any residual moisture. The dried material was then milled by a hammer mill. Thereafter, the milled tassel was sieved to a particle size of 150-500 μm. An electronic weighing balance was used to measure 500 g of the milled tassel powder (Sekhula *et al.*, 2012).

3.2.2 Characterization of the maize tassel fibre

Physical characteristics of the raw and loaded adsorbent which include proximate analysis (Moisture content, Ash content, bulk density), BET, FT-IR and SEM.

3.2.2.1 Determination of moisture content

Petri dishes where washed, placed in the oven to dry and left to cool in the desiccator. Each of the dishes was weighed with a digital weighing balance and the mass was recorded and noted as (M_1). An unknown mass of maize tassel powder was placed in the dish and the mass of the dish plus the dried sample was recorded and noted as (M_2). The dried sample containing the maize tassel was placed in an oven to dry under the temperature of 70 °C and it was left over night to dry. The sample was removed the next morning and the new mass was weighed and recorded as (M_3) (Ekpete *et al.*, 2017). The moisture content was calculated as described by equation (3.1);

_____

3.2.2.2 Determination of ash content

4 g of the maize tassel was placed in a crucible of weight (M_1); then the weight of the crucible plus the sample was weighed and recorded as (M_2). The sample was kindled on a bursen flame inside a fume cupboard to remove some of the smoke, and then it was transferred to a furnace at 650 °C for 1 hour until a grey colour was noticed. The crucible was placed in a desiccator to cool and the weight was taken and recorded as (M_3) (Ekpete *et al.*, 2017). The Ash of the maize tassel powder was calculated as described by equation (3.2);

_____)

3.2.2.3 Determination of bulk density/ apparent density

An electronic weighing balance was used to weigh 20 g of the maize tassel in a 100 ml measuring cylinder. The cylinder was tapped 10 times against the palm and placed on the table to record the final volume (Ekpete *et al.*, 2017). The equation below was used to calculate the bulk density;

3.2.2.4 Determination of iodine number

0.5 g of maize tassel powder was transferred to a clean and dry 250 ml Erlenmeyer flask equipped with a ground glass stopper. 10 ml of 5 wt % hydrochloric acid solution was transferred into each of the flask containing the maize tassel. Each of the flasks was stoppered and twirled gently until the maize tassel is completely wetted. The stoppers were undone to vent the flasks, and they were placed on a hot plate in a fume hood and brought to boil. The contents were boiled gently for 30 seconds to expel any sulphur content which may obstruct the test results. The flasks were removed from the hot plate and left to cool at room temperature. 100 ml of 0.1 N iodine solutions was transferred with the aid of a pipet into each flask and the flasks were stoppered. The contents were shaken briskly for 30 seconds and filtered immediately through a sheet of folded filter paper (Whatman 110 mm) into a beaker. 20 ml of the filtrate was used to rinse the pipet and discarded and the remaining was collected in clean beakers. 50 ml of the filtrate were transferred into a clean 250 ml Erlenmeyer flask with the aid of a measuring cylinder. Each of the filtrate was titrated with standardized 0.1 N sodium thiosulfate solutions until the solution turns pale yellow. 2 ml of the starch indicator solution were added and continue the titration with sodium thiosulfate until one drop produces a colourless solution. The volume of sodium thiosulfate used for determination of the amount of iodine adsorbed on to the carbon (mg/g) was recorded and blank iodine was titrated with sodium thiosulphate and a starch indicator was used until the solution turns colourless and the volume of sodium thiosulphate used was recorded. The equation below was used to determine the iodine number of maize tassel;

( ) (3.4)

Where *v* is the volume of iodine, T_i is the sodium thiosulphate solution used for titration of the iodine solution without maize tassel, T_f is the amount of sodium thiosulphate used for titration of iodine and the maize tassel, C_i is the concentration of iodine, M_i is the molar weight of iodine and w is the weight of the maize tassel (Wang *et al.*, 2008).

3.2.2.5 Determination of point zero charge

The salt addition approach was done by the inclusion of same quantity of substrate to a set of solutions of similar ionic strength at different pH values. In a series of 50 mL centrifuge tubes, 20 mL of 0.1 M $NaNO_3$ solution was added to a weighed sample of 0.1 g of maize tassel and the pH was altered with 0.1 M HNO_3 and 0.1 M NaOH to achieve the appropriate pH range of 2, 3, 4, 5, 6, 7, 8, 9, 10, and 11 (± 0.1 pH units). The pH values of the supernatant in each tube were denoted as pHi. The samples were shaken for 30 minutes using a centrifuge at 3500 rpm. After settling, the pH values of the supernatant in each tube were measured and denoted as pHf. The PZC was obtained from the plot of ΔpH (=pHf – pHi) against pHi. Experiments were repeated with a 0.05 M $NaNO_3$ solution. Each set of experiments was done thrice and the average value was recorded (Bakatula *et al.*, 2018).

3.2.2.6 Determination of crude protein

An electronic weighing balance was used to weigh 0.5 g of maize tassel and poured into the digestion tube with the addition of 20 ml of concentrated Hydrogen tetraoxosulphate (VI) acid. A selenium tablet was added to the mixture as a catalyst. The content in the tube was heated at a temperature of 350 ^{o}C for 6 hours until a clear solution (digest) was achieved. This solution was poured into a measuring cylinder and made up to 100 ml. 10 ml of 2 % boric acid was taken into a 100 ml conical flask and added with three

drops of mixed indicator (Bromocresol green and Methyl red) and the colour changes to pink which was then placed under the collecting spot. 10 ml of the digested sample was pipetted into the open chamber of the makhamps apparatus then followed by 10 ml of 40 % NaOH. The mixture was hereby boiled by the steam produced by the boiling water in the flat bottom flask. As the mixtures boils, a gas (ammonia) was evolve and condense by the condenser of the apparatus which was collected inform of liquid into the boric acid. As the ammonia is collected in the boric acid, the solution turns blue. The distillate collected was titrated using 0.1M HCl until an end point is reached by the colour change of the distillate to pink colour. Crude protein is calculated with the equation (3.5);

——————————— (3.5)

Where TV is the titre value of hydrochloric acid used, 0.014 is nitrogen standard, M_A is the molar concentration of hydrochloric acid, D_F is the dilution factor and S is the weight of maize tassel used (Onwuka, 2005).

3.2.2.7 Determination of oxygen containing functional groups

The Boehm titration method was used for this analysis. 1 g of the maize tassel were added to each 15 ml solution of $NaHCO_3$ (0.1 M), Na_2CO_3 (0.05 M) and NaOH (0.1 M) for acidic groups and 0.1 M HCl for basic groups sites respectively at ambient temperature for more than 2 days. Direct titration process was carried out to determine the functional groups present. The number and type of acidic sites were calculated in view that NaOH neutralizes carboxylic, lactonic and phenolic groups, Na_2CO_3 neutralizes carboxylic and lactonic groups and that $NaHCO_3$ neutralizes only carboxylic groups. Carboxylic groups were therefore quantified by direct titration with $NaHCO_3$. The change between the groups titrated with Na_2CO_3 and those titrated with $NaHCO_3$

was inferred to be lactones and the change between the groups titrated with NaOH and those titrated with Na_2CO_3 was presumed to be phenol. Neutralization points were known using pH indicators of phenolphthalein solution for titration of strong base and strong acid, methyl red solution for weak base with strong acid and pH together. In order to neutralize basic group sites, remaining HCl in the solution was back titrated with 0.1 M NaOH (Ekpete and Horsfall, 2011). The equation (3.6) was used to solve for the functional groups present in the maize tassel;

[] ( ) — (3.6)

Where [B] is the concentration of base, V_B is the volume of the reaction base, n_{csf} is the moles of maize tassel surface functionalities on the surface of carbon that reacted with the base, V_a volume of the aliquot taken from V_B, [HCl] is the concentration of HCl and V_{HCl} is the volume of acid used (Goertzen *et al.*, 2010).

3.2.2.8 Determination of surface functional groups

FT-IR spectra were used to study the structure of maize tassel fibres using a Nicolet 560 spectrophotometer. The size of the maize tassel fibres were reduced and mixed with KBr powders and the mixture was compressed into plates for FT-IR analysis. The FT-IR spectra of the samples were obtained in the wavelength range of 4000–650 cm^{-1}. A total of 32 scans were co-added in order to achieve an acceptable signal-to-noise ratio. In all cases, spectra resolution was maintained at 4 cm^{-1} (Mwangi *et al.*, 2011).

3.2.2.9 Determination of surface area and pore volume

The porosity and specific surface area were determined by the modelling of N_2-adsorption data with the Brunauer–Emmett–Teller (BET) isotherm. The particle size distribution was gotten by the fitting of an algorithm to patterns generated by the diffraction of a laser beam by suspended adsorbent particles. A Novastation D (version

11.03) was used to achieve textural analysis on the maize tassel powder and after immobilizing with polyvinyl alcohol determined by nitrogen adsorption–desorption at an analysis bath temperature of 273 k, outgas temperature of 250 ºC, analysis time of 79 minutes and an equilibration interval of 12 s. The sample was automatically degassed. A sample mass of 0.08 g was used and the adsorptive properties of nitrogen were analysed. The multiple-point BET surface area, adsorption total pore volume and the pore diameter were determined (Zvinowanda *et al.,* 2008).

3.2.2.10 Surface morphology determination

This is carried out according to the method reported by Wang *et al.,* 2008, the outer surface micro porosity and pore size of the raw and loaded Maize tassel PVA beads was examined using a scanning electron microscope (SEM) with an accelerating voltage of 15 kV at various magnifications of x500 and x1000. A thin layer of the adsorbent was mounted on the Al specimen holder by a double sided tape and coated with Au/Pb to a thickness of about 30 nm.

3.2.2.11 Phosphate determination

Colorimetric method was used using EPA 365.3, 5 ml of the digested sample was put into a conical flask and 4 ml of ammonium molybdate-antimony potassium tartate was added together with 2 ml of ascorbic acid solution. After 5 minutes, a UV-spectrophotometer U-4100 with absorbance of 650 nm was used to determine the concentration with a standard calibration curve.

3.2.3 Preparation of maize tassel-PVA beads

An electronic weighing balance was used to measure 8.5 g of PVA powder and poured into a 250 mL beaker containing 50 mL of distilled water. The mixture was stirred at a speed of 800 rpm at 80 °C for 5 h and 17 g of sieved tassel powder added to the mixture while stirring. The mixture was stirred for another 1 h with a magnetic stirrer to get a

homogeneous mixture until the tassel powder blended well with the PVA and the temperature of the mixture reduced to 50 °C. After that, the homogeneous mixture was cooled and added drop wise via the aid of a syringe to a beaker containing 99 % methanol for an hour. It was rinsed with distilled water and dried in an oven at a very low temperature before storing in an air tight container. The diameters of the beads were measured using a vernier calliper (Sekhula *et al.*, 2012).

3.3 Collection and characterization of the surface water

The surface water used was collected from Lapai Gwari fish pond in Minna, Niger state.

3.3.1 pH

The pH of the surface water was analysed before and after treatment with the aid of a pH meter, PH 25. The pH meter was firstly calibrated with a buffer solution of 2, 6.8 and 9 then the probe was rinsed with distilled water and cleaned with a dry cloth. The probe was inserted into the surface water and the readings were taken.

3.3.2 Dissolved Oxygen

This was determined by electrometric method using APHA 4500-O G, the dissolved oxygen measurement was submerged into the sample and the reading taken in mg/L.

3.3.3 Chemical Oxygen Demand

This was determined by colorimetric method using PPHA 5220D. The culture tubes were washed with 20 % sulphuric acid and rinsed with distilled water to avoid impurities before the analysis was carried out. 2 ml of the surface water, 1 ml of digestion solution and 3 ml of sulphuric acid were poured into the culture tubes. The mixture was placed in a block digester which has been preheated to a temperature for 150 ºC for 2 hrs and was allowed to cool at ambient temperature after the reading of the concentration was taken.

3.3.4 Biochemical Oxygen Demand

The water sample was gotten using APHA 5210B method. 95 ml of the sample was poured into the BOD Trak sample bottles and BOD nutrient buffer pillow was added in each bottle for the growth of the bacteria. Magnetic bar was placed inside the sample bottles with the contents were kept in the Chassis of the BOD Trak and incubated at 20 ^{o}C for five days and the BOD value was taken digitally from the instrument.

3.4 Column Adsorption Studies

This is carried out according to the method reported by Sekhula *et al.,* (2012) and Yahya (2015); the study was carried out with the aid of a glass column of internal diameters (I.D) of 3cm and 50 cm in length. The beads were allowed to fall into the column under force of gravity. The cotton wool which acts as a support by preventing it from flowing through the outlet was packed before and after packing the maize tassel-PVA beads. The flow rates of the effluent from the tank were controlled with the aid of Medical set. The following parameters were studied during the process such as; flow rate, bed height and initial concentration of the effluent. The column was open to the atmosphere in order to maintain the internal pressure in the columns near atmospheric pressure. The solution entering and leaving the top of the column was collected at various time intervals and the samples were analysed and studied with the aid of a UV-spectrophotometer. All experiments were conducted at room temperature and the direction of flow was from top to bottom and the flow continues until the effluent concentration almost equal influent concentration.

3.4.1 Effect of bed height

The effect of bed height on the breakthrough curve was studied by altering the height of the adsorbent (Maize tassel PVA) ranging from 2, 4 and 6 cm equivalent to 6.3, 12.6 and 18.9 g respectively while the initial concentration of the effluent and the flow rate

were kept constant at 2 mg/l, 6.13 mg/L, 11.23 mg/L and 8 mL/min respectively. The wastewater was introduced from the top of the column to the bottom and the samples were taken from 15 to 1620 min for analysis.

3.4.2 Effect of initial concentration

The effect of the initial concentration on the breakthrough curve, the concentrations of the surface water were passed into the column from the top while keeping the flow rate and bed height constant at a value of 8 ml/min and 4 cm respectively. The samples were taken for analysis between 15 to 1620 minutes.

3.4.3 Effect of inlet flow rates

The effect of flow rates were investigated on the breakthrough curve by varying the flow rates between 4 - 12 mL/min while the concentration and bed height were kept constant at a value of 2 mg/L, 6.13 mg/L 11.23 mg/L and 4 cm respectively. The samples were taken for analysis between the time intervals of 15 – 1620 minutes.

3.5 Modelling of fixed bed column breakthrough

The two models that would be considered for the kinetic studies for the column sorption process of phosphoric compounds using maize tassel in PVA as an adsorbent in this work are Thomas and Clark model.

CHAPTER FOUR

4.0 RESULTS AND DISCUSSION

4.1 Proximate analysis of maize tassel

Adsorption is reliant on material characteristics such as surface area, particle size and number of carbon atoms present. In this study, characterization and the preparation of the maize tassel immobilized in Polyvinyl Alcohol and used to study the removal efficiency of phosphoric compounds from surface water. Adsorbents materials are generally valued on a moisture free basis but some moisture content is stipulated except its being packaged in air tight containers. They can adsorb moisture and still remain dry, this moisture content doesn't affect the adsorptive power but it reduces the carbon content present in the adsorbent materials. The permissible limit of moisture content allowed in adsorbent materials is within the range of 3-6 % (ISI standards). This statement is true when taking maize tassel into consideration. The values of the surface characterization of maize tassel are shown in Table 4.1

Table 4.1: Surface characterization of maize tassel

Parameter	Value
Moisture content (%)	4.51
Ash content (%)	2.134
Apparent density (g/cm^3)	0.41
Iodine number	423.05
Particle size (μm)	300
Crude protein (%)	4.06
Acid soluble matter (%)	79

From the table above, it shows that maize tassel moisture and ash content are at a low level having values of 4.51 and 2.134 % respectively.

According to Ekpete *et al.,* (2017) the presence of low amount of moisture and ash content present in adsorbent materials shows that the density of the particles are small and it would be a remarkable unprocessed material for adsorption purposes in a fixed bed or column reactor. The lower the moisture and ash value the greater the adsorbents and the value should be within the ranges of 1-20 % hereby making maize tassel a viable sorbent for the extraction of pollutants from waste water.

The apparent density is a vital physical parameter which evaluates the filterability of a sorbent material because the amount of carbon present in a filter of given solids can be determined by the amount of treated liquid retained by the filter cake. The apparent density of the adsorbent material has an effect on adsorption per unit volume but does not affect the efficiency of measured in adsorption per unit weight. If the density of the material is high, small amount of the sample is sufficient for carrying out adsorption studies (Ekpete and Horsfall, 2011). From Table 4.1 the apparent density of maize tassel gotten is 0.41 g/ml.

The acid soluble matter is vital because when the waste water being treated is acidic, the adsorbent becomes soluble and the effluent contains the material. Maize tassel cannot be used efficiently adsorption in an acidic medium because it is highly soluble in acid.

4.1.1 Surface characterization of maize tassel

Iodine number is used solely for the purpose of evaluating the surface area of sorbent materials at ambient temperature conditions to aid in evaluating the porosity and adsorbent capacity of the materials. The increase in iodine number of carbon atoms has been attributed to the occurrence of enormous micro-pores structure and to the immense

possibility of carbons present in the adsorbent materials to have enormous surface area as a result of the increase of their pore structure (Ekpete *et al.,* 2017).

As observed in the table above, the iodine number for maize tassel is 423.05 which show that it has large micro-pores thereby leading to large surface area which is a necessity for adsorption process.

The capability of an adsorbent material to adsorb contaminants is an essential property due to its specific surface area. Mostly, the increase in surface area of the sorbent material determines the capability of adsorbing more contaminants. The table 4.2 below shows the result of the surface area and pore volume on the maize tassel;

Table 4.2: Adsorption parameters obtained by the application of the bet model to adsorption isotherms of maize tassel

Sample	**Surface area (m^2/g)**	**Pore volume (cm^3/g)**	**Pore size (nm)**
Maize tassel	652.3	0.4056	2.144

The point of zero charge is an essential measurable property of any sorbent material. They are pH values at which the surface charge components sum up to 0 under given conditions such as temperature, pressure and composition which implies equal amounts of positive and negative charges. At pH below the point zero charge the sorbent material is positively charged which implies the material will adsorb anions while at pH values above the point zero charge the sorbent material is negatively charged which results to the material adsorbing cations. The point zero charge values might aid in the selection of a material for the removal of pollutants from effluents. Sorbent materials that have low point zero charge would be appropriate to remove pollutants that possess positive

ions, while materials with high PZC values would be best to remove negative ions (Bakatula *et al.*, 2018).

The curves gotten from the (plots of ΔpH vs pHi) following the salt addition technique at both ionic strengths of (0.05 and 0.1 M of $NaNO_3$) were done in triplicates and the average was taken are presented in figure 4.1

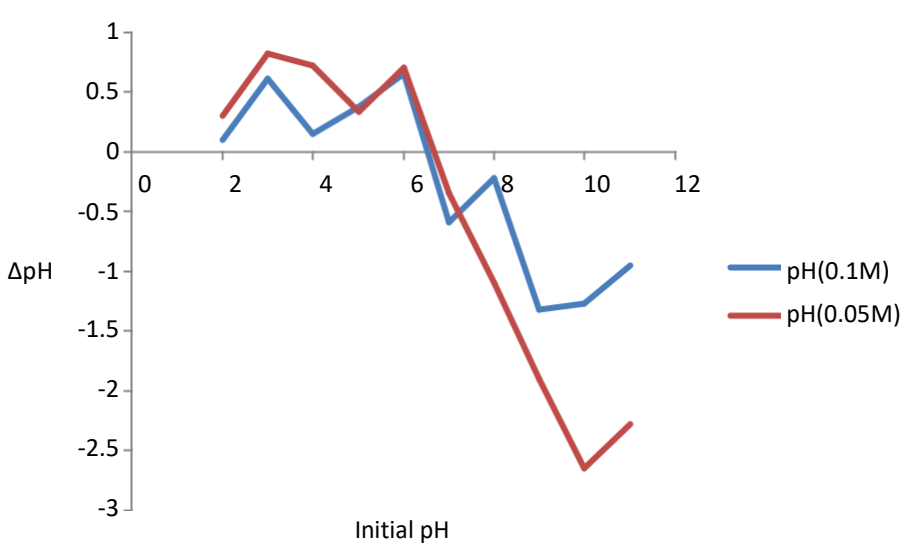

Figure 4.1: A plot of the Change in Final pH and Initial pH against the Initial pH for maize tassel

In 0.05 M $NaNO_3$, the point zero charge values of maize tassel was 6.8. When the ionic strength was increased to 0.1 M, the point zero charge reduced to 6.6 with a minor decrease of PZC (0.2 pH unit). This work is in agreement with Boparai *et al.*, (2013) with the same salts and ionic strength with pHZPC of 6.25. According to Sillerova *et al.*, (2013) the point zero charge of peat and sawdust using the same ionic strength and same salts as stated above were 3.42 and 4.26 respectively.

4.1.2 Surface chemistry characterization of the maize tassel fibre

Boehm's method gives a semi-quantitative degree of surface functionalities since the chemical groups are more difficult and are shown in Boehm titrations. With $NaHCO_3$, Na_2CO_3, NaOH, and HCl assumed to be neutralizing carboxylic groups, lactonic and carboxylic groups, lactonic, carboxylic, and phenolic groups, and all basic groups, the nominal observation of the values showed that there was no much change existing between the carbon samples when the acidic sites are taken into consideration. The table 4.3 shows the oxygenated functional groups of maize tassel plant below;

Table 4.3: The oxygen functional groups of maize tassel

Groups	Maize Tassel (mmol/g)
Carboxyl	0.9
Lactones	0.6
Phenols	-0.66
Total non-carbonyl	0.84

The oxygen containing groups were analysed and evaluated with the aid of FT-IR. Due to the distinctive property of absorbing energy from the different bonds in each group, FTIR spectra discloses the specific surface functional groups on the maize tassel fibre (Ismadji *et al.*, 2010)

The affirmations of the chemical structures of maize tassel fibres were gotten from FT-IR analysis. The composition changes observed for maize tassel fibres are shown in Figure 4.2

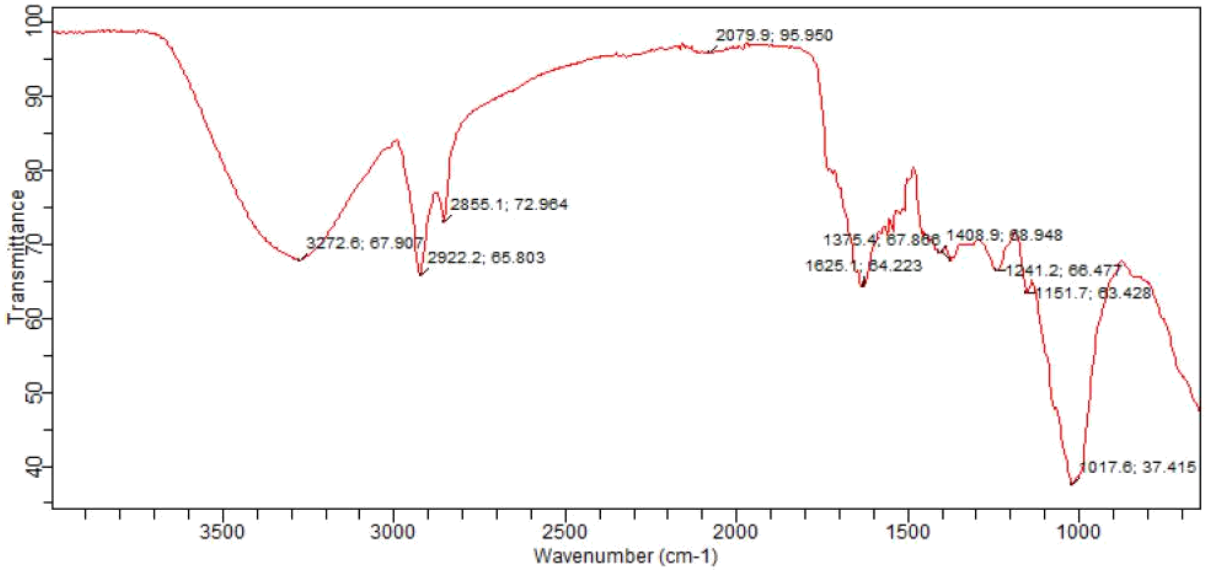

Figure 4.2: FT-IR spectrum of maize tassel

Table 4.4: The bonds present in maize tassel fibre

Maize tassel peaks (cm^{-1})	Bonds indicative	**Reference**
3272	Alcohol stretching vibration	Jin *et al., 2019*
2922.2-2855.1	Alkanes stretching vibration	Jin *et al.*, 2019
1625.1	Alkenes (CH_2) bending vibrations	
1241.2- 1151.7	Alkyl,ArylorEther stretching vibration	Nguyen *et al.*, 2015

The spectrum shows the presence of hydroxyl, carbonyl, ether groups, and absorbed water in the maize tassel fibre which can be bonded with cations easily (Zvinowanda *et al.,* 2008). As shown in Figure 4.2 above, the hemicellulose intensity of the peak appeared at around 1730 and 1240 cm^{-1} in the maize tassel which is in agreement to Obi *et al.,* (2014).

The functional groups present in maize tassel fibre presented in figure 4.2 above indicates strong bonds between 3272 and 2922 cm^{-1} attributed to hydroxyl groups, alcohol, alkanes or Amine groups (I.R Spectrum table and chart, n.d). The two bands at 2855.1 and 1625.1 cm^{-1} were ascribed to the alkanes and alkenes groups respectively while the band at 1625.1 cm^{-1} which was assigned to stretching of carbonyl group. This work is in agreement with the reports of Mwangi *et al.*, (2011).

The concentration of phosphorus in the maize tassel plant determined with the aid of a UV-spectrophotometer was 0.139 mg/L.

4.1.3 Surface chemistry characterization of the maize tassel fibre immobilized in PVA

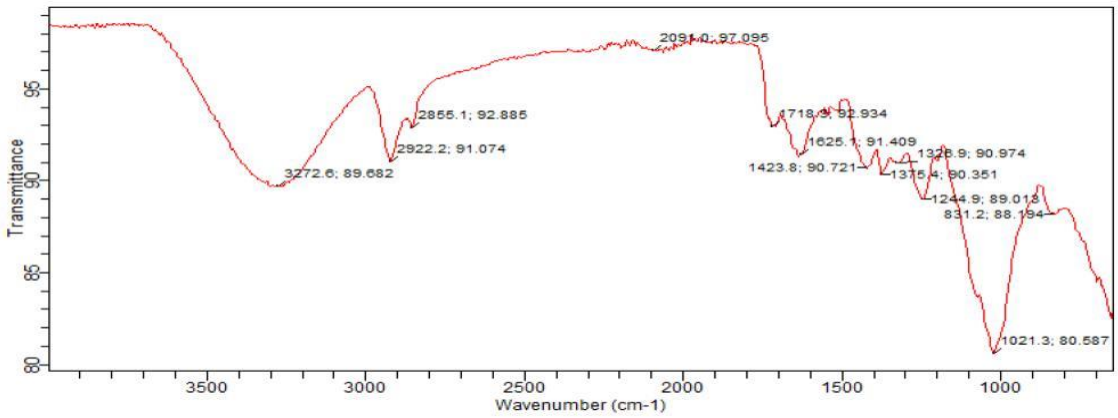

Figure 4.3: FT-IR Result for Maize Tassel Fibre Immobilized with PVA

Table 4.5: The Bonds Present in Maize Tassel Immobilized in PVA

Maize tassel peaks (cm^{-1})	Bonds indicative	Reference
3272.6	Alcohol stretching vibration	Jin *et al.*, 2019
2922.2	Alkanes stretching vibration	Jin *et al.*, 2019
1625.1	Alkenes (CH_2) bending vibrations	Jin et al., 2019

Table 4.5:	**Contd**.
1244.9	Alkyl, Aryl or Ether stretching vibration	Nguyen *et al.*, 2015

4.1.4 Surface chemistry characterization of the maize tassel fibre immobilized in PVA after Adsorption of phosphoric compounds

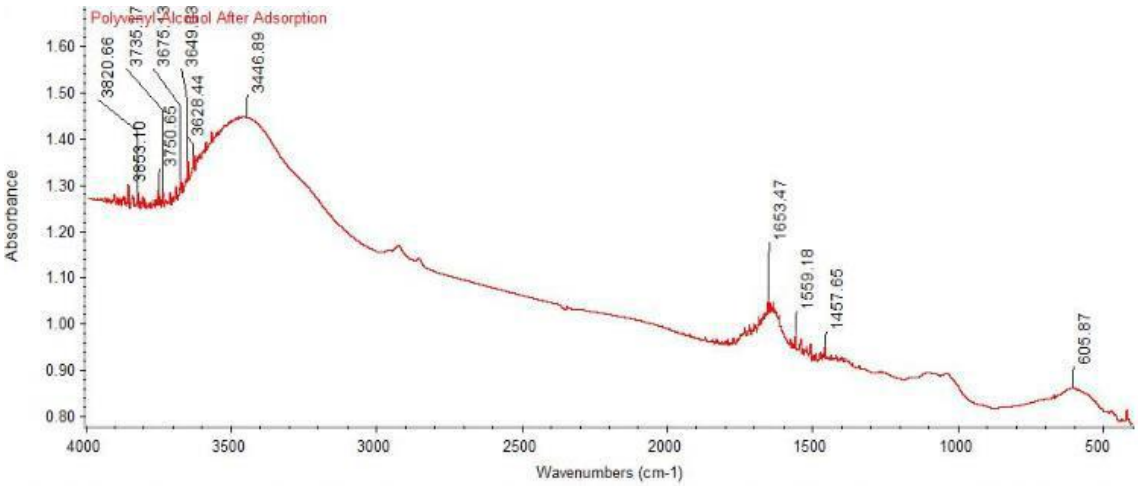

Figure 4.4: FT-IR Result of phosphoric compounds loaded in Maize Tassel Immobilized with PVA

The spectra of maize tassel immobilized in PVA and phosphoric compounds loaded in maize tassel immobilized in PVA are shown in Figure 4.3 and 4.4. The broad and strong bands at 3272.6 – 3446.89 cm^{-1} were ascribed to hydroxyl and amines groups of maize tassel immobilized in PVA before and after adsorption (Jin *et al.*, 2019). The peaks at 2922, 1653.47 and 1653.47 cm^{-1} were due to –CH group and stretching vibration of –C=O group of maize tassel respectively. The peak noticed at 1035 cm^{-1} after adsorption can be attributed to –C–O stretching of carboxylic acids and alcohols. The functional groups of maize tassel changed significantly after PVA modification. Maize tassel in PVA exhibited major absorption bands at 3272 – 3446.89 cm^{-1} and 1021 cm^{-1}, were corresponding to stretching of hydroxyl and carbonyl groups. The results confirmed that

maize tassel was successfully modified by PVA and the peak at 3272.6 cm^{-1} shifted to 3446.89 cm^{-1} for phosphoric compounds loaded with maize tassel immobilized in PVA adsorbent, indicating that hydroxyl group was mainly involved in the adsorption process.

4.1.5 Surface Morphology Determination of the Maize tassel Immobilized in PVA before and after Adsorption

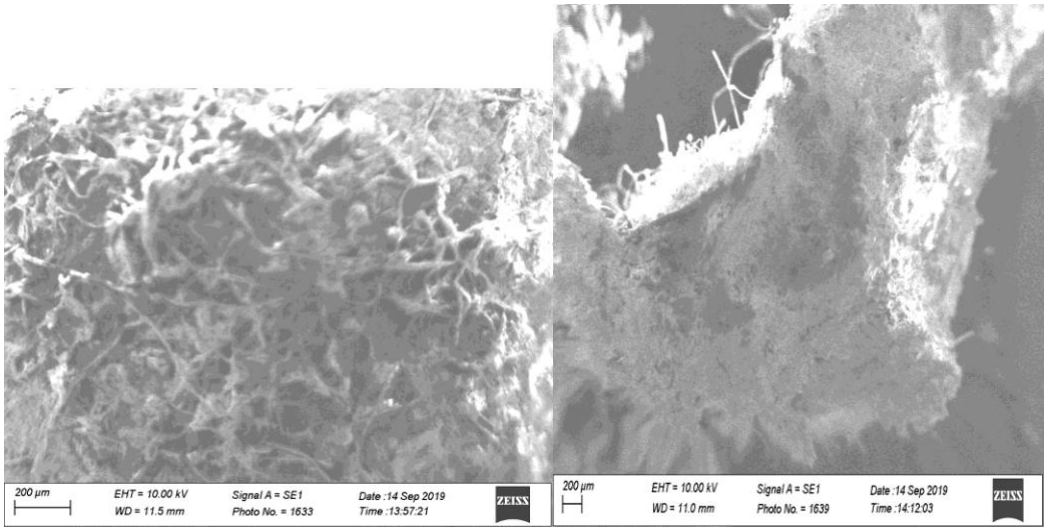

(a) **(b)**

Figure 4.5 SEM Micrograph of maize tassel immobilized in PVA before (a) and after (b) adsorption

Figure 4a and b shows the scanning electron micrographs of maize tassel-PVA beads before and after adsorption. From Figure 4a, the maize tassel immobilized in PVA appeared as elongated fibrous particles which are bound tightly to PVA but after adsorption it shows that the adsorbate has taken over the adsorbent.

4.2 Characterization of the Surface Water

Table 4.6: Table showing the values gotten from the surface water

Characterization	Results
Dissolved oxygen (mg/l)	4
COD (mg/L)	16
pH	7.78
BOD	5

4.3 Effect of Bed Study

4.3.1 Effect of bed height

The figure below shows the breakthrough curve obtained for adsorption of phosphoric compounds on maize tassel immobilized in PVA for three different bed heights of 2, 4 and 6 cm.

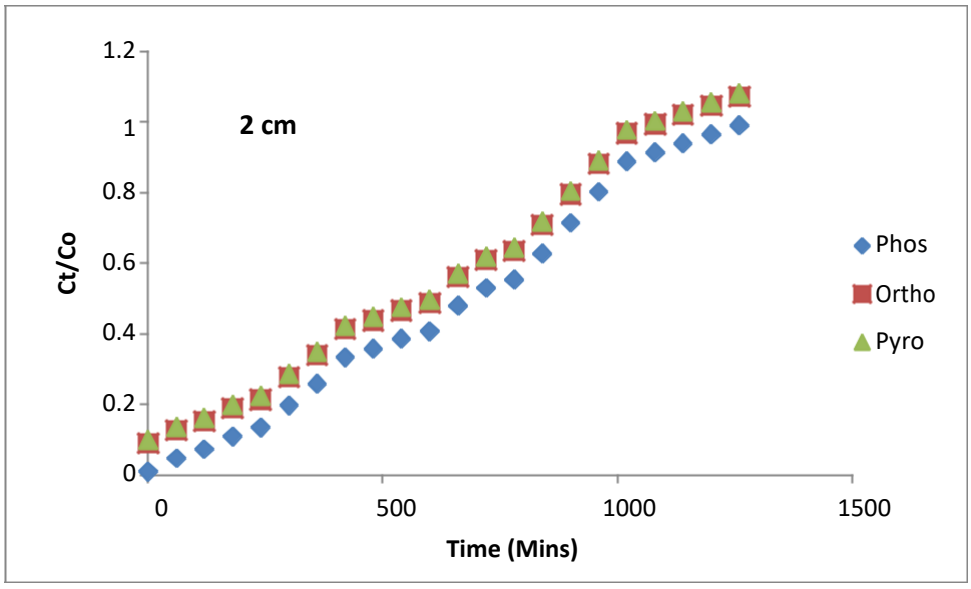

Figure 4.6: Breakthrough curve showing the removal of phosphoric compounds at a bed height of 2 cm

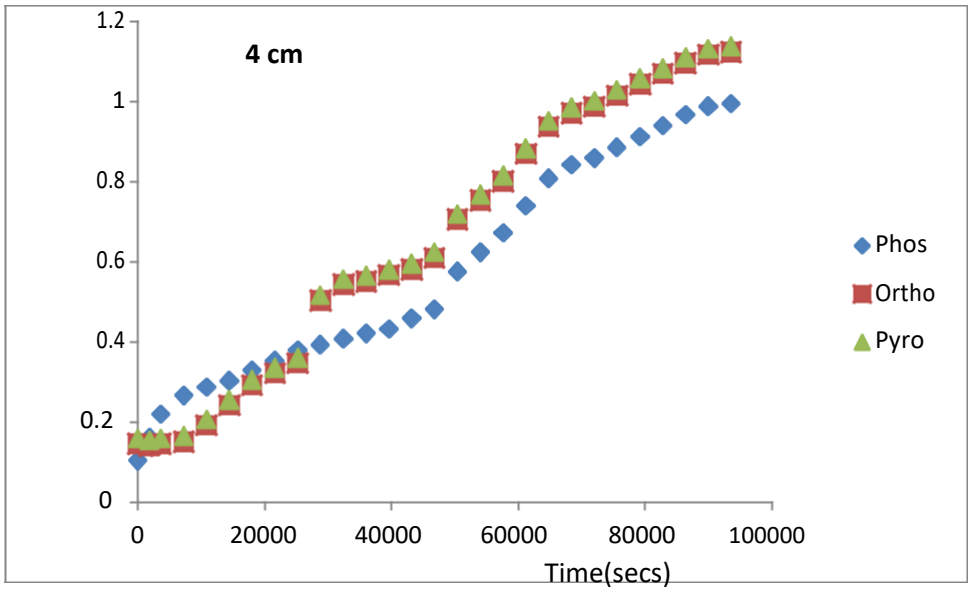

Figure 4.7: Breakthrough curve showing the removal of phosphoric compounds at a bed height of 4 cm

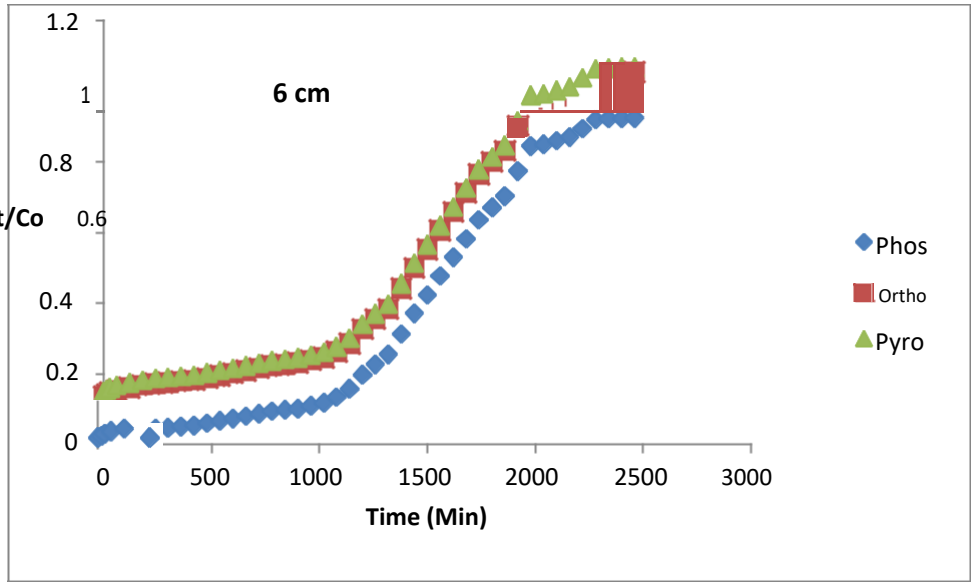

Figure 4.8: Breakthrough curve showing the removal of phosphoric compounds at a bed height of 6 cm

Breakthrough curves for the removal of phosphoric compounds on maize tassel immobilized in PVA for different Bed height (concentration of 2, 6.13 and 11.23 mg/L of phosphorus, orthophosphates and pyrophosphates respectively and at a flow rate of 8 mL/min).

As can be seen from the plots above the break through time and exhaustion time were found to increase with increasing bed height. The plots represent the shape and gradient of the breakthrough curves which were slightly different with the variation of bed depth which is expected also. A higher uptake was observed at higher bed height due to the increase in the amount of the maize tassel immobilized in PVA which provided more fixations of the anions with active binding sites for the adsorption process to commence which will lead to the increase in bed height and increase the mass transfer zone. The mass transfer zone in a column moves from the entrance of the bed and proceed towards the exit. Hence for same influent concentration and fixed bed system, an increase in bed height would create a longer distance for the mass transfer zone to reach the exit subsequently resulting an extended breakthrough time. For higher bed depth, the increase of adsorbent mass would provide a larger service area leading to an increase in the volume of the treated solution.

The breakthrough time of phosphorus at a bed height of 2 cm is at 183 minutes while at an increased bed height of 6 cm, the time increased to 750 minutes. Furthermore, the exhaustion time of phosphoric compounds also increased from 1250-2500 minutes as the height of the bed increased.

4.3.2 Effect of Flow rate

The breakthrough curves at various flow rates are shown in Fig 4 below at different flow rates of 4, 8 and 12ml/min and at a constant bed height of 4 cm and initial concentration of the influents at 2, 6.13 and 11.23 mg/L for phosphorus, orthophosphates and pyrophosphates respectively.

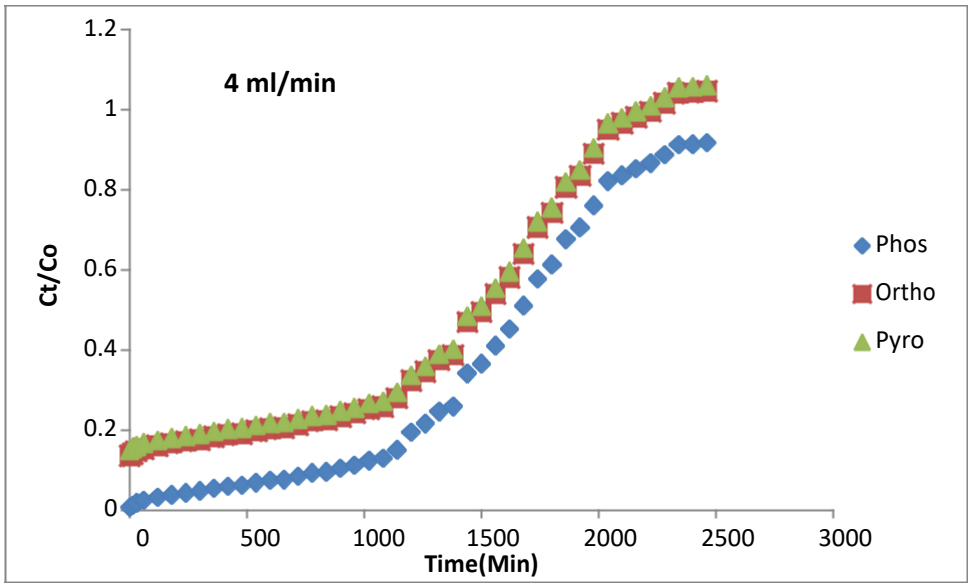

Figure 4.9: Breakthrough curve showing the removal of phosphoric compounds at a flow rate of 4 ml/min

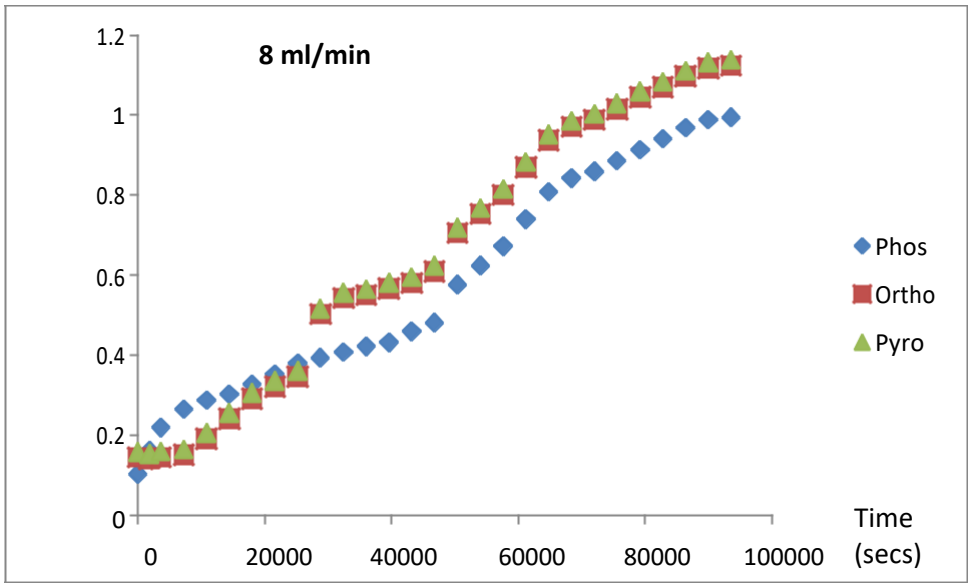

Figure 4.10: Breakthrough curve showing the removal of phosphoric compounds at a flow rate of 8 ml/min

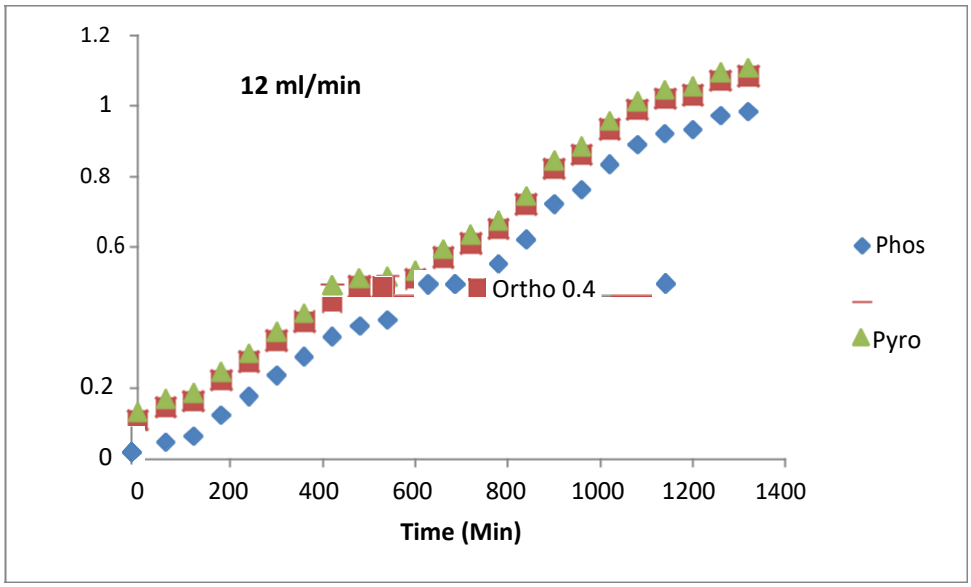

Figure 4.11: Breakthrough curve showing the removal of phosphoric compounds at a flow rate of 12 ml/min

It reveals that the breakthrough generally occurred faster with a higher flow rate. Breakthrough time reaching saturation was increased significantly with a decrease in the flow rate. At a low rate of influent, Phosphoric compounds had more time to be in contact with adsorbent, which resulted in a greater removal of the contaminants in column.

When the flow rate increased from 4 to 12 ml/min, the breakthrough time decreased from 867 to 200 minutes and the exhaustion time decreased from 2500 to 1300 minutes.

4.3.3 Effect of Initial Concentration

The effect of influent phosphoric concentration on the shape of the breakthrough curves is shown in the Figures below;

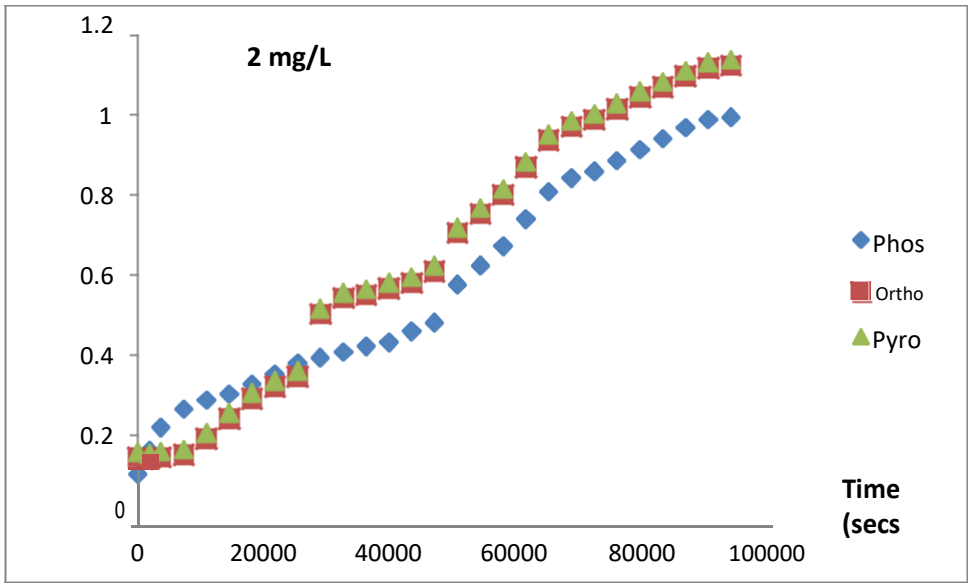

Figure 4.12: Breakthrough curve showing the removal of phosphoric compounds at initial phosphoric concentration of 2, 6.13 and 11.23 mg/L

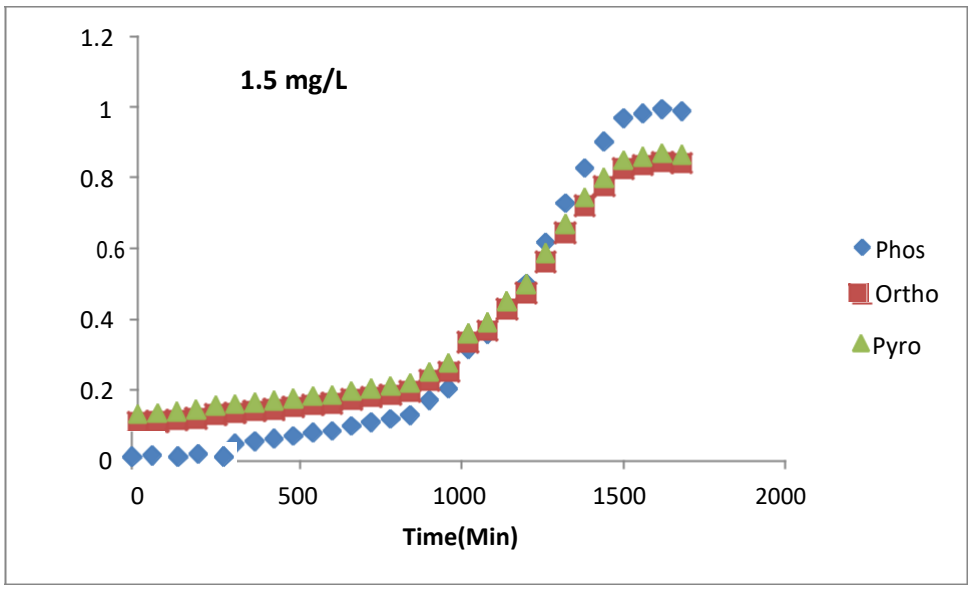

Figure 4.13: Breakthrough curve showing the removal of phosphoric compounds at initial phosphoric concentration of 1.5, 4.8 and 8.9 mg/L

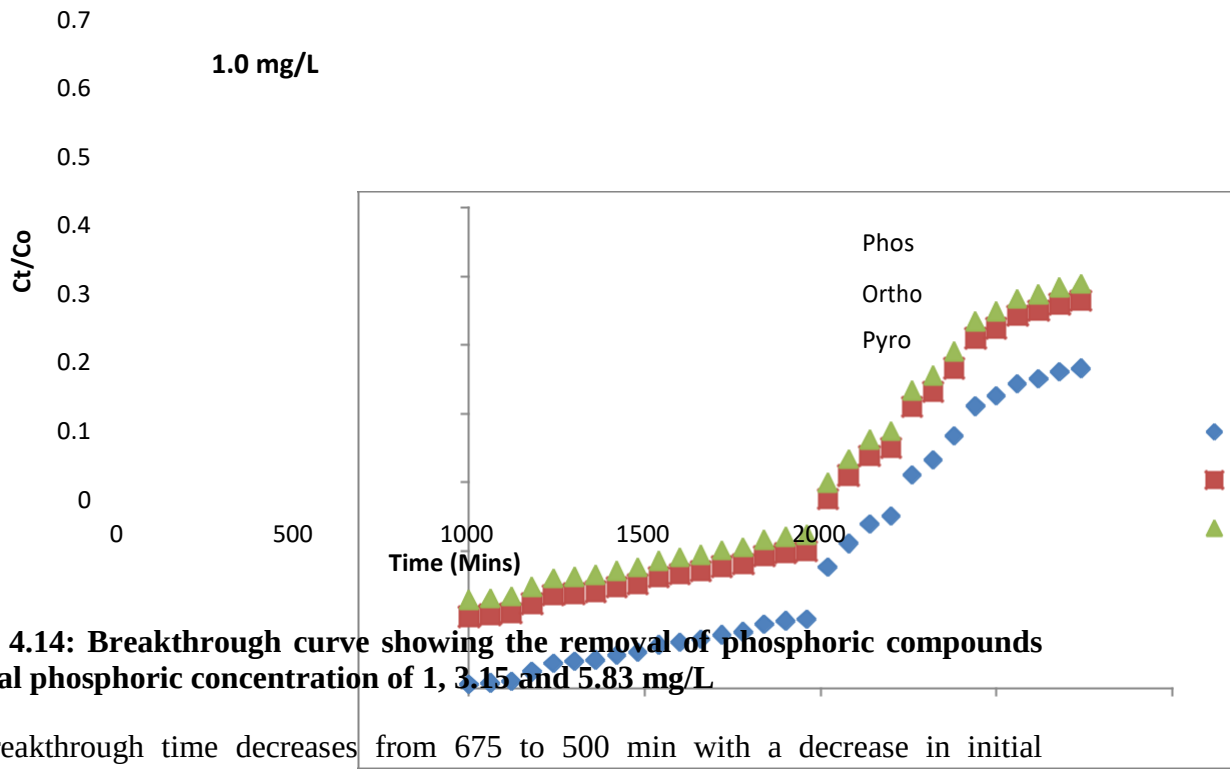

Figure 4.14: Breakthrough curve showing the removal of phosphoric compounds at initial phosphoric concentration of 1, 3.15 and 5.83 mg/L

The breakthrough time decreases from 675 to 500 min with a decrease in initial concentration of phosphoric compounds which is due to a larger mass transfer coefficient. The presence of more phosphates ions provided an increased competition for the lesser available biding sites on the adsorbent (Singh *et al.*, 2015). Therefore it is concluded that the adsorption process is concentration dependent.

When the concentration was reduced, the break through time increased from 0 – 367 minutes and the exhaustion time increased from 1560- 1777.8 minutes.

4.4 Evaluation of the column performance

Table 4.7: Column data parameter obtained on sorption characteristics of maize tassel immobilized in PVA at varying bed height

Bed height(cm)	t_{total} (mins)	V_{eff} (ml)	m_{total} (mg)	q_{total} (mg)	% Removal
Phosphorus					
2	1260	10,080	20.16	13.91	69
4	1380	11,040	22.08	16.56	75
6	2500	20,000	41.44	37.296	90
Orthophosphates					
2	1260	10,080	61.79	33.98	55
4	1380	11,040	67.67	46	68
6	2500	20,000	127	104	82
Pyrophosphates					
2	1260	10,080	113	73.45	65
4	1380	11,040	123.97	89.26	72
6	2500	20,000	233	213.7	91.7

The following parameters volume of the effluent treated (V_{eff}), maximum adsorption capacity (q_{total}), the total phosphoric compounds sent to the column (m_{total}) and the percentage removal of phosphoric compounds were calculated with Equation 2.1, 2.2, 2.3 and 2.4 respectively.

From Table 4.7, the following results were obtained for phosphoric compounds adsorption: the total phosphorus sent to the column at a bed height of 2 cm was 20.16 mg out of which 13.91 mg was adsorbed; at bed height of 4 cm, total phosphorus sent was 22.08 mg and 16.56 mg was absorbed, while at a bed height of 6 cm, total phosphorus sent was 41.44 mg and 37.296 mg was adsorbed. The percentage removal of phosphorus at a height of 6 cm was higher (69 %) than the percentage removal at 4 and 2 cm which was 75 and 69 % respectively. This applies also for orthophosphates and pyrophosphates. The increase is as a result of increase in the amount of sorbent in the column which provided more binding sites for the phosphoric compounds.

Table 4.8: Column data parameter obtained on sorption characteristics of maize tassel immobilized in PVA at varying flow rates

Flow-rate (ml/min)	t_{total} (mins)	V_{eff} (ml)	m_{total} (mg)	q_{total} (mg)	% Removal
Phosphorus					
4	2460	9,840	19.68	18	92
8	1380	11,040	22.08	16.34	74
12	1200	14,400	28.8	15.84	55

Orthophosphates					
4	2460	9,840	60	58	97
8	1380	11,040	67.67	51.43	76
12	1200	14,400	88.27	42.37	48
Pyrophosphates					
4	2460	9,840	111	97.37	91
8	1380	11,040	123.97	57.03	46
12	1200	14,400	162	56.7	35

From Table 4.8, the amount of phosphoric compound adsorbed and percentage removal decreased with increase in flow rate. This is obvious in the results given in table 4.7. For phosphorus adsorption, there is a decrease in the amount adsorbed from 18 to 15.84 mg as the flow rate increased from 4 to 12 ml/min which led to the reduction of the percentage removal from 92 % at 4 ml/min to 55 % at 12 ml/min. The percentage removal of orthophosphates and pyrophosphates reduced also from (97-48 %) and (91-35 %) respectively as the flow rate reduced. This is because at high flow rates, the contact time gets shorter; thereby leading to the active sites of the phosphoric compounds not reaching full saturation and leads to a decrease in the amount of phosphoric compounds adsorbed (Chen *et al*., 2012).

Table 4.9: Column data parameter obtained on sorption characteristics of maize tassel immobilized in PVA at varying initial concentration

Initial concentration (mg/L)	t_{total} (mins)	V_{eff} (ml)	m_{total} (mg)	q_{total} (mg)	% Removal
Phosphorus					
2	1260	10,080	20	14.8	74
1.5	1500	12,000	18	14.94	83
1	1680	13,440	13.44	13.04	97
Orthophosphates					
6.13	1260	10,080	61.8	46.96	76
4.8	1500	12,000	57.6	50.11	87
3.15	1680	13,440	42.3	39.34	93
Pyrophosphates					
11.23	1260	10,080	113	51.98	46
8.9	1500	12,000	107	73.83	69
5.83	1680	13,440	78.4	63.5	81

In the same way, from Table 4.8, the percentage removal of phosphoric compounds increased while the influent concentration decreased. The percentage removal of

phosphorus increased from 74-97 % when there was a reduction in the influent concentration from 2-1 mg/L. The percentage removal of orthophosphates and pyrophosphates increased from (76-93 %) and (46-81 %) when there was a reduction in the influent concentration from (6.13-3.15 mg/L) and (11.23-5.83 mg/L) respectively. This could be due to the longer service time of the column as the phosphoric compounds concentration decreases.

4.5 Analysis of Fixed Bed Models

4.5.1 Clark Model

This model is based on Freundlich isotherm model where Freundlich constant n=2.06 is used for the calculation of Clark model parameters A and r (min^{-1}) (Singh *et al.,* 2015).

4.5.1.1 Effect of bed height on Clark model

Table 4.10: Clark model constants at different bed heights of 2-6 cm and flow rate of 8 ml/min and initial concentration of phosphoric compounds

Phosphoric compounds	**A**	**r (L/min)**	**R^2**
2 cm			
Phosphorus	39.67	0.0056	0.9498
Orthophosphates	7.613	0.0033	0.5498
Pyrophosphates	5.698	0.0026	0.5354
4 cm			
Phosphorus	54.57	0.0052	0.9567

Orthophosphates	4.052	0.002	0.4009
Pyrophosphates	3.395	0.0017	0.3551
6 cm			
Phosphorus	92.85	0.0029	0.975
Orthophosphates	10.858	0.0018	0.5394
Pyrophosphates	-0.00016	-5919	0.558

As can be seen from the table above the R^2 values using Clark model for the removal of phosphorus increased from 0.9498-0.975. It shows that at an increase in bed height the removal efficiency of phosphoric compounds increases. The increase in bed height shows a great increment in the rate constant and constant A for phosphorus while for the phosphoric compounds, an increase in bed height gave a resultant increase in constant A.

4.5.1.2 Effect of flow rate on Clark model

Table 4.11: Clark model constants at different flow rate of 4-12 ml/min and bed height of 4 cm and initial concentration of phosphoric compounds

Phosphoric compounds	A	r (L/min)	R^2
4 ml/min			
Phosphorus	86.84	0.0027	0.9746
Orthophosphates	10.887	0.0018	0.6242
Pyrophosphates	8.321	0.0009	0.9648
8 ml/min			
Phosphorus	54.57	0.0052	0.9567
Orthophosphates	4.052	0.002	0.4009
Pyrophosphates	3.395	0.0017	0.3551
12 ml/min			
Phosphorus	31.81	0.0052	0.9479
Orthophosphates	4.84	0.0025	0.4781
Pyrophosphates	3.5194	0.00197	0.4456

The decrease in flow rate from 12-4 ml/min brought about an increase in R^2 value from 0.9479-0.9746 (Phosphorus), 0.4009-0.6242 (Orthophosphates) and 0.3551-0.9648

(Pyrophosphates). It shows that Clark model is viable at a low flow rate for the removal of phosphoric compounds.

As the flow rates increases, the rate constant increased and also the R^2 values decreased for the phosphoric compounds.

4.5.1.3 Effect of initial concentration on Clark model

Table 4.12: Clark model constants at different initial concentration of phosphoric compounds with flow rate of 8 ml/min and bed height of 4 cm

Phosphoric compounds	A	r (L/min)	R^2
Phosphorus (2 mg/L)	54.57	0.0052	0.9567
Orthophosphates (6.13 mg/L)	4.052	0.002	0.4009
Pyrophosphates (11.23 mg/L)	3.395	0.0017	0.3551
Phosphorus (1.5 mg/L)	199.437	0.0051	0.912
Orthophosphates (4.8 mg/L)	19.12	0.0025	0.8928
Pyrophosphates (8.9 mg/L)	15.48	0.0025	0.877
Phosphorus (1 mg/L)	108	0.0028	0.9547
Orthophosphates (3 mg/L)	13	0.0016	0.9477
Pyrophosphates (6 mg/L)	10.31	0.0015	0.9403

A reduction in the concentration of the surface water brought about a resultant decrease in the R^2 values, rate constant and A.

4.5.2 Thomas Model

4.5.2.1 Effect of bed height on Thomas model

Table 4.13: Thomas parameters at different bed heights of 2-6 cm, Flow rate 8ml/min and Initial concentration of the phosphoric compounds

Phosphoric compounds	K_{th} (——)	Q_o (mg/g)	R^2
2 cm			
Phosphorus	-1669	0.0028	0.95
Orthophosphates	-0.00052	-4604.151	0.5295
Pyrophosphates	-0.00022	-9213	0.5084
4 cm			
Phosphorus	0.00255	947.2	0.9578
Orthophosphates	-0.000169	-4744.998	0.3761
Pyrophosphates	0.000142	-4866.979	0.3274
6 cm			
Phosphorus	-0.0014	-1301	0.974
Orthophosphates	-0.00029	-3265.5	0.5228
Pyrophosphates	-0.00022	-3941	0.5149

The R^2 value using Thomas model for the removal of phosphorus increased from 0.95-0.974 (phosphorus), 0.5228-0.6083 (Orthophosphates) and 0.5084-0.5509. It shows that at an increase in bed height the removal efficiency of phosphoric compounds is high.

4.5.2.2 Effect of flow rate

Table 4.14: Thomas parameters at different flow rates of 4-8ml/min, bed height of 4 cm and Initial concentration of the phosphoric compounds

Phosphoric compounds	K_{th} (——)	Q_o (mg/g)	R^2
4 ml/min			
Phosphorus		-0.0003895	0.9735
Orthophosphates	0.3656	-0.00148	0.6083
Pyrophosphates	0.1817	-0.00262	0.5509
8 ml/min			
Phosphorus	0.00255	947.2	0.9578
Orthophosphates	-0.000169	-4744.998	0.3761
Pyrophosphates	0.000142	-4866.979	0.3274
12 ml/min			
Phosphorus	-0.00255	-1227.973	0.9495
Orthophosphates	0.000004	-34276	0.4536
Pyrophosphates	-0.00016	-6694.64	0.4139

The R^2 value using Thomas model for the removal of phosphoric compounds decreased from 0.9735-0.9495 (phosphorus), 0.6083-0.4536 (Orthophosphates) and 0.5509-0.4139 (Pyrophosphates) with increase in flow rate from 4 – 12 ml/min.

4.5.2.3 Effect of initial concentration

Table 4.15: Thomas parameters at different initial concentration of phosphoric compounds with flow rates of 8ml/min and bed height of 4 cm

Phosphoric compounds	K_{th} (——)	Q_o (mg/g)	R^2
Phosphorus (2 mg/ L)	0.00255	947.2	0.9578
Orthophosphates (6.13 mg/L)	-0.000169	-4744.998	0.3761
Pyrophosphates (11.23 mg/L)	0.000142	-4866.979	0.3274
Phosphorus (1.5 mg/L)	-981.6	-0.00327	0.9064
Orthophosphates (4.8 mg/L)	-0.00052	-3410	0.8902
Pyrophosphates (8.9 mg/L)	-0.000269	-6117.66	0.8745
Phosphorus (1 mg/L)	-0.0027	-1101.21	0.9562
Orthophosphates (3 mg/L)	-0.0005	-3258	0.9467
Pyrophosphates (6 mg/L)	-0.00023	-6043	0.9393

A reduction in the concentration of the adsorbate gave a decrease in R^2 values for orthophosphates and pyrophosphates with the following values 0.6083-0.9467 and

0.5509-0.9393 respectively while a decrease in concentration of phosphorus brought about a decrease in R^2 value from 0.9735- 0.9562.

4.6 Comparison of the Experimental Data and the Applied Models

The Thomas model adequately predicted the experimental data better than the Clarks model when considering phosphorus ranging from 0.9064-0.974, while for orthophosphates and pyrophosphates (0.3761-0.9467) and (0.3274-0.9393) respectively. The adsorption capacities were moderately high at increased bed heights, increase in flow rate brought about a decrease in the correlation coefficient which were both similar to the experimental data but there was a difference between the experimental data and the Thomas model while varying initial concentration. The kinetic (kTh) constant decreases with increase in flow rate from 4 ml/min to 12 ml/min with values ranging from (2.119-0.00255 ml mg/min) for phosphorus which implies that breakthrough curve is favourable at lower flow rate.

For the Clark model, the correlation coefficient of the phosphoric compounds ranges from (0.3551-0.972). The Clark constant increased with increased in bed height with values (39.67-92.85) and had a reduction with values (86.84-31.81) when the flow rate was increased. These results to increase in the values of correlation coefficient from (0.9498-0.975) when considering increase in bed height and decrease in correlation coefficient (0.9746-0.9479) when considering increase in flow rate. This is similar to the experimental data gotten for the removal of phosphorus.

CHAPTER FIVE

5.0 CONCLUSION AND RECOMMENDATIONS

5.1 Conclusion

The results from this study have shown the removal efficiency of the adsorbent and it was successful shown on the breakthrough curves gotten after column sorption process. The application of the adsorbent reveals the extent of removal based on the time it got its breakthrough by getting to the permissible limit. The following deductions were gotten from this study;

Maize tassel immobilized in polyvinyl alcohol was obtained at a temperature of 80 ºC and left to cool.

The concentration of phosphoric compounds after adsorption was characterized with the aid of a UV-Vis spectrophotometer.

The maize tassel immobilized in PVA was characterized before and after adsorption with FT-IR, SEM-EDX and BET surface analyser. The FT-IR shows the functional group responsible for the adsorption of phosphoric compounds which is the hydroxyl group.

The column studies showed that increase in bed height, flow rates and inlet concentrations had a significant effect on the breakthrough time and exhaustion time.

The Thomas Model was found to predict the breakthrough of the phosphoric compounds better than the Clark model with R^2 value of 97.5 % for bed heights and flow rates.

5.2 Recommendations

These following recommendations could be executed with further research;

1. XRF and XRD should be carried out on the maize tassel immobilized in PVA to check its oxides composition and its crystallinity.

2. Further research should be carried out on the use of the adsorbent to treat Industrial effluents

3. Other models should be used to determine the column efficiency using the same adsorbent materials.

REFERENCES

American Public Health Association (APHA). (2017). Standard methods for the examination of water and wastewater, American Water Works Association (AWWA), Water Environment Federation(WEF), ISBN: 9870875532875.

Arias, M., Silva-Carballal, J.D., Garcia-Rio, L., Mejuto, J and Nunez, A. (2006). Retention of Phosphorus by Iron and Aluminum-Oxides-Coated Quartz Particles. *Journal of Colloid and Interface Science,* 295 (1), 65-70. Retrieved from https://doi.org/10.1016/j.jcis.2005.08.001

Agyei, N.M., Shofolahan, A.M and Okonkwo, J.O (2016). Utilization of Chemically Activated Maize Tassel for Remediation of Eutrophic Phosphorus. *Fresenius Environmental Bulletin*, 2514. Retrieved from https://scholar.google.com/32FEB_15_420

Aslam, M., Kalyar, M.A and Raza, Z.A (2018). Polyvinyl Alcohol: A Review of Research Status and use of Polyvinyl Alcohol Based Nano-composites. Polymer Engineering and Science, 58 (12), 2119- 2132. Retrieved from https://doi.org/10.1002/pen.24855

Bakatula, E., Richard, D and Neculita, C. (2018). Determination of point of zero charge of natural organic materials. *Environmental Science and Pollution Research*, 25 (8), 7823-7833. Doi:10.1007/s11356-017-1115-7

Bhatnagar, .A and Sillanpaa, .M (2010). Utilization of Agro-industrial and Municipal Waste Materials as Potential Adsorbents for Water Treatment: A Review. *Chemical Engineering Journal*, 157 (2-3), 277-296. Retrieved from https://doi.org/10.1016/j.cej.2010.01.007

Birbas, D. (2011). *Preparation of Activated Carbon: Forest residues activated with Phosphoric Acid and Zinc Sulfate* (Master's thesis, Department of Chemical Engineering Royal Institute of Technology (KTH) Stockholm, Sweden).

Boparai, H.K., Joseph, M and O'Carroll, D.M. (2013). Cadmium Removal by Nano Zerovalent Iron: Surface Analysis, Effects of Solution Chemistry and Surface Complexation Modelling. *Environmental Science and Pollution Research*, 20 (9), 6210-6221. Doi: 10.1007/s11356-013-1651-8

Capodaglio, A.G., Daneshgar, S., Callegari, A and Vaccari, .D (2018). The Potential Phosphorus Crisis: Resource Conservation and Possible Escape Technologies: A Review. *Resources,* 7 (2), 37. Retrieved from https://doi.org/10.3390/resources7020037

Christopher, A.T and Wayne, E.M (2002). Copper Ion Removal by Almond Shell Carbons And Commercial Carbons: Batch And Column Studies. *Separation Science and Technology*, 37 (10), 2369-2383. Retrieved from https://doi.org/10.1081/SS-120003518

Chu, K. H and Hashim, M.A (2006). Copper bio-sorption on immobilized seaweed biomass: Column breakthrough characteristics. *Journal of Environmental Sciences*, *21* (4) 295-306. doi.10.1002/1521-3846(200111)21:43.0.CO;2-F

Demirbas, A. (2008). Heavy Metal Adsorption onto Agro-Based Waste Materials: A Review. *Journal of Hazardous Materials,* 157 (2-3), 220-229. Retrieved from https://doi.org/10.1016/j.jhazmat.2008.01.024

Duangpapeng, P., Ketthaisong, D., Lomthaisong, K., Lertrat, K., Scott, M.P and Suriharn, B. (2018). Corn Tassel: A New Source of Phytochemicals and Antioxidant Potential for Value-Added Product Development in the Agro-Industry. *Agronomy*, *8* (11), 1-9. Retrieved from https://doi.org/10.3390/agronomy8110242

Edgar, J. K and Pawar, S.N (2012). Alginate Derivatization: A Review of Chemistry, Properties and Applications. *Biomaterials*, 33, 3279-3305. doi:10.1016/j.biomaterials.2012.01.007

Ekpete, O. A and Marcus, A. C. (2017). Preparation and Characterization of Activated Carbon Obtained from Plantain (Musa paradisiaca) Fruit Stem. *Journal of Chemistry*, 1-6. Retrieved from https://doi.org/10.1155/2017/8635615.

Ekpete, O. A and Horsfall, M. (2011). Preparation and Characterization of Activated Carbon Derived from Fluted Pumpkin Stem Waste (Telfairia occidentalis Hook F). *Research Journal of Chemical Sciences,* 1(3), 10-17. Retrieved from https://www.isca.in

Eljamal, O., Okawauchi, J., Hiramatsu, K and Harada, M. (2013). Phosphorus Sorption From Aqueous Solution Using Natural Materials. *Environmental Earth Sciences,* 68, 859–863. DOI 10.1007/s12665-012-1789-6

Fadhil, A and Deyab, M. (2008). Conversion of Some Fruit Stones and Shells Into Activated Carbons. *Arabian Journal for Science and Engineering*, 33 (2A), 175-184. Retrieved from https://inis.iaea.org/search/search.aspx?orig_q=RN:41045160

Farooq, U., Kozinski, J.A., Khan, M.A and Athar, M. (2010). Bio-sorption of heavy metal ions using wheat based bio-sorbents: A review of the recent literature. *Bio-resource Technology*, 101 (14), 5043-5053. doi:10.1016/j.biortech.2010.02.030.

Filippelli, G.M (2010). Bio-geochemistry: Phosphorus and The Gust of Fresh Air. *Nature*, 467 (7319), 1052. Doi:10.1038/4671052a

Food and Agriculture Organization Corporate Statistical Database (2014). *Maize, rice, wheat farming must become more sustainable.* Retrieved from https://fao.org/news/story/en/item/273303/icode

Gautam, R. K., Banerjee, S., Gautam, P. K., and Chattopadhyaya, M. (2014). Remediation Technology for Phosphate Removal from Waste Water: An Overview. *Advances in Environmental Research*, *36*: 1-23. Retrieved from https://www.researchgate.net/publication/268046263

Ghulam, S.S., Altaf, A.S., Muhammad, M.B and Pirah, S. (2018). Evaluation of Surface Water Quality Index and the Synthetic Pollution Index: A Case Study of Indus Delta Region of Pakistan. *Desalination and Water Treatment,*118, 39-48. Doi:10.5004/dwt.2018.22407

Goertzen, S.L., Theriault, K.D., Oickle, A.M., Tarasuk, A.C and Andreas, H.A. (2010). Standardization of the Boehm Titration. Part I. CO_2 Expulsion and End Point Determination. *Carbon*, 48 (4), 1252-1261. Retrieved from https://doi.org/10.1016/j.carbon.2009.11.050

Guo, X., Liang, S., Feng, N and Tian, Q. (2009). Adsorption of Cu^{2+} and Cd^{2+} from aqueous solution by mercapto-acetic acid modified orange peel. *Colloids and Surfaces B: Bio-interfaces , 73* (1) 10–14. Retrieved from https://doi.org/10.1016/j.colsurfb.2009.04.021

Han, R., Wang, Y., Zhao, X., Wang, Y., Xie, F., Cheng, J and Tang, M. (2009). Adsorption of methylene blue by phoenix tree leaf powder in a fixed-bed column: Experiments and Prediction of Breakthrough Curves. *Desalination,* 245(1-3), 284–297. Retrieved from https://doi.org/10.1016/j.desal.2008.07.013

Hashem, M.A (2007). Adsorption of lead ions from aqueous solution by okra wastes. *International Journal of Physical Sciences, 2* (7) 178-184. Retrieved from http://www.academicjournals.org/IJPS

Inoue, K., Biswas, K.B., Ghimire, K.N., Ohta, S., Harada, H., Ohto, K and Kawakita, H. (2007). The Adsorption of Phosphate from an Aquatic Environment Using Metal-Loaded Orange Waste. *Journal of Colloid and Interface Science*, 312 (2), 214-223. Retrieved from https://doi.org/10.1016/j.jcis.2007.03.072.

I.R Spectrum table and chart. (n.d). Retrieved from https://www.sigmaaldrich.com/technical-documents/articles/biology/ir-spectrum-table.html

International Institute of Tropical Agriculture (2017). *Maize production.* Retrieved from https://www.iita.org/cropsnew/maize

Ismadji, S., Ismanto, A and Wang, S. S. (2010). Preparation of Capacitor's Electrode from Cassava Peel Waste. *Bio-resource Technology*, 101 (10), 3534–3540.

Jang, J and Lee, D.S (2016). Enhanced Adsorption of Cesium on PVA-Alginate Encapsulated Prussian Blue-Graphene Oxide Hydrogel Beads in a Fixed-Bed Column System. *Bio-resource Technology*, 218, 294-300. Retrieved from https://doi.org/10.1016/j.biortech.2016.06.100

Jarvie, H.P., Withers, J.A and Neal, C. (2002). Review of Robust Measurement of Phosphorus in River Water: Sampling, Storage, Fractionation and Sensitivity. *Hydrology and Earth System Sciences*, 6 (1), 113-131. Retrieved from https://doi.org/10.5194/hess-6-113-2002

Jha, K.V., Kameshima, Y., Nakajima, A and Okada, K. (2008). Utilization of Steel Making Slag for the Uptake of Ammonium and Phosphate Ions from Aqueous Solution. *Journal of Hazardous Materials*, 156 (1-3), 156-162. Retrieved from https://doi.org/10.1016/j.jhazmat.2007.12.009

Jin, Y., Qu, J., Song, T., Liang, J., Bai, X., Wei, Y., Huang, S and Dong, L. (2019). Adsorption Of Lead (Ⅱ) From Aqueous Solution By Modified Auricularia Matrix Waste: A Fixed-Bed Column Study. *Ecotoxicology and Environmental Safety*, 169, 722−729. Retrieved from https://doi.org/10.1016/j.ecoenv.2018.11.085.

Kahn, M.N and Wahab, M.F. (2007). Characterization of Chemically Modified Corncobs and its Application In The Removal Of Metal Ions From Aqueous Solution. *Journal of Hazardous materials*, *141* (1) 237- 244. Retrieved from https://doi.org/10.1016/j.jhazmat.2006.06.119

Klemm, D., Heublein, B and Fink, H. B. (2005). Cellulose: Fascinating Biopolymer and Sustainable Raw Material. *Polymer Science*, 3359-3393 doi: 10.1002/anie.200460587.

Kose, T.E and Kivanc, B. (2011). Adsorption of Phosphate from Aqueous Solutions Using Calcined Waste Egg Shell. *Chemical Engineering Journal*, 178 (15), 34-39. Retrieved from https://doi.org/10.1016/j.cej.2011.09.129

Krishnani, K.K., Xiaoguang, M., Christodoulatos, C and Boddu, V.M. (2007). Bio-sorption mechanism of Nine Different Heavy Metals Onto Bio-matrix From Rice husk. *Journal of harzardous materials, 153* (3) 1222- 1234. Retrieved from https://doi.org/10.1016/j.jhazmat.2007.09.113

Li, Y., Zhang, Y., Li, X., Yang, L., Bai, X., Ye, Z., Zhou, L and Wang, L. (2010).Selective Removal for Pb^{2+} in Aqueous Environment by Using Novel Macroreticular PVA Beads. *Journal of Hazardous Materials*, 181 (1-3), 898-907. Retrieved from https://doi.org/10.1016/j.jhazmat.2010.05.097

Li, H., Ru, J., Yin, W., Liu, X., Wang, J and Zhang, W. (2009). Removal of Phosphate from Polluted Water by Lanthanum Doped Vesuvianite. *Journal of Hazardous Materials*, 168 (1), 326-330. Retrieved from https://doi.org/10.1016/j.jhazmat.2009.02.025

Maepa, C. E., Jayaramudu, J., Okonkwo, J. O., Ray, S. S and Sadiku, E. R. (2015). Extraction and Characterization of Natural Cellulose Fibers from Maize Tassel. *International Journal of Polymer Analysis and characterization,* 20 (2), 99-109. Retrieved from https://doi.org/10.1080/1023666X.2014.961118

Mambaa, B., Olorundare, O., Krause, R and Okonkwo, J. (2012). Potential Application of Activated Carbon from Maize Tassel for the Removal of Heavy Metals In Water. *Physics and Chemistry of the Earth,* 50, 104–110. Retrieved from https://doi.org/10.1016/j.pce.2012.06.001

Markou, G., Mitrogiannis, D., Muylaert, K., Celekli, A and Bozkurt, H., (2016). *Journal of Environmental Sciences,* 45, 49-49. Retrieved from https://dx.doi.org/10.1016/j.jes2015.12.009

Moyo, M and Okonkwo, J. O. (2013). Horseradish Peroxidase Biosensor Based On Maize Tassel–Mwcntscomposite For Cadmium Detection. *Sensors and Actuators B,* 193, 515– 521. Retrieved from http://dx.doi.org/10.1016/j.snb.2013.11.086

Moyo, M., Okonkwo, J. O and Agyei, N. (2014). Maize Tassel-Modified Carbon Paste Electrode for Volta metric Determination of Copper (II*). Environmental Monitoring and Assessment,* 186 (8) 4807–4817. Retrieved from https://doi.org/10.1007/s10661-014-3739-0

Mwangi, I.W., Ngila, J.C and Okonkwo, J.O (2011). A Comparative Study Of Modified And Unmodified Maize Tassels For Removal Of Selected Trace Metals In Contaminated Water. *Toxicological and Environmental Chemistry,* 94, 20-39. Retrieved from https://doi.org/10.1080/02772248.2011.638636

Nasiruddin, K. M and Wahab, F. M. (2007). Characterization Of Chemically Modified Corncobs And Its Application In The Removal Of Metal Ions From Aqueous Solution. *Journal of Hazardous Materials*, 141, 237–244.

Nazarian, R. (2017). *Advanced phosphate removal in dialysis employing lanthanum impregnated activated carbon fixed bed column* (Master's Thesis, The University of Cincinnati, United States). Retrieved from http://orcid.org/0000-0001-5216-4857

Nehrenheim, E and Gustafsson, J. (2008). Kinetic Sorption Modelling of Cu, Ni, Zn, Pb and Cr ions to Pine Bark and Blast Furnace Slag by Using Batch Experiments. *Bio-resource Technology,* 99(6), 1571. Doi:10.1016/j.biortech.2007.04.017

Ngila, J., Mwangi, I and Okonkwo, J. (2012). A comparative study of modified and unmodified maize tassels for removal of selected trace metals in contaminated water. Toxicological & Environmental Chemistry, 94(1), 20–39. Retrieved from http://dx.doi.org/10.1016/j.jenvman.2013.12.031

Nguyen, N.T (2015). *Adsorption Of Phosphorus From Wastewater Onto Biochar: Batch And Fixed-bed Column Studies.* (Bachelor of Engineering, Helsinki Metropolia University of Applied Sciences). Retrieved from https://pdfs.semanticscholarlar.org

Odysseas. (2016). Fixed Bed Column Studies In Laboratory And Pilot Scale For Methylene Blue Removal And Recovery By Untreated, Auto-hydrolized And Brine Hydrolized Spruce. *Journal of Environmental Science and Engineering*, 5, 489-497. Doi:10.17265/2162-5298/2016.10.001

Oguz, E. (2004). Removal of Phosphate from Aqueous Solution with Blast Furnace Slag. *Journal of Harzardous Materials*, 114(1-3), 131-137.Retrieved from https://doi.org/10.1016/j.jhazmat.2004.07.010

Oladipo, A.A and Gazi, M. (2014). Fixed-Bed Column Sorption of Borate onto Pomegranate Seed Powder-PVA Beads: A Response Surface Methodology Approach. *Toxicology and Environmental Chemistry*, 96 (6), 837-848. Retrieved from https://doi.org/10.1080/02772248.2014.989854

Olorundare, O., Msagatia, T., Krauseb, R., Okonkwo, J and Mambaa, B. (2014). Steam Activation, Characterisation And Adsorption Studies Of Activated Carbon From Maize Tassels. *Chemistry and Ecology*, 30 (5), 473–490. Retrieved from https://doi.org/10.1080/02757540.2013.877001

Onwuka, G. (2005). Food Analysis and Instrumentation Theory and Practice. Umuahia, Nigeria: Naphthali Prints A Division of HG Support Nigeria Limited No 6 Adeniyi Jones Close Surulere, Lagos, Nigeria.

Pagnanellia, F., Toro, L and Veglio, F. (2002). Olive Mill Solid Residues as Heavy Metal Sorbent Material: A Preliminary Study. *Waste Management*, 22 (8), 901–907. Retrieved from https://doi.org/10.1016/S0956-053X(02)00086-7

Paripurnanda, .L., Saravanamuthu, V., Jaya, K and Nanthi, S.B. (2014). Removal and Recovery of Phosphate from Water Using Sorption. *Critical Reviews in Environmental Science and Technology*, 44 (8), 847-907. Retrieved from http://dx.doi.org/10.1080/10643389.2012.741311

Patel, H. (2019). Fixed-bed Column Adsorption Study: A Comprehensive Review. *Applied Water Science*, 9 (3), 45. Retrieved from https://link.springer.com/article/10.1007/s13201-019-0927-7

Qu, F., Tang, X., Ding, A., Jia, R., Chang, H., Cheng, X., Liu, B., Li, G and Liang, H. (2016). Effect Of Operation Parameters On The Flux Of Stabilization Of Gravity-Driven Membrane (GDM) Filtration System For Decentralized Water Supply. *Environmental Science and pollution Research, 23* (16), 16771-16780. Retrieved from https://link.springer.com/article/10.1007/s11356-016-6857-0

Sasaki, K and Koilraj, P. (2017). Selective Removal of Phosphate Using La-Porous Carbon Composites from Aqueous Solutions: Batch and Column Studies. *Chemical Engineering Journal,* Retrieved from http://dx.doi.org/10.1016/j.cej.2017.02.075.

Sekhula, M. M., Okonkwo, J. O., Zvinowanda, C. M., Agyei, N. N and Chaudhary, A. J. (2012). Fixed bed Column Adsorption of Cu (II) onto Maize Tassel-PVA Beads. *Chemical Engineering and Process Technology,* 3 (2) 1-5. Retrieved from https://dx.doi.org/10.4172/2157-7048.1000131

Sibrell, P. L and Tucker, W.T. (2012). Fixed Bed Sorption of Phosphorus from Wastewater Using Iron Oxide-Based Media Derived from Acid Mine Drainage. *Water Air Soil Pollution,* 223, 5105–5117. DOI 10.1007/s11270-012-1262-x

Sibrell, P. L., Montgomery, G. A., Ritenour, K. L and Tucker, T.W. (2009). Removal Of Phosphorus From Agricultural Wastewaters Using Adsorption Media Prepared From Acid Mine Drainage Sludge. *Water research,* 43, 2240 – 2250. doi:10.1016/j.watres.2009.02.010

Sillerova, H., Komarek, M., Chrastny, V., Novak, M., Vanek, A and Drabek, O. (2013). Brewers Draff as a New Low-Cost Sorbent for Chromium (VI): Comparison with other Bio-sorbents. *Journal of Colloid and Interface Science,* 396, 227-233. Retrieved from https://doi.org/10.1016/j.jcis.2013.01.029

Singh, S. K., Katoria, D., Mehta, D and Sehgal, D. (2015). Fixed Bed Column Study And Adsorption Modelling On The Adsorption Of Malachite Green Dye From Wastewater Using Acid Activated Sawdust. *International Journal of Advanced Research*, 3(7), 521-529. Retrieved from https://www.researchgate.net/publication/280610841

Soleimani, M and Kaghazchi, T. (2008). Adsorption of Gold Ions From Industrial Wastewater Using Activated Carbon Derived From Hard Shell Of Apricot Stones – An Agricultural Waste. Bio-resource Technology, 99 (13), 5374- 5383. Retrieved from https://doi.org/10.1016/j.biortech.2007.11.021

Unuabonah, E.I., Olu-Owolabi, B.I., Fasuyi, E.I and Adebowale, K.O. (2010) Modelling Of Fixed-Bed Column Studies for the Adsorption of Cadmium onto Novel Polymer–Clay Composite Adsorbent. *Journal of Hazardous Materials,* 179 (1-3), 415-423. Retrieved from https://doi.org/10.1016/j.jhazmat.2010.03.020

Viswanathan, T., Ramasahayam, S. K., Guzman, L and Gunawan, G. (2014). A Comprehensive Review of Phosphorus. *Journal of Macromolecular Science, Part A:Pure and Applied Chemistry,* (51) 538–545. doi: 10.1080/10601325.2014.906271

Wang, L and Lin, C. (2008). Adsorption Of Lead(II)Ion From Aqueous Solution Using Rice Hull Ash. *Industrial Engineering chemistry Research,* (47), 4891-4897. doi:10.1021/ie071521z

Worsfold, P., McKelvie, I and Monbet, P. (2016). Determination of Phosphorus in Natural Waters: A Historical Review. *Analytica Chimica Acta, 918, 8-20.* Retrieved from https:doi.org/10.1016/j.aca.2016.02.047

Yagub, M., Sen, T. K., Afroze, S and Ang, H. (2015). Fixed-Bed Dynamic Column Adsorption Study Of Methylene Blue (MB) Onto Pine Cone. *Desalination and Water Treatment,* 55, 1026–1039. Retrieved from http://www.tandfonline.com/loi/tdwt20

Yahya, M.D and Odigure, J.O (2015). Fixed Bed Column Study for Pb(II) Adsorption Using Calcium-Alginate Treated Shea Butter Husk (TSBH). Proceedings of the 2015 International Conference on Industrial Engineering and Operations Management
Dubai, United Arab Emirates (UAE). Doi: 10.1109/IEOM.2015.7093936

Zhang, Y., Li, Y., Yang, L., Ma, X., Wang, L and Ye, Z. (2010). Characterization and Adsorption Mechanism of Zn^{2+} Removal by PVA/EDTA Resin in Polluted Water. *Journal of Hazardous Materials,* 178 (1-3), 1046-1054. Retrieved from https://doi.org/10.1016/j.jhazmat.2010.02.046

Zhu, C., Wang, L and Chen, W. (2009). Removal of Cu (II) From Aqueous Solution by Agricultural By-Product: Peanut Hull. *Journal of Hazardous Materials,* 168 (2-3), 739-746. Retrieved from https://doi.org/10.1016/j.jhazmat.2009.02.085

Zia, K., Zia, F and Zuber, M. R. (2015). Alginate Based Polyurethanes: A Review of recent advances and Perspective. *International Journal of Biological Macromolecules,* 1-46 http://dx.doi.org/doi:10.1016/j.ijbiomac.2015.04.076.

Zvinowanda, C. M., Okonkwo, J. O., Sekhulaa, M. M., Agyei, N. M and Sadiku, R. (2009). Application of maize tassel for the removal of Pb, Se, Sr, U and V from borehole water contaminated with mine wastewater in the presence of alkaline metals. *Journal of Hazardous Materials,* (164), 884–891. doi:10.1016/j.jhazmat.2008.08.110

Zvinowanda, C., Okonkwo, J., Agyei, N and Shabalala, P.N. (2008). Physiochemical Characterization of Maize Tassel as an Adsorbent. I. Surface Texture, Microstructure and Thermal Stability. *Journal of Applied Polymer Science,* (111), 1923–1930. Retrieved from http://www.interscience.wiley.com/

APPENDICIES

6.1 Effect of bed height using Clarks Model

For 2 cm

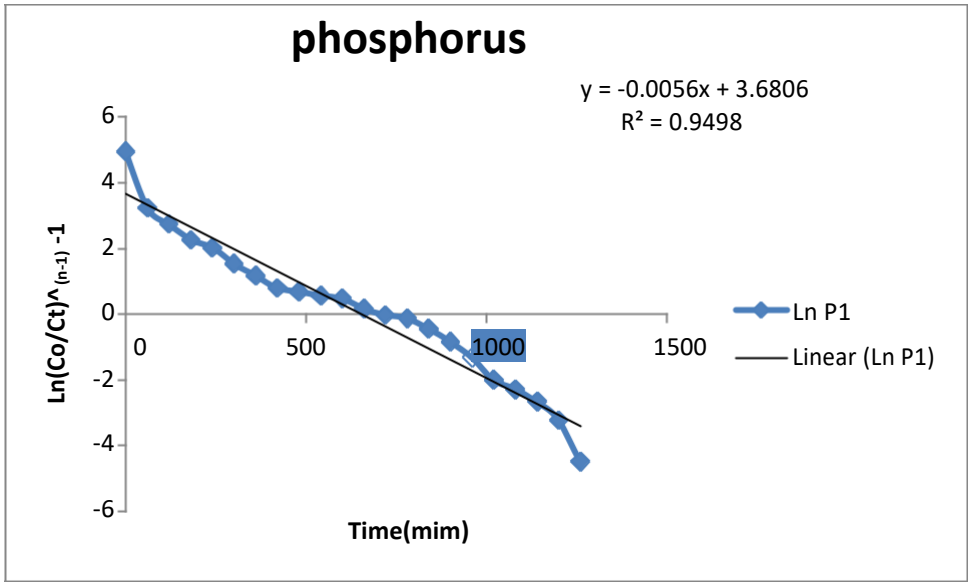

Figure 6.1: Clark model showing the R^2 value at constant flow rate and initial concentration at a bed height of 2 cm

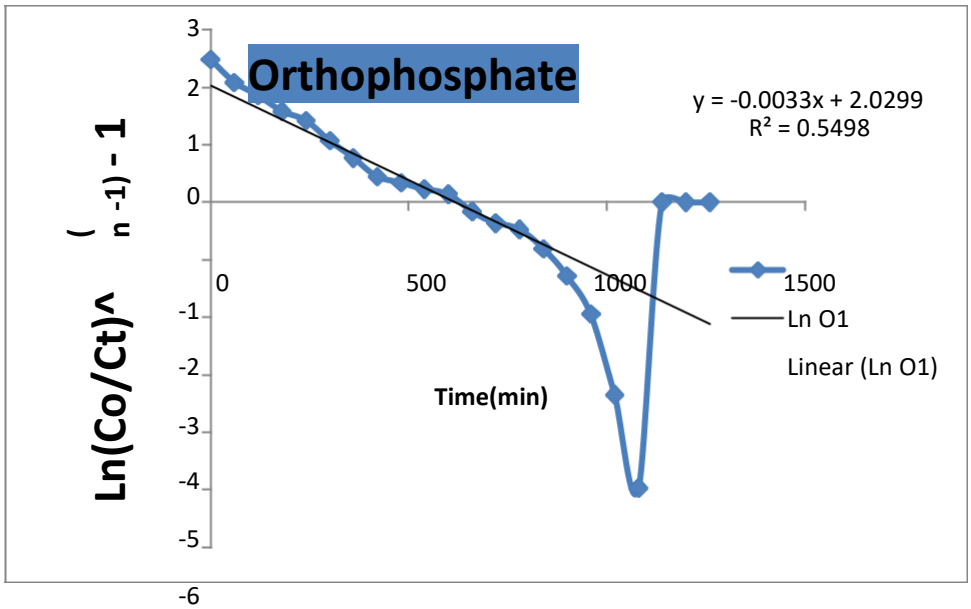

Figure 6.2: Clark model showing the R^2 value at constant flow rate and initial concentration at a bed height of 2 cm

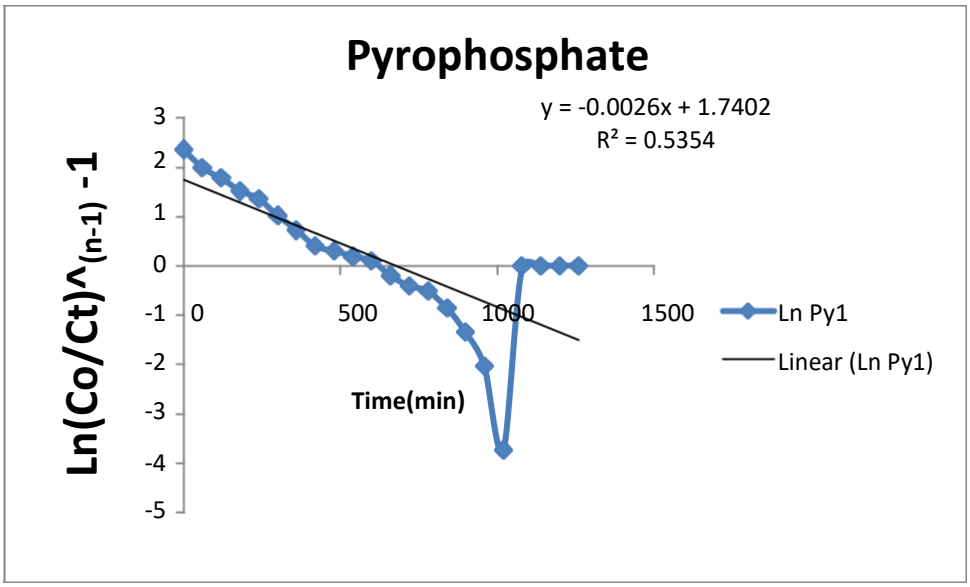

Figure 6.3: Clark model showing the R^2 value at constant flow rate and initial concentration at a bed height of 2 cm

For 4 cm

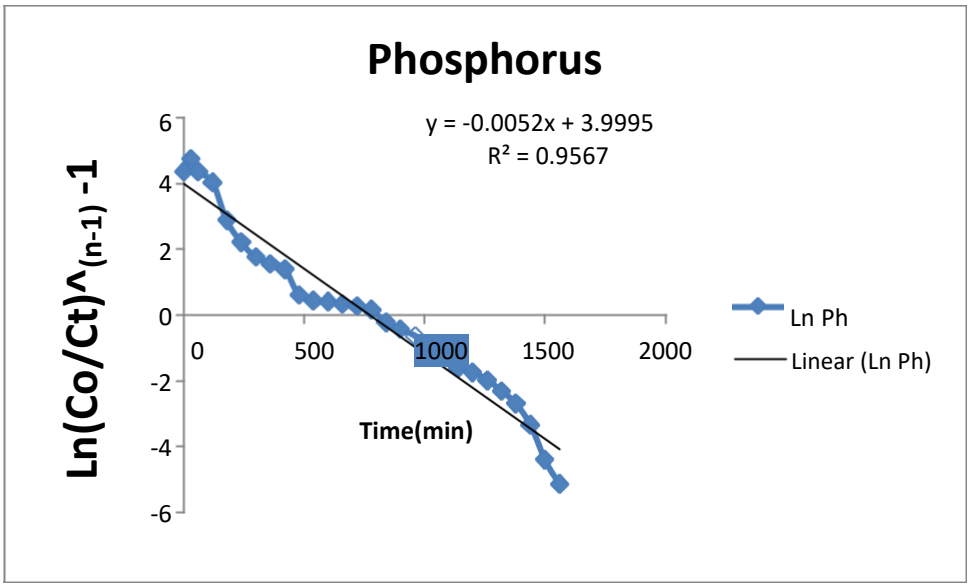

Figure 6.4: Clark model showing the R^2 value at constant flow rate and initial concentration at a bed height of 4 cm

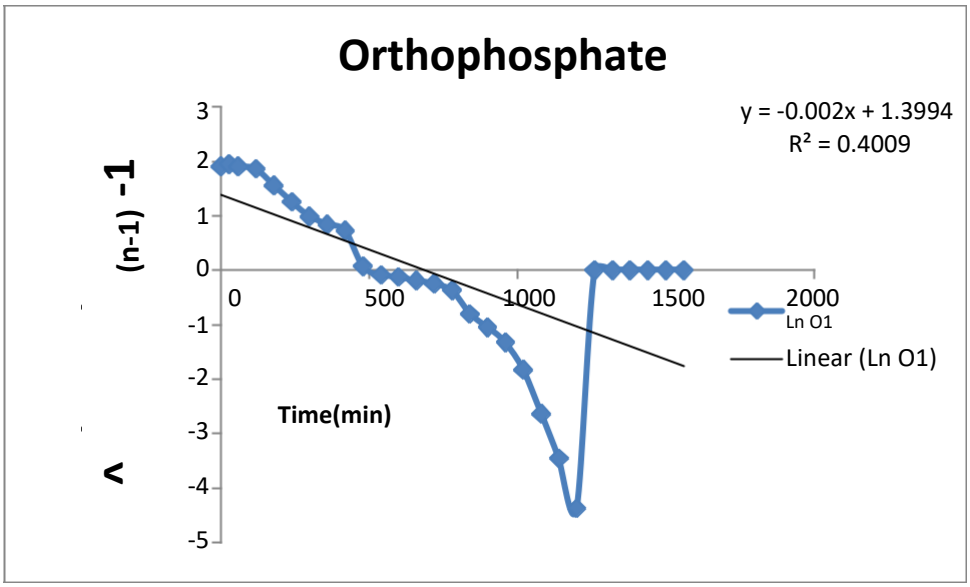

Figure 6.5: Clark model showing the R^2 value at constant flow rate and initial concentration at a bed height of 4 cm

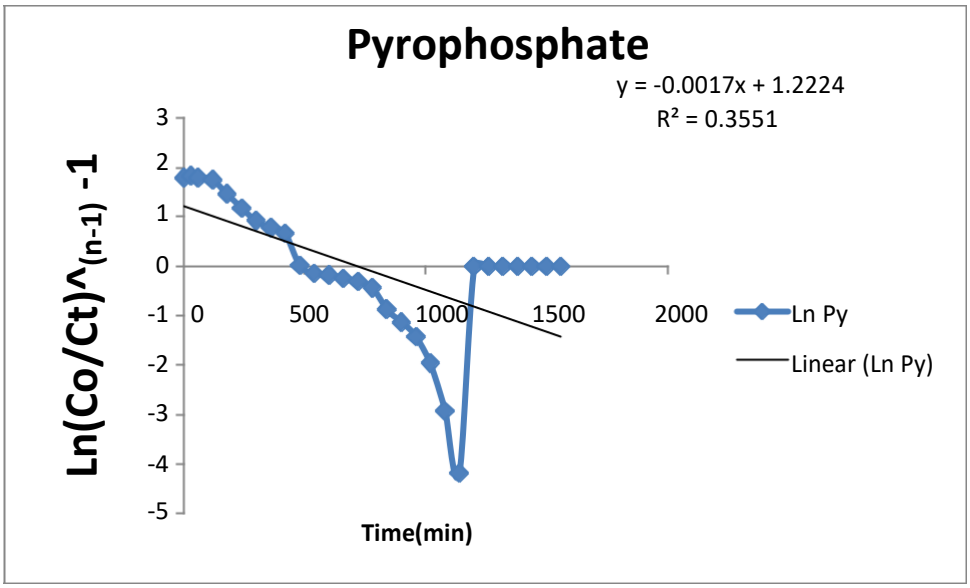

Figure 6.6: Clark model showing the R^2 value at constant flow rate and initial concentration at a bed height of 4 cm

For 6 cm

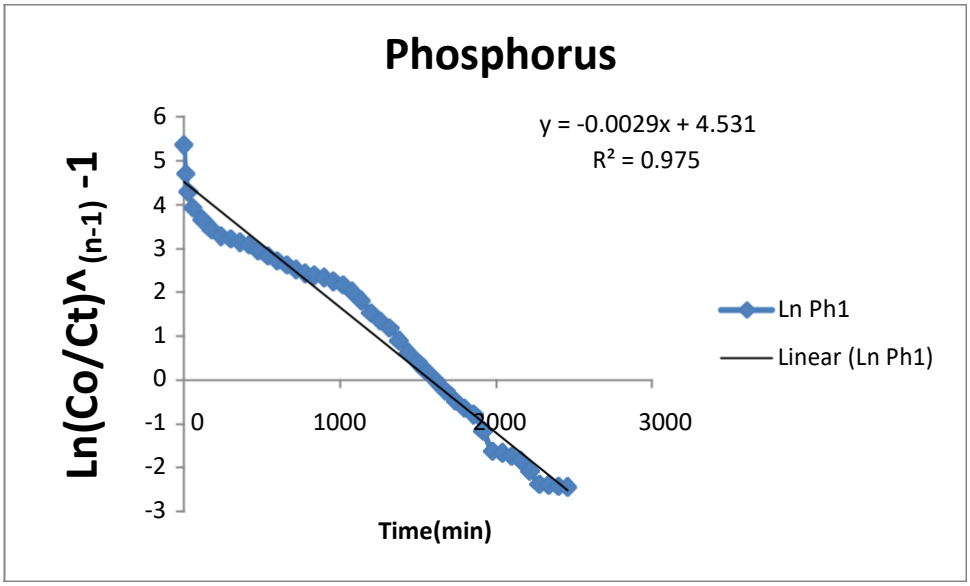

Figure 6.7: Clark model showing the R^2 value at constant flow rate and initial concentration at a bed height of 6 cm

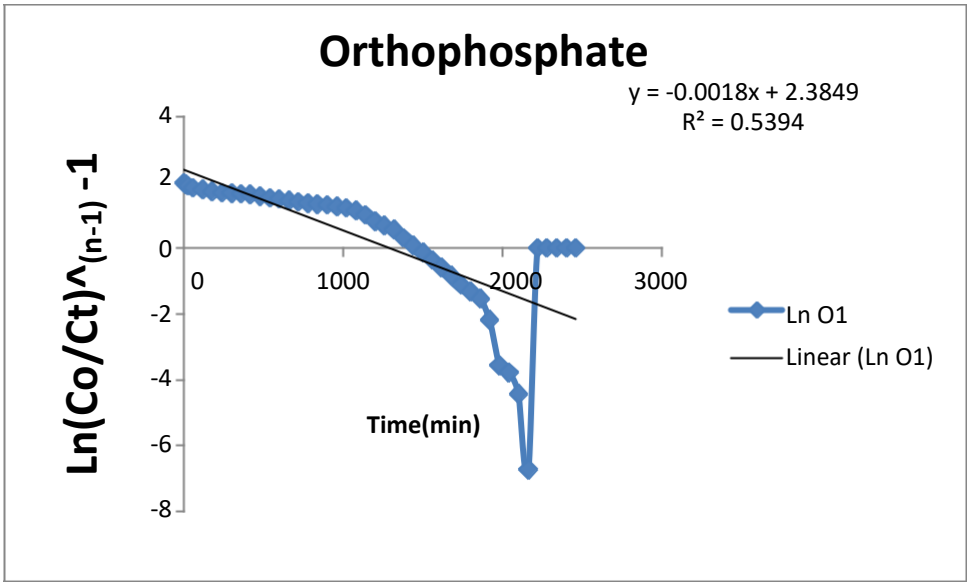

Figure 6.8: Clark model showing the R^2 value at constant flow rate and initial concentration at a bed height of 6 cm

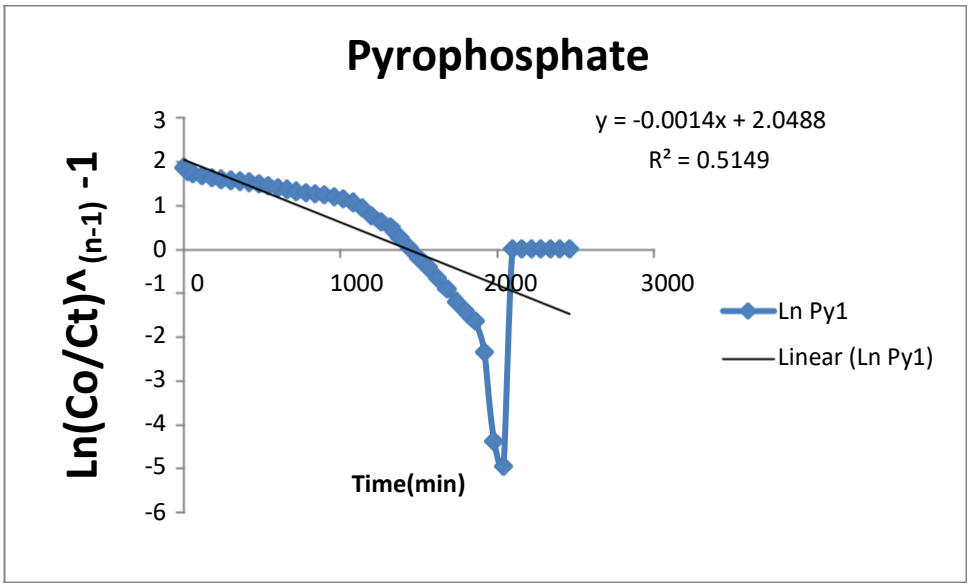

Figure 6.9: Clark model showing the R^2 value at constant flow rate and initial concentration at a bed height of 6 cm

4.4.1.2 Effect of flow rate using Clark model

For 4 ml/min

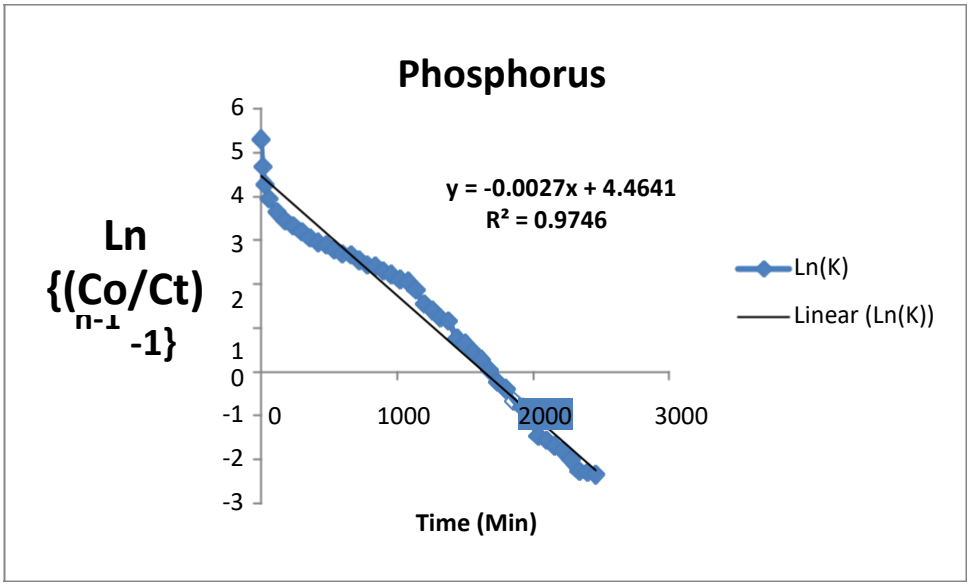

Figure 6.10: Clark model showing R^2 value at constant bed height and initial concentration at a flow rate of 4 ml/min

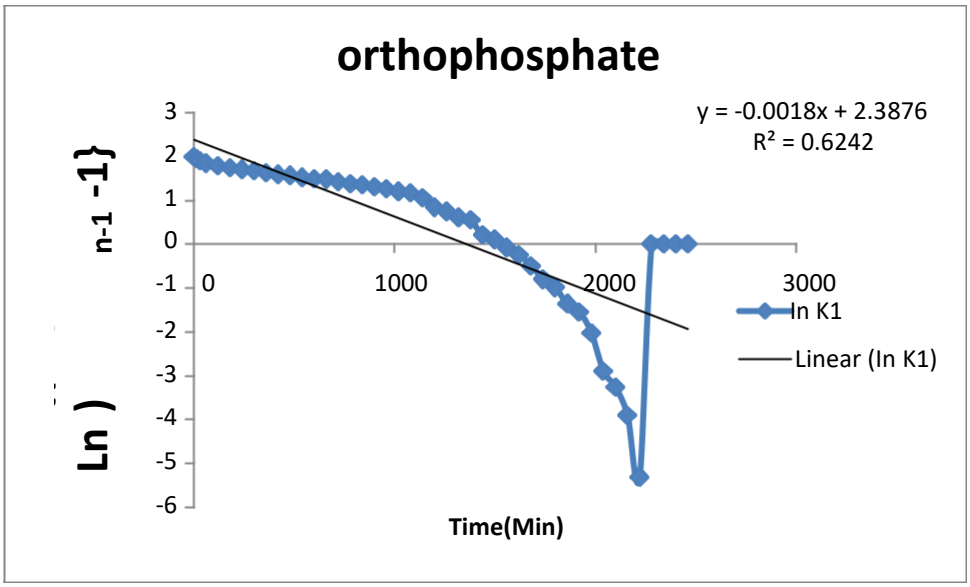

Figure 6.11: Clark model showing R^2 value at constant bed height and initial concentration at a flow rate of 4 ml/min

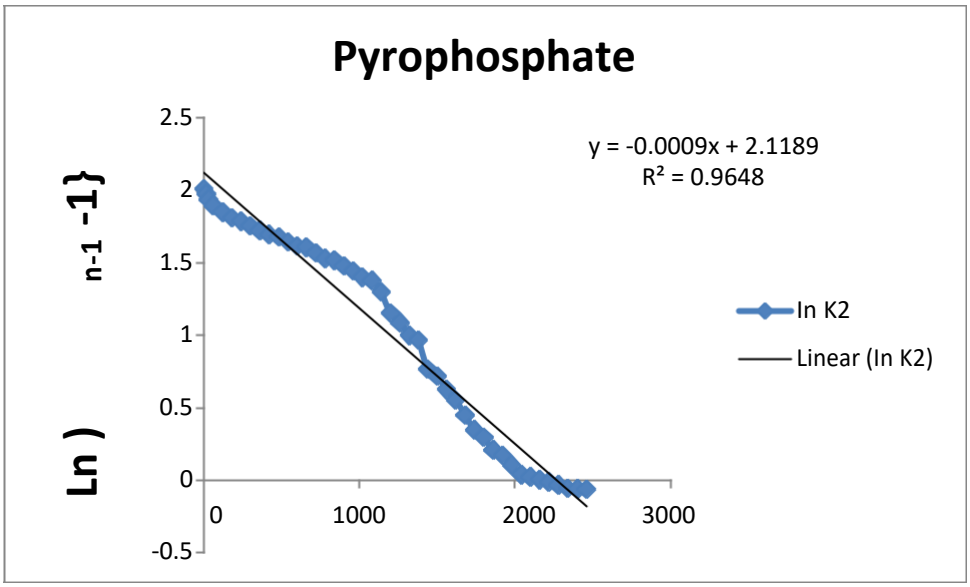

Figure 6.12: Clark model showing R^2 value at constant bed height and initial concentration at a flow rate of 4 ml/min

For 8 ml/min

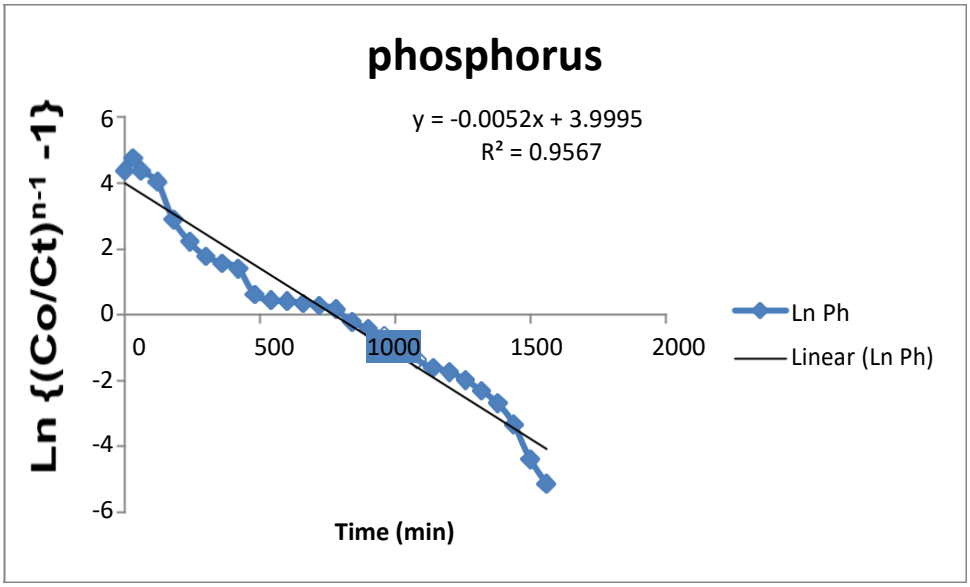

Figure 6.13: Clark model showing R^2 value at constant bed height and initial concentration at a flow rate of 8 ml/min

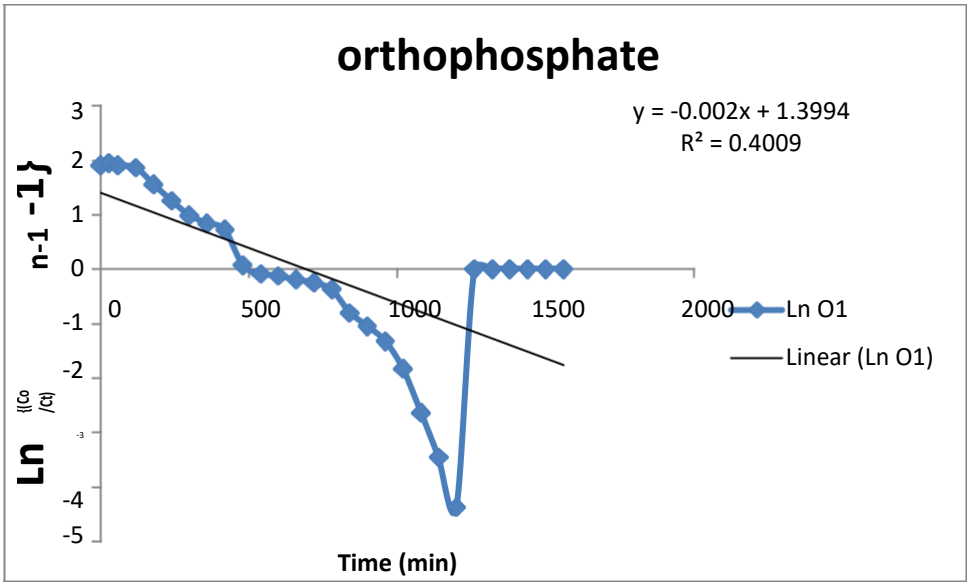

Figure 6.14: Clark model showing R^2 value at constant bed height and initial concentration at a flow rate of 8 ml/min

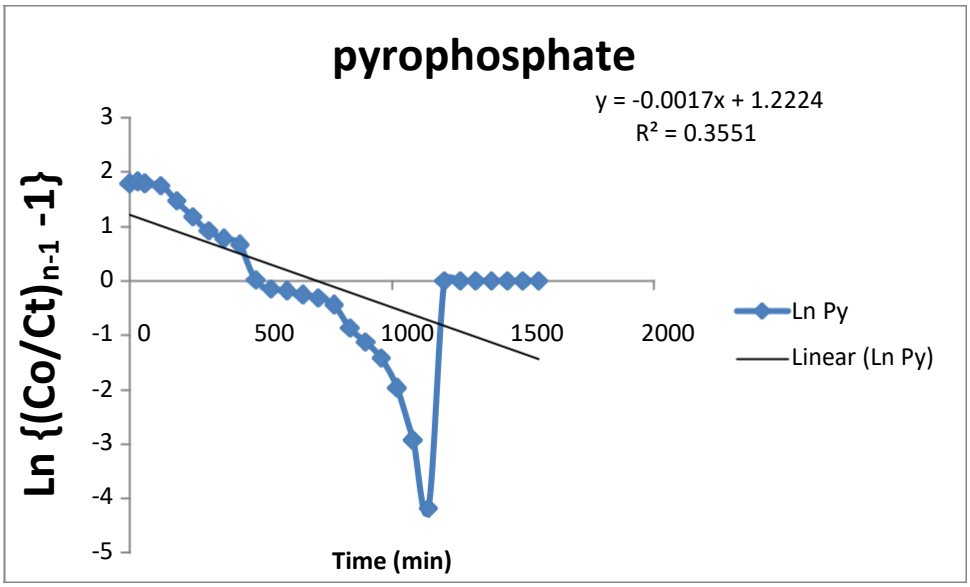

Figure 6.15: Clark model showing R^2 value at constant bed height and initial concentration at a flow rate of 8 ml/min

12 ml/min

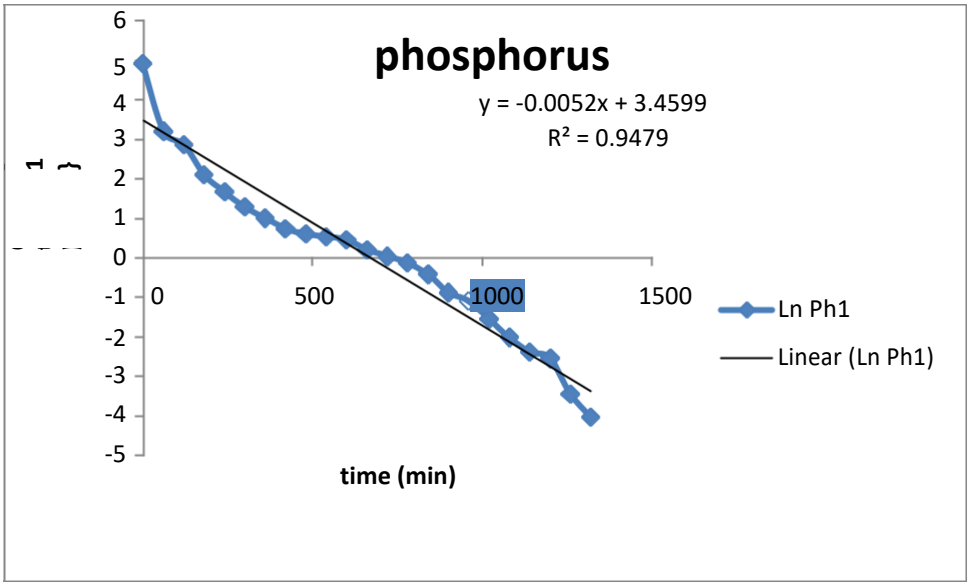

Figure 6.16: Clark model showing R^2 value at constant bed height and initial concentration at a flow rate of 12 ml/min

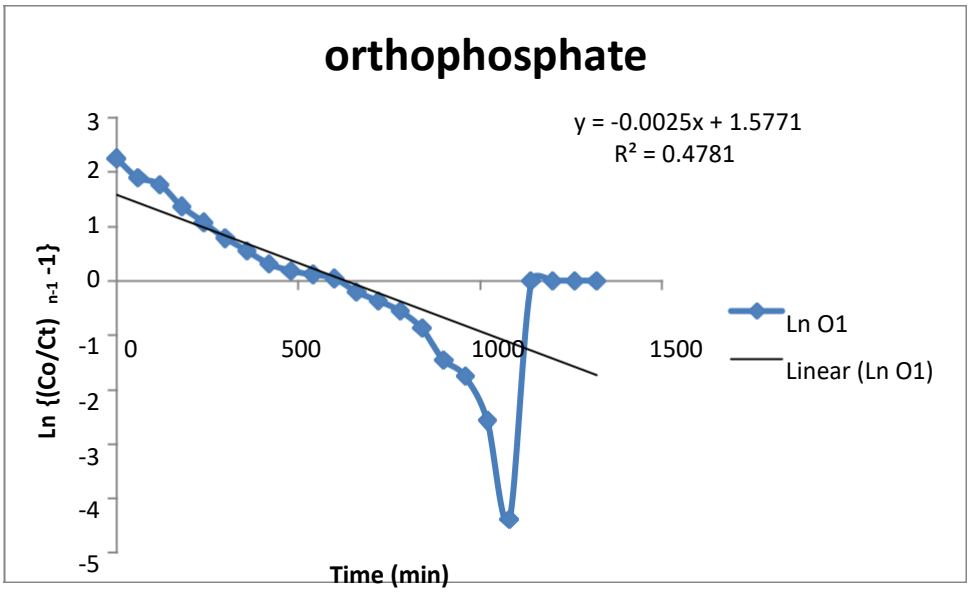

Figure 6.17: Clark model showing R^2 value at constant bed height and initial concentration at a flow rate of 12 ml/min

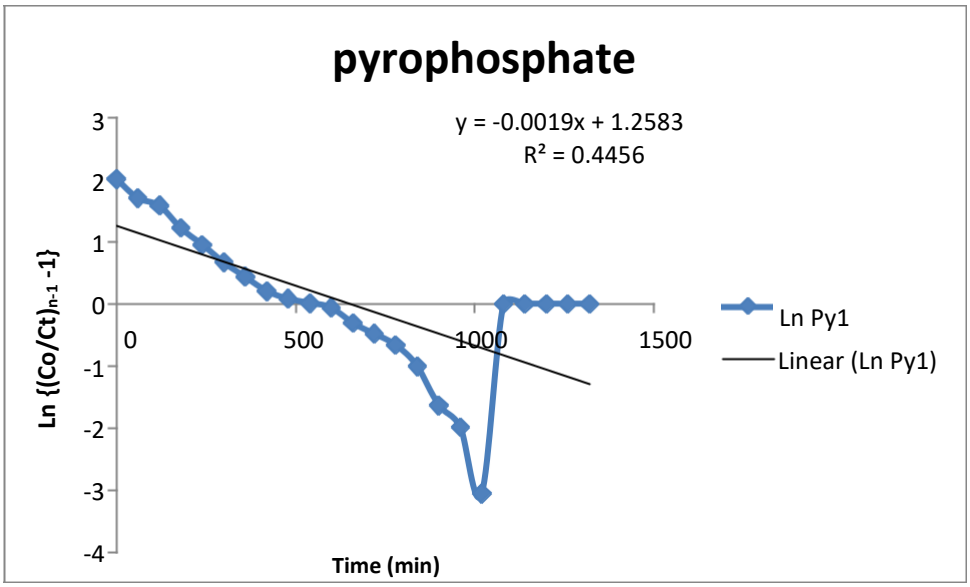

Figure 6.18: Clark model showing R^2 value at constant bed height and initial concentration at a flow rate of 12 ml/min

4.4.1.3 Effect of initial concentration on Clark model

Initial concentration of phosphoric compounds from 2-11.23 mg/L

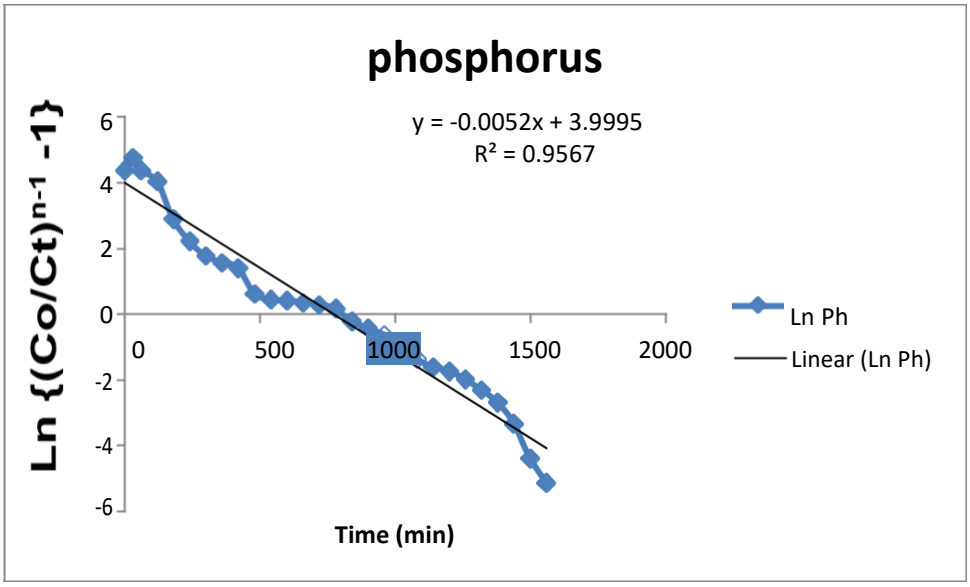

Figure 6.19: Clark model showing the R^2 at constant bed height and flow rate at a concentration of 2 mg/L

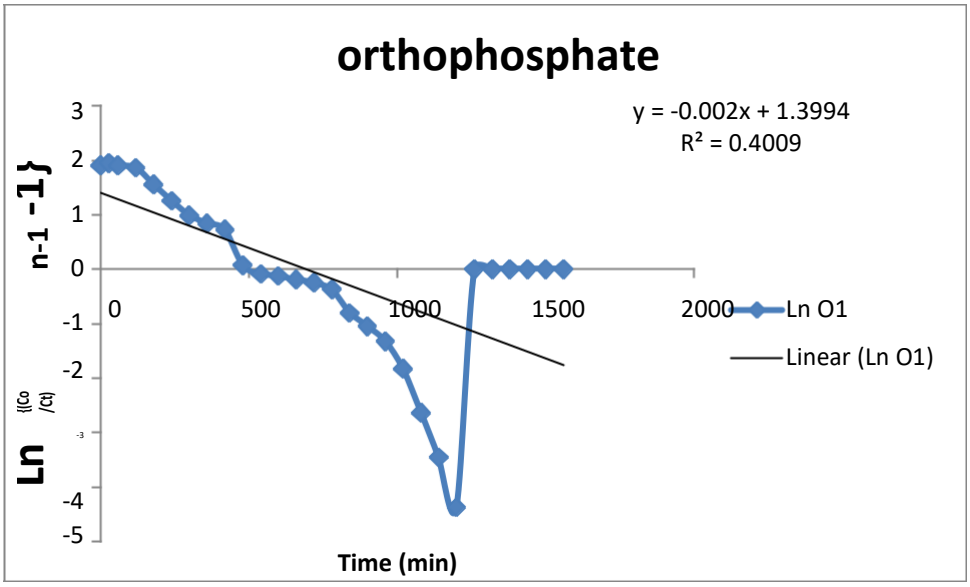

Figure 6.20: Clark model showing the R^2 at constant bed height and flow rate at a concentration of 6.13 mg/L

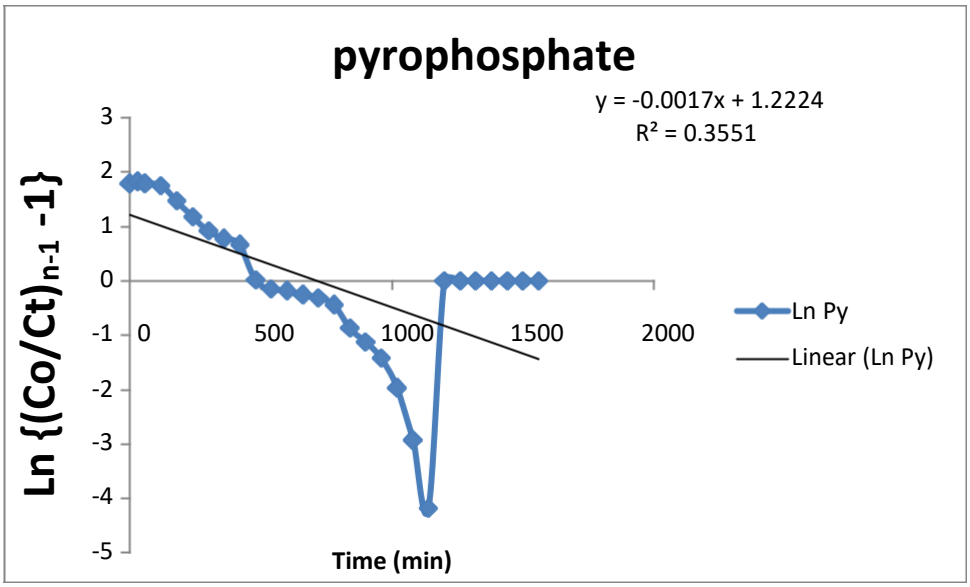

Figure 6.21: Clark model showing the R^2 at constant bed height and flow rate at a concentration of 11.2 mg/L

Initial concentration of phosphoric compounds from 1.5-8.9 mg/L

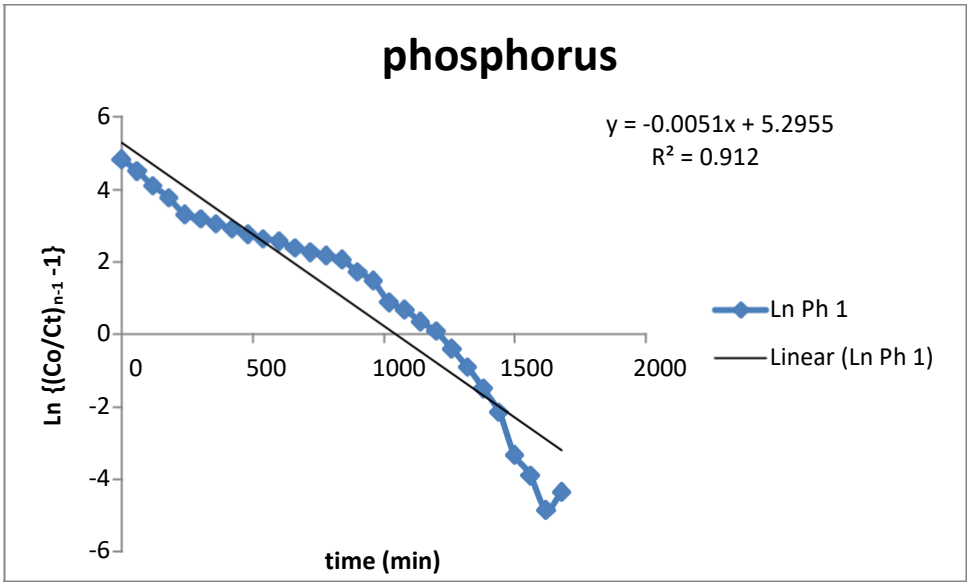

Figure 6.22: Clark model showing the R^2 at constant bed height and flow rate at initial concentration of 1.5 mg/L

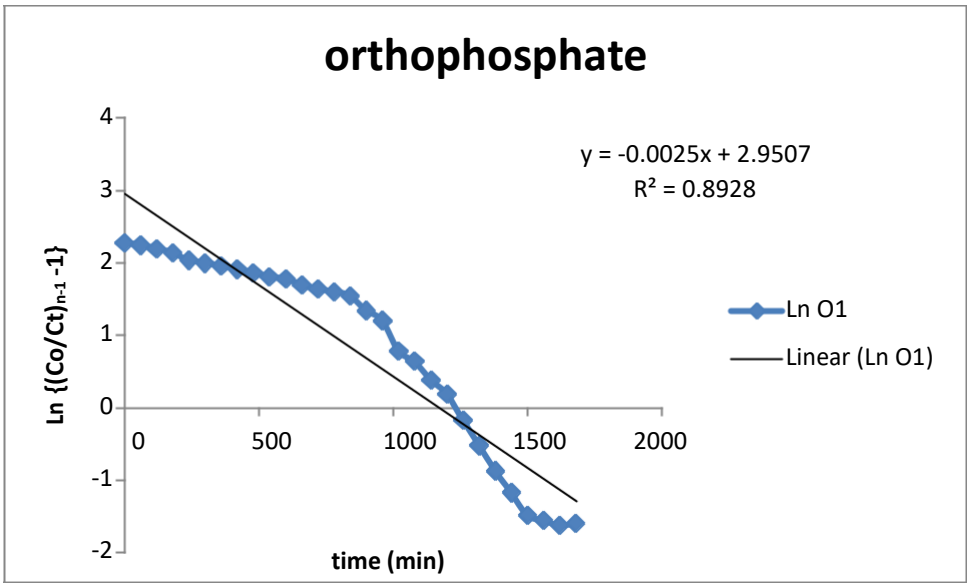

Figure 6.23: Clark model showing the R^2 at constant bed height and flow rate at initial concentration of 4.8 mg/L

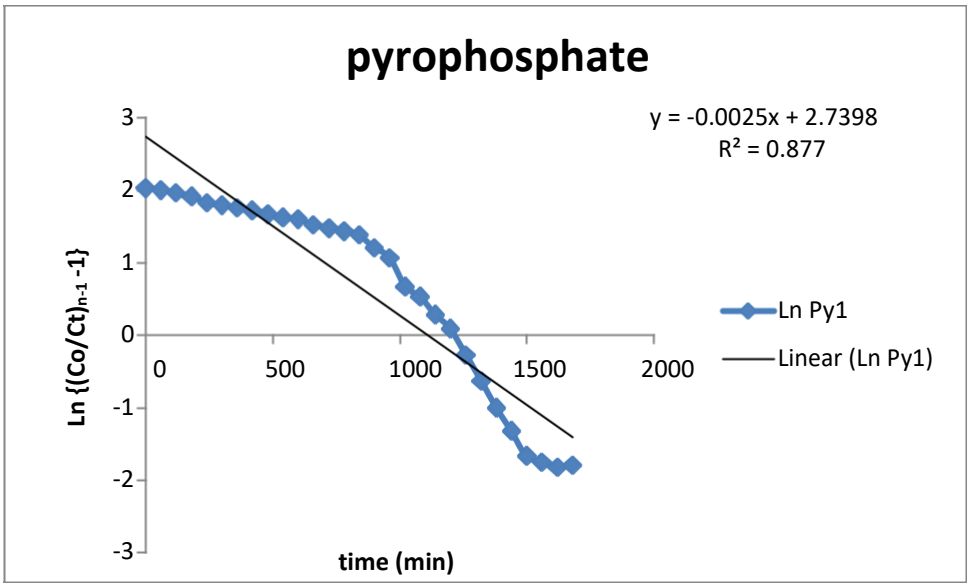

Figure 6.24: Clark model showing the R^2 at constant bed height and flow rate at initial concentration of 8.9 mg/L

Initial concentration of phosphoric compounds from 1, 3 and 6 mg/L

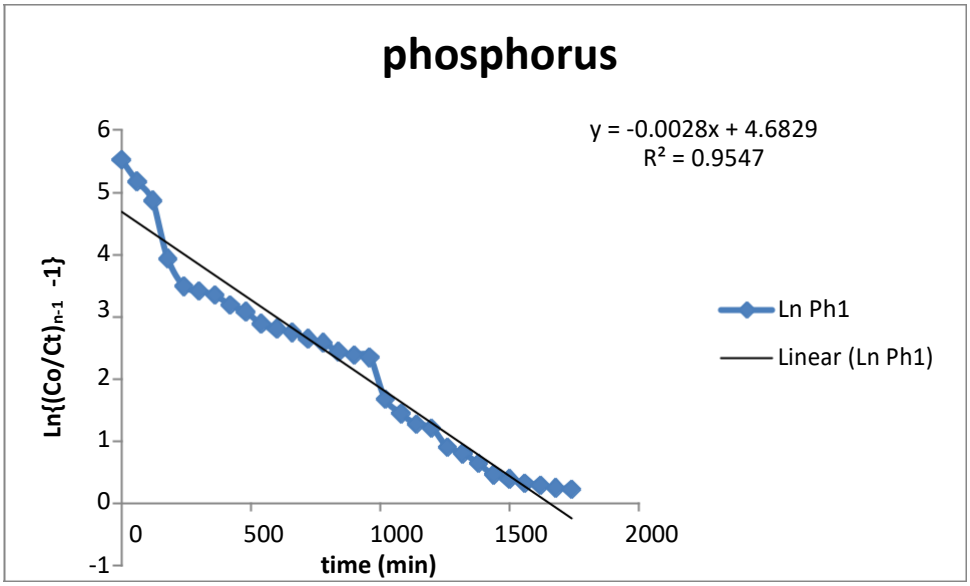

Figure 6.25: Clark model showing the R^2 at constant bed height and flow rate at initial concentration of 1 mg/L

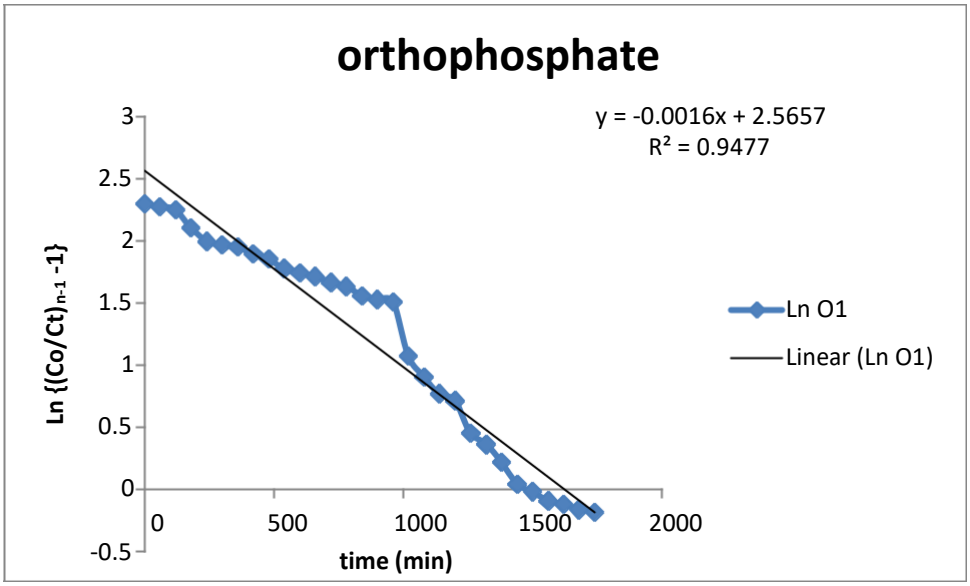

Figure 6.26: Clark model showing the R^2 at constant bed height and flow rate at initial concentration of 3 mg/L

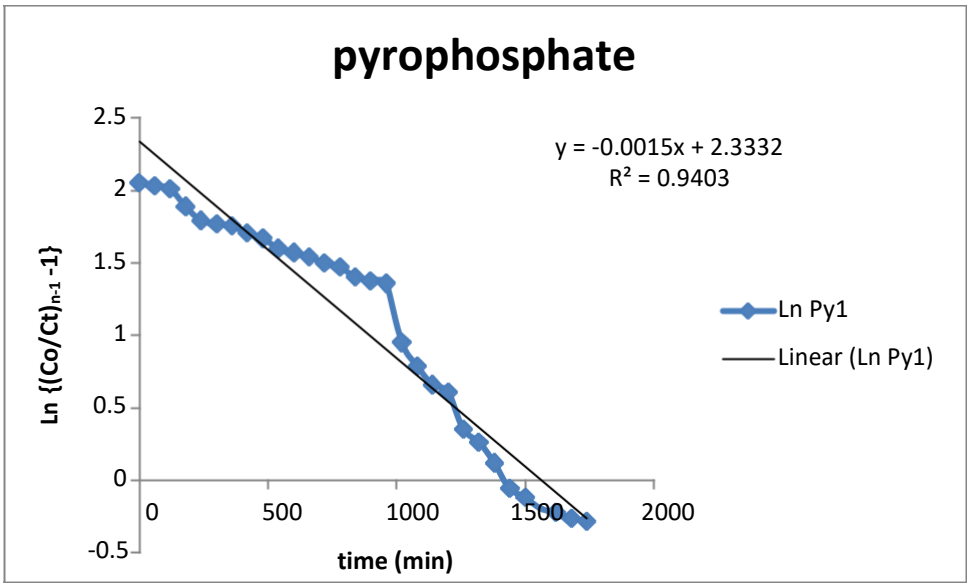

Figure 6.27: Clark model showing the R^2 at constant bed height and flow rate at initial concentration of 6 mg/L

4.4.2 Thomas Model

2 cm

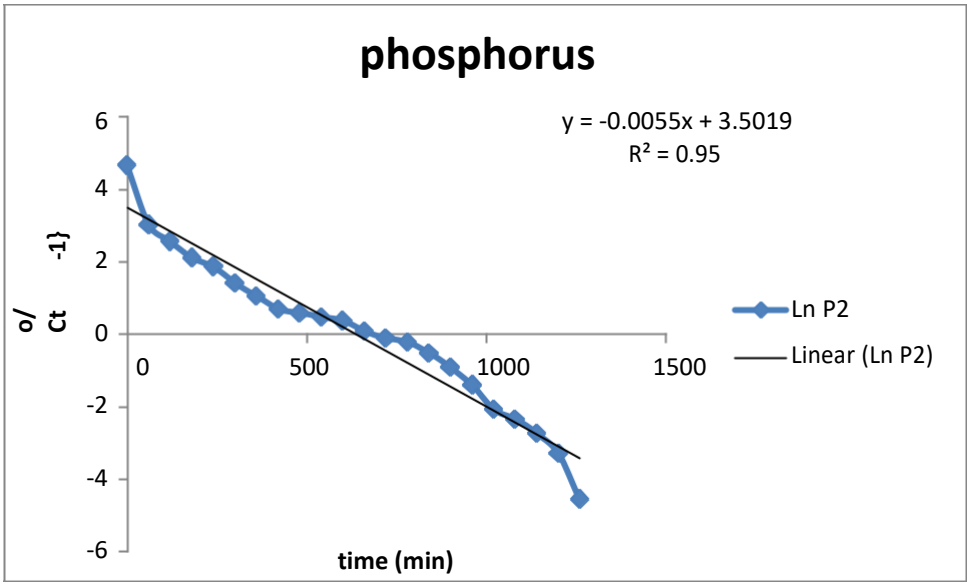

Figure 6.28: Thomas model showing the R^2 at constant flow rate at initial concentration at a bed height of 2 cm

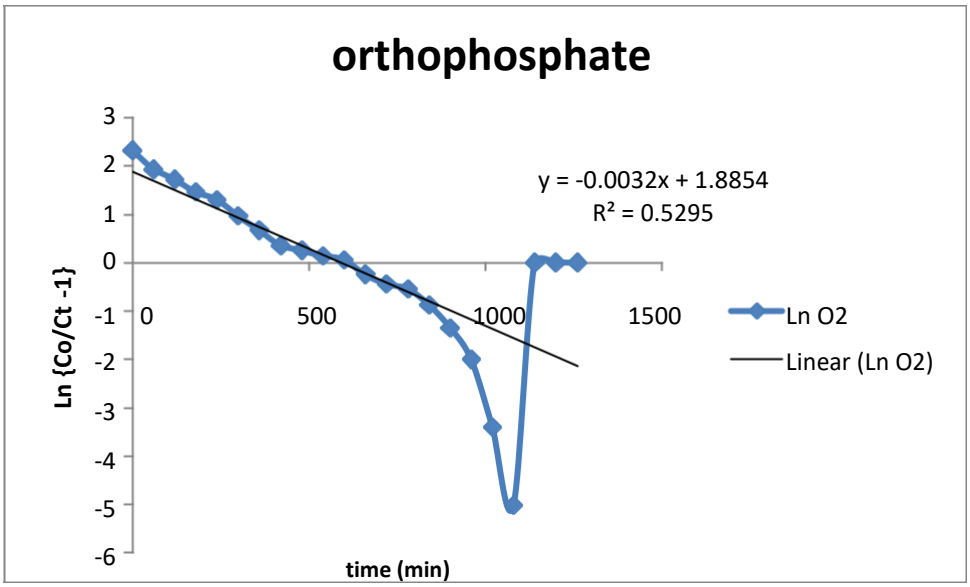

Figure 6.29: Thomas model showing the R^2 at constant flow rate at initial concentration at a bed height of 2 cm

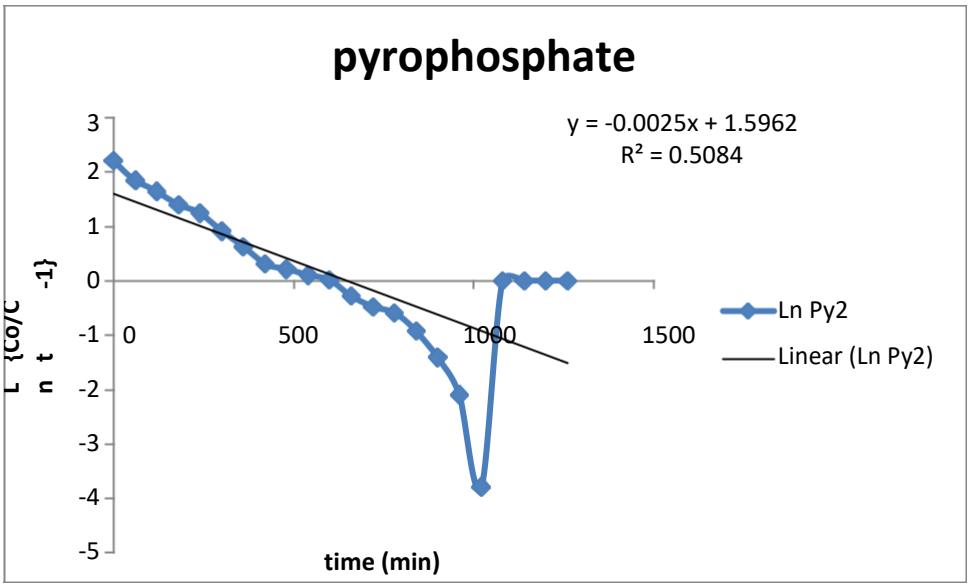

Figure 6.30: Thomas model showing the R^2 at constant flow rate at initial concentration at a bed height of 2 cm

4 cm

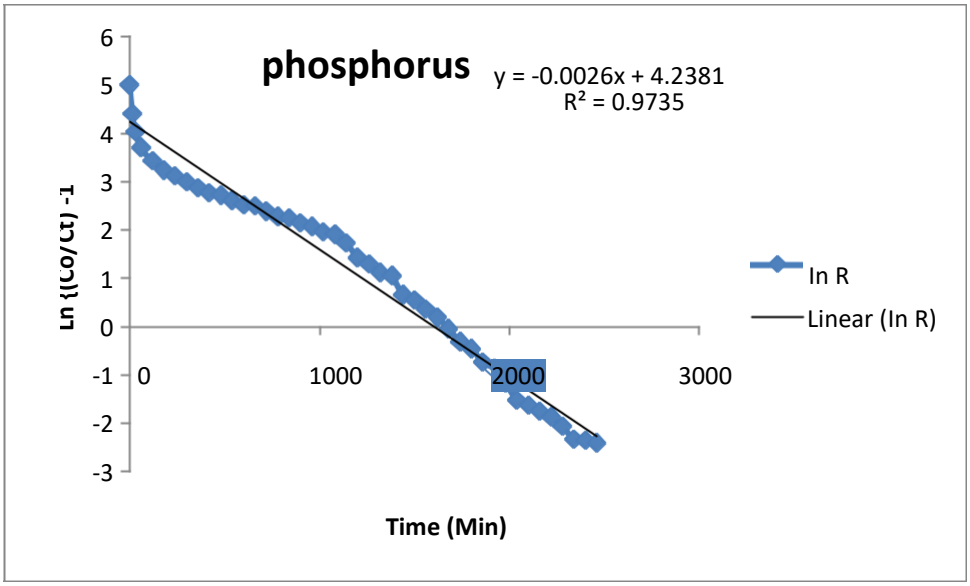

Figure 6.31: Thomas model showing the R^2 at constant flow rate at initial concentration at a bed height of 4 cm

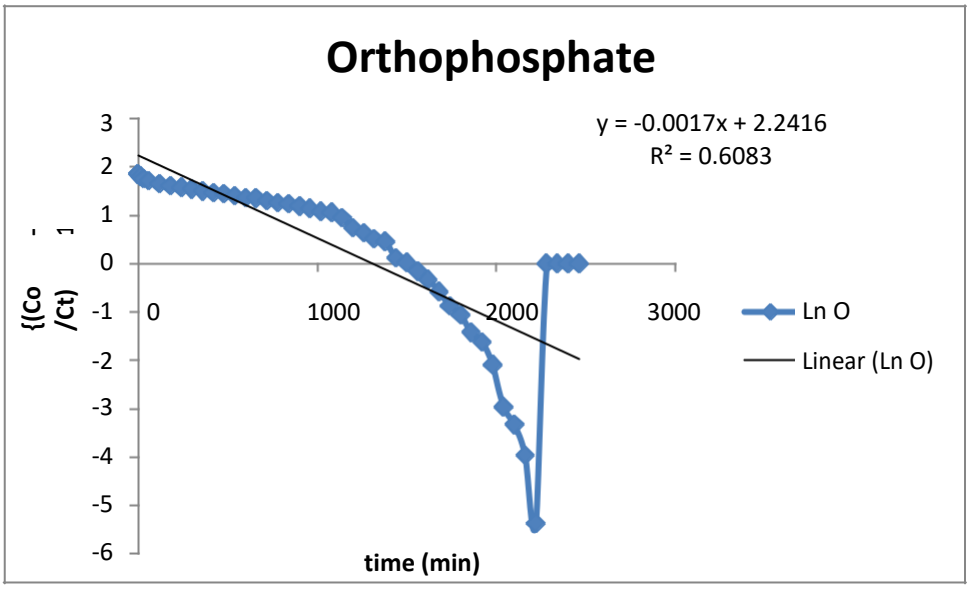

Figure 6.32: Thomas model showing the R^2 at constant flow rate at initial concentration at a bed height of 4 cm

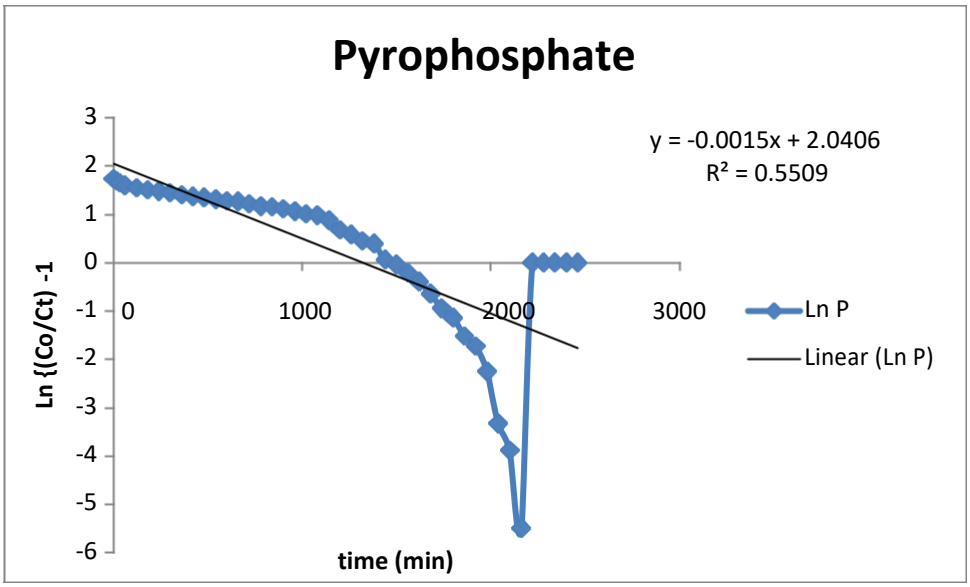

Figure 6.33: Thomas model showing the R^2 at constant flow rate at initial concentration at a bed height of 4 cm

6 cm

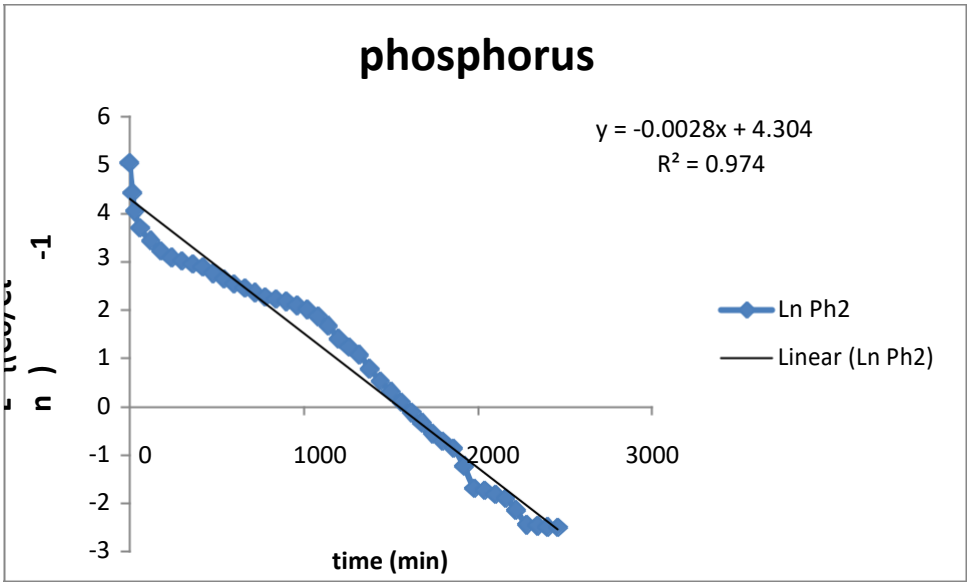

Figure 6.34: Thomas model showing the R^2 at constant flow rate at initial concentration at a bed height of 6 cm

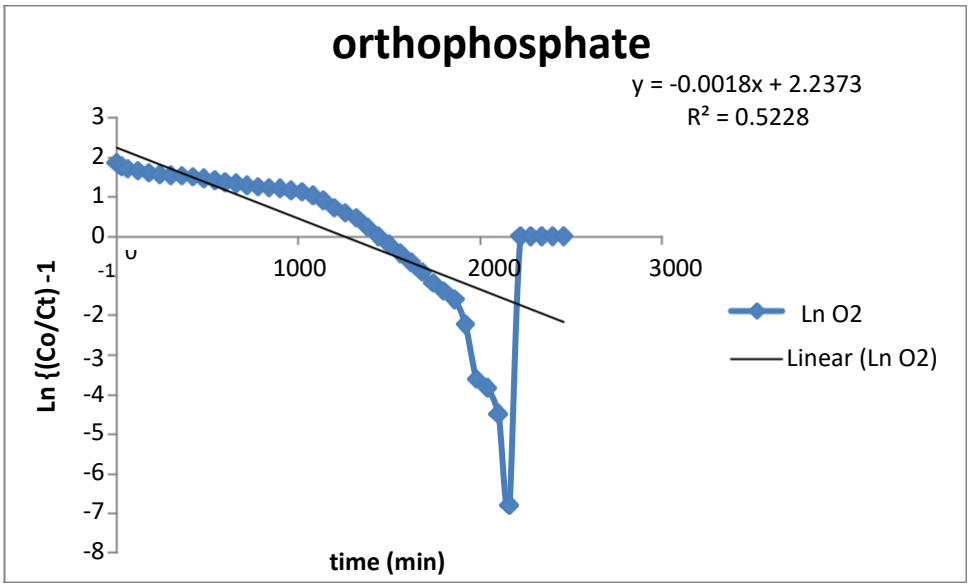

Figure 6.35: Thomas model showing the R^2 at constant flow rate at initial concentration at a bed height of 6 cm

4 ml/min

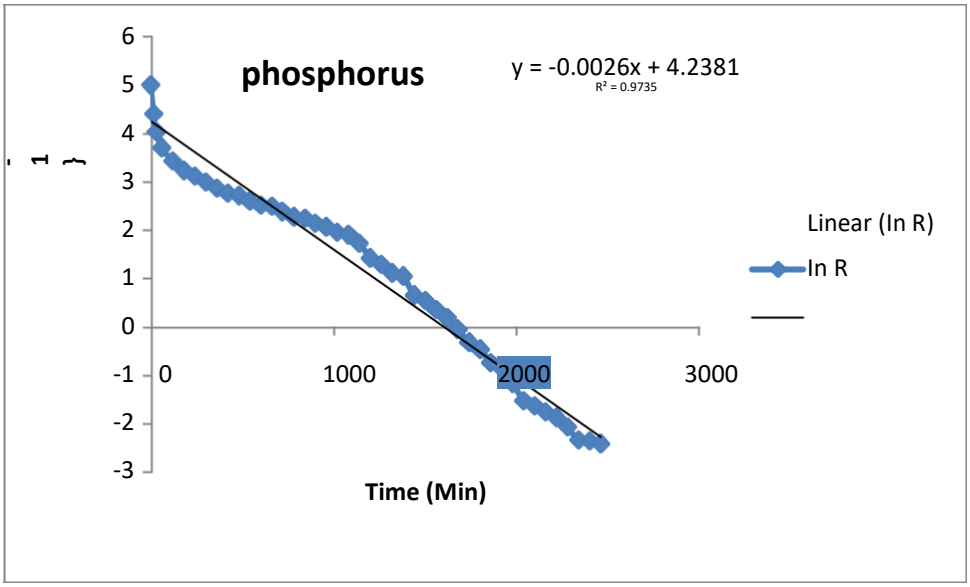

Figure 6.36: Thomas model showing the R^2 at constant bed height and at initial concentration at flow rate of 4 ml/min

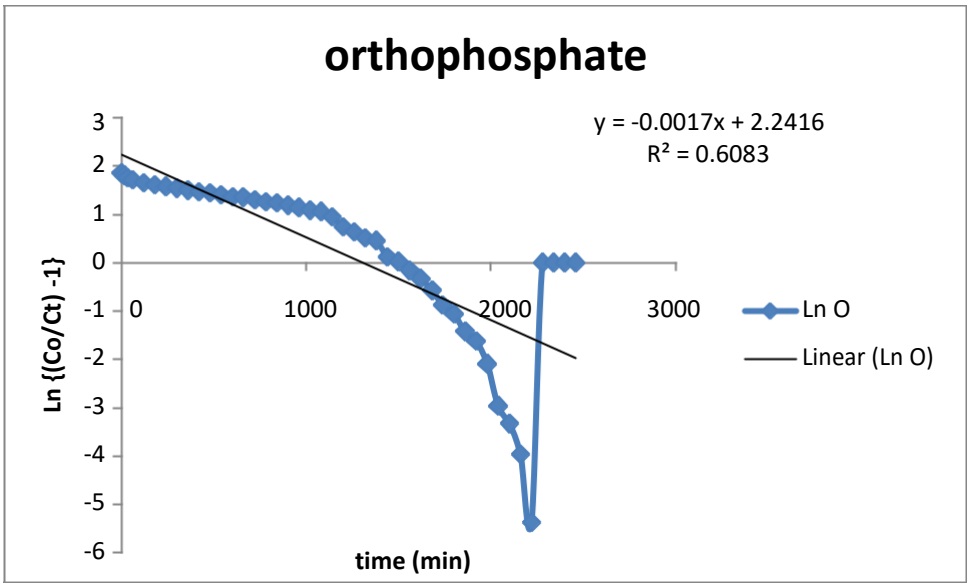

Figure 6.37: Thomas model showing the R^2 at constant bed height and at initial concentration at flow rate of 4 ml/min

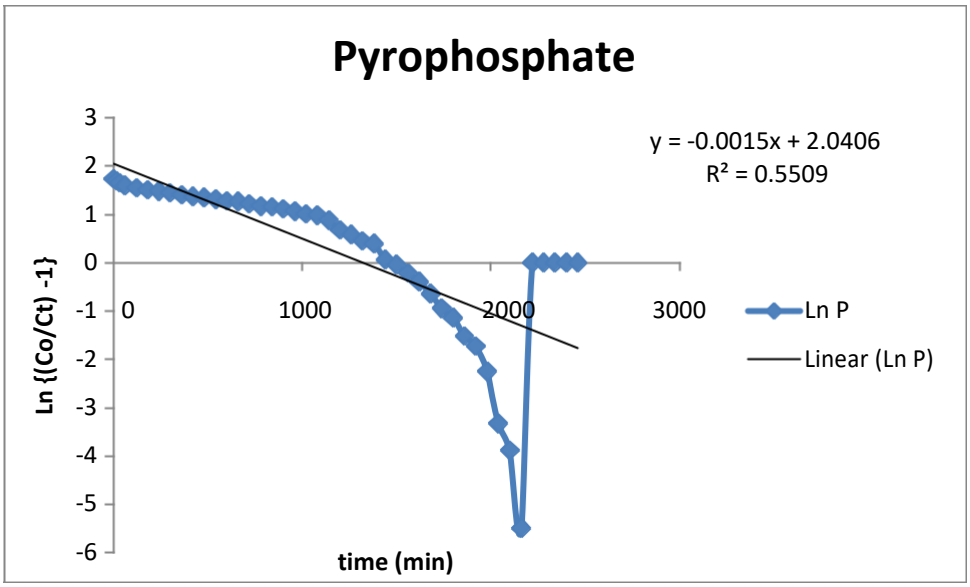

Figure 6.38: Thomas model showing the R^2 at constant bed height and at initial concentration at flow rate of 4 ml/min

8 ml/min

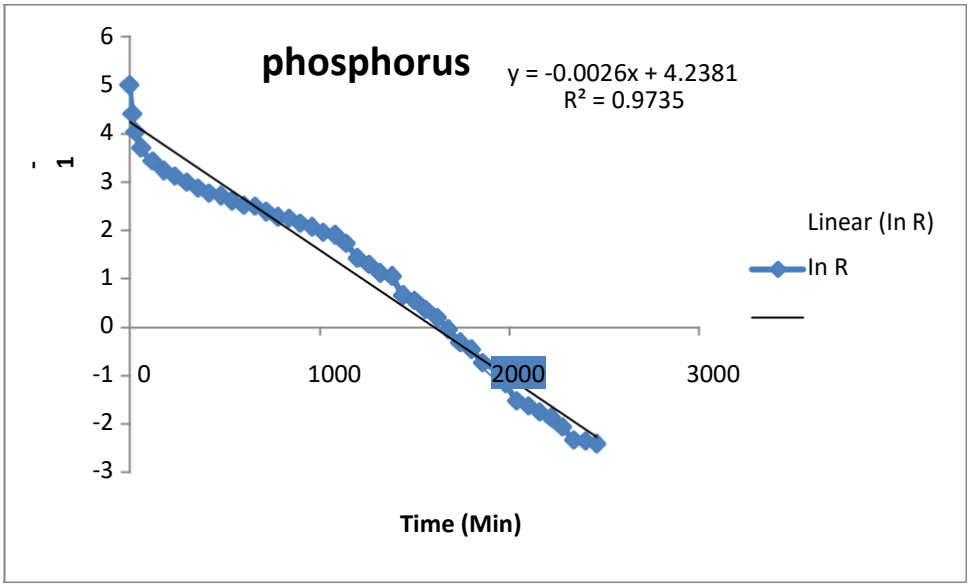

Figure 6.39: Thomas model showing the R^2 at constant bed height and at initial concentration at flow rate of 8 ml/min

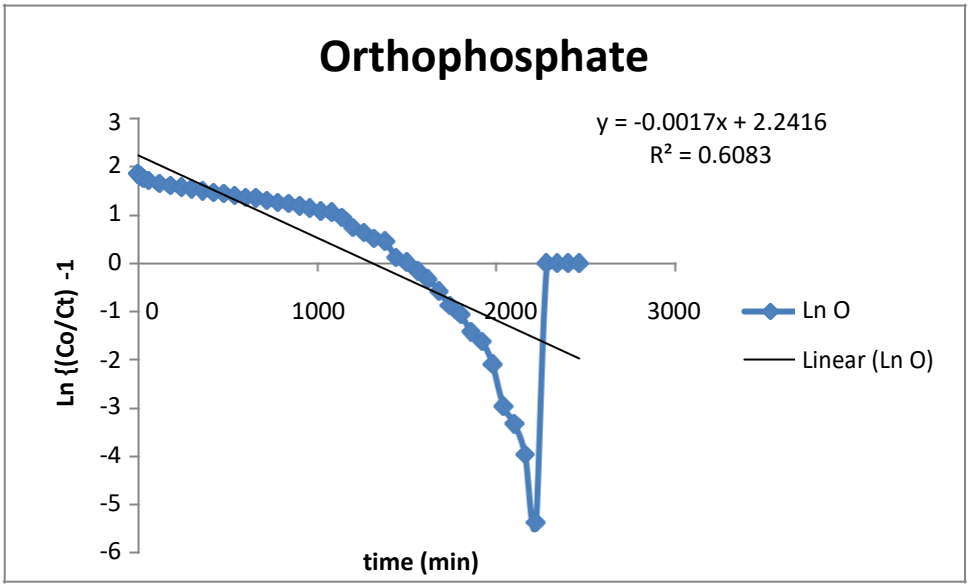

Figure 6.40: Thomas model showing the R^2 at constant bed height and at initial concentration at flow rate of 8 ml/min

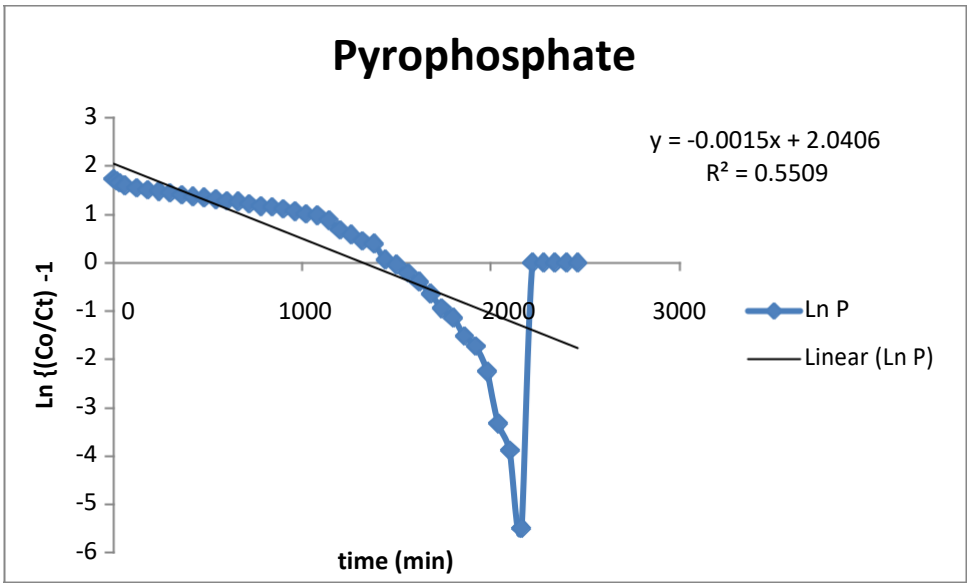

Figure 6.41: Thomas model showing the R^2 at constant bed height and at initial concentration at flow rate of 8 ml/min

12 ml/min

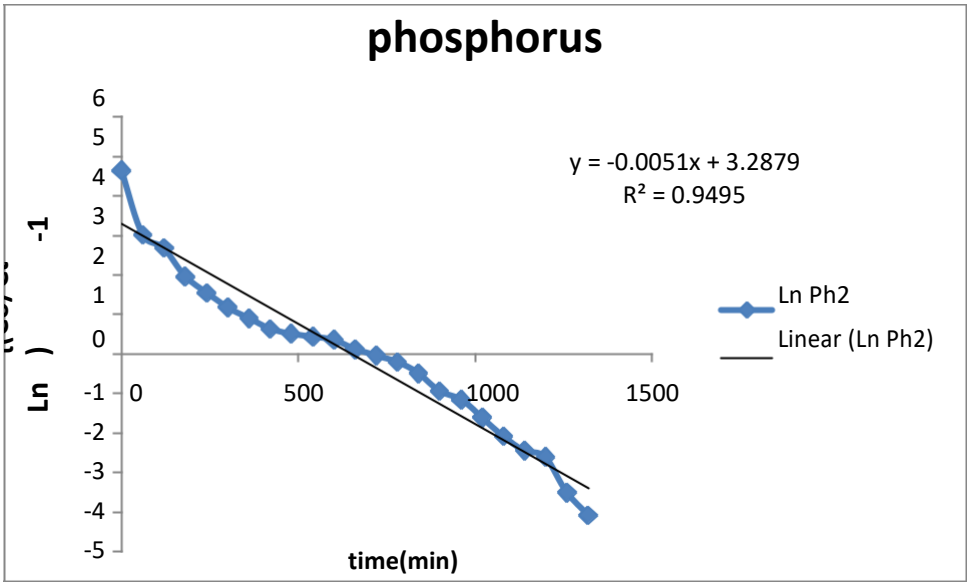

Figure 6.42: Thomas model showing the R^2 at constant bed height and at initial concentration at flow rate of 12 ml/min

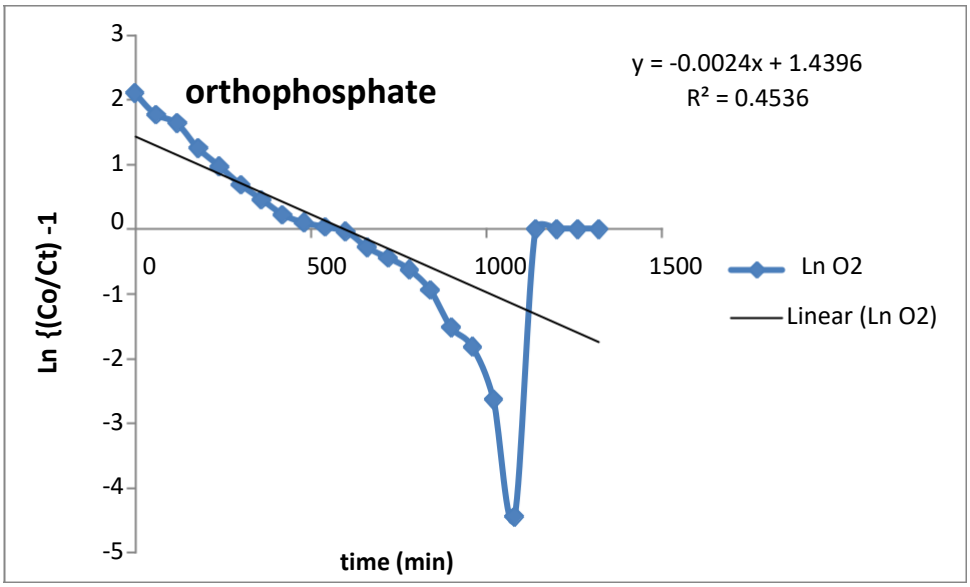

Figure 6.43: Thomas model showing the R^2 at constant bed height and at initial concentration at flow rate of 12 ml/min

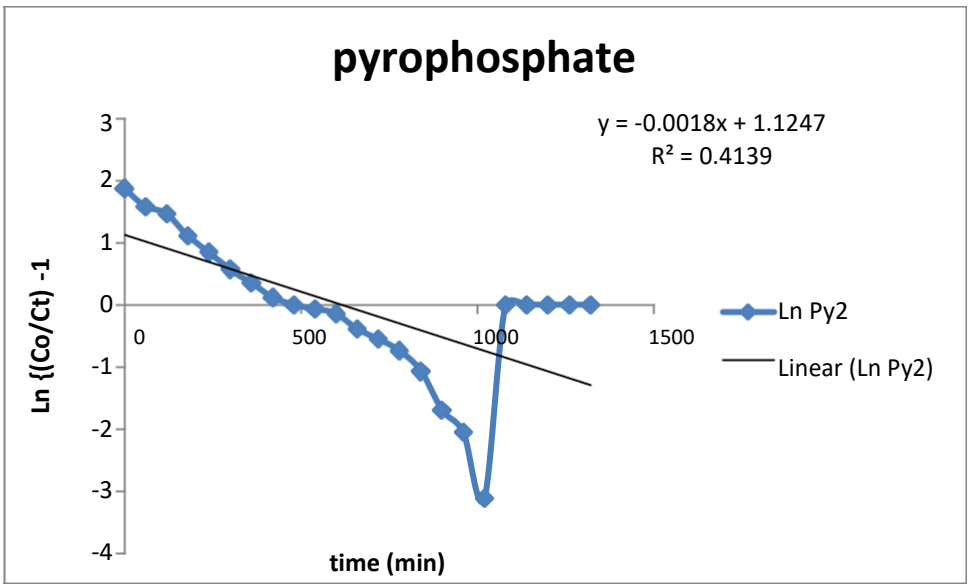

Figure 6.44: Thomas model showing the R^2 at constant bed height and at initial concentration at flow rate of 12 ml/min

Initial concentration of phosphoric compounds from 2-11.23 mg/L

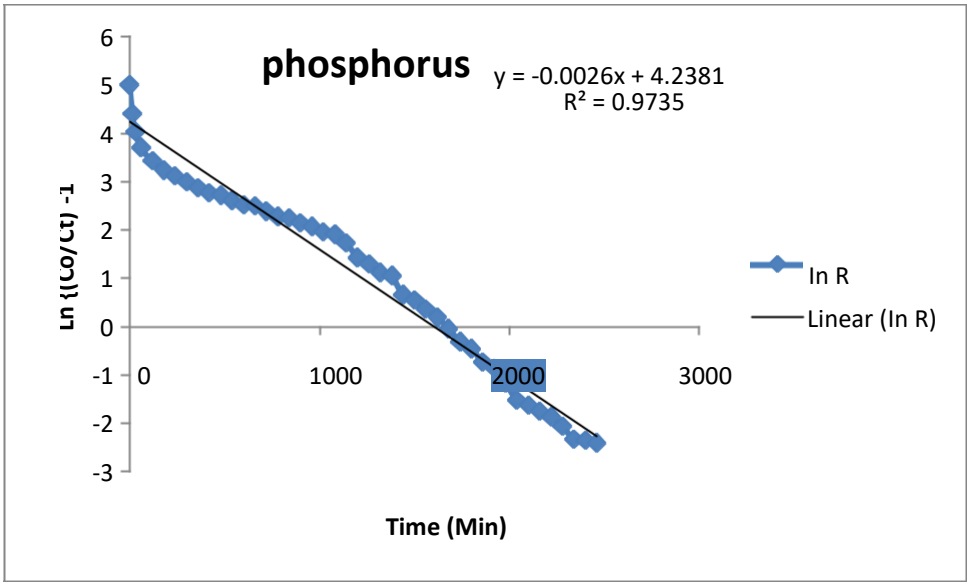

Figure 6.45: Thomas model showing the R^2 value at constant bed height and flow rate at a concentration of 2 mg/L

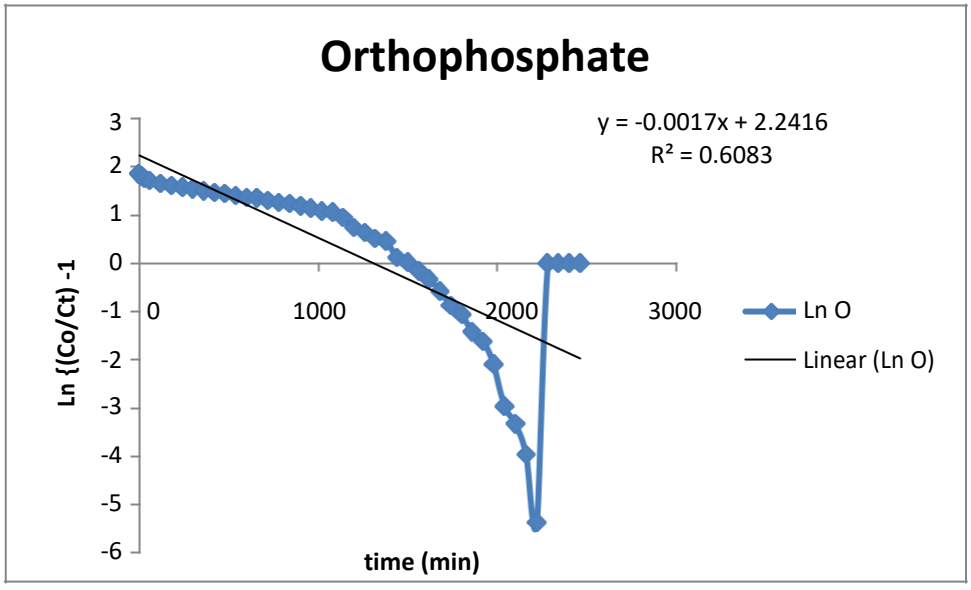

Figure 6.46: Thomas model showing the R^2 value at constant bed height and flow rate at a concentration of 6.13 mg/L

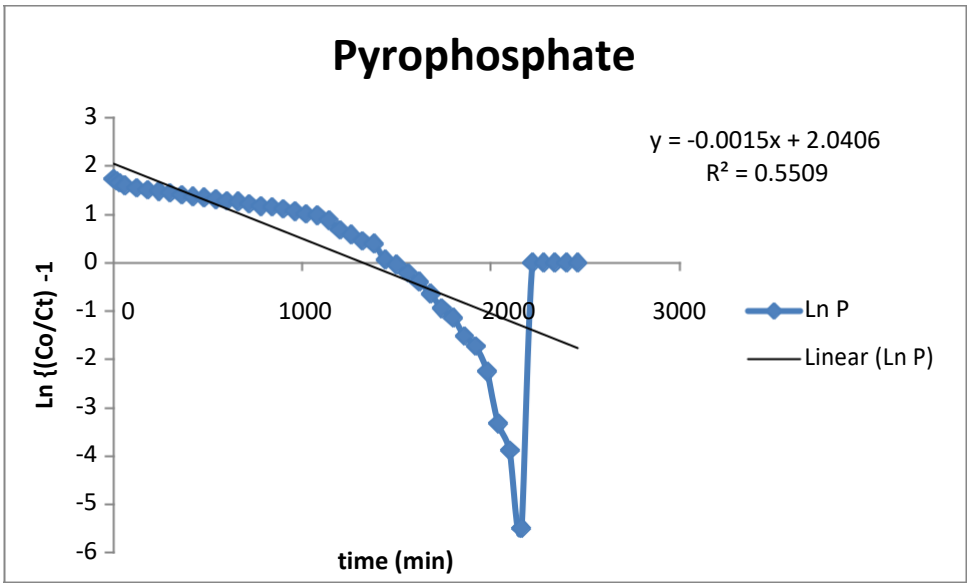

Figure 6.47: Thomas model showing the R^2 value at constant bed height and flow rate at a concentration of 11.23 mg/L

Initial concentration of phosphoric compounds from 1.5 – 8.9 mg/L

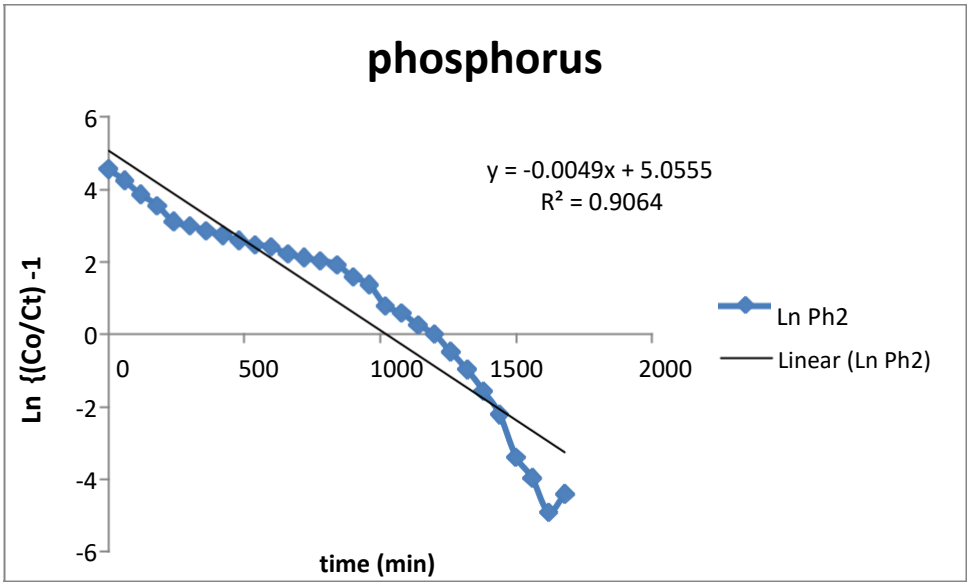

Figure 6.48: Thomas model showing the R^2 value at constant bed height and flow rate at a concentration of 1.5 mg/L

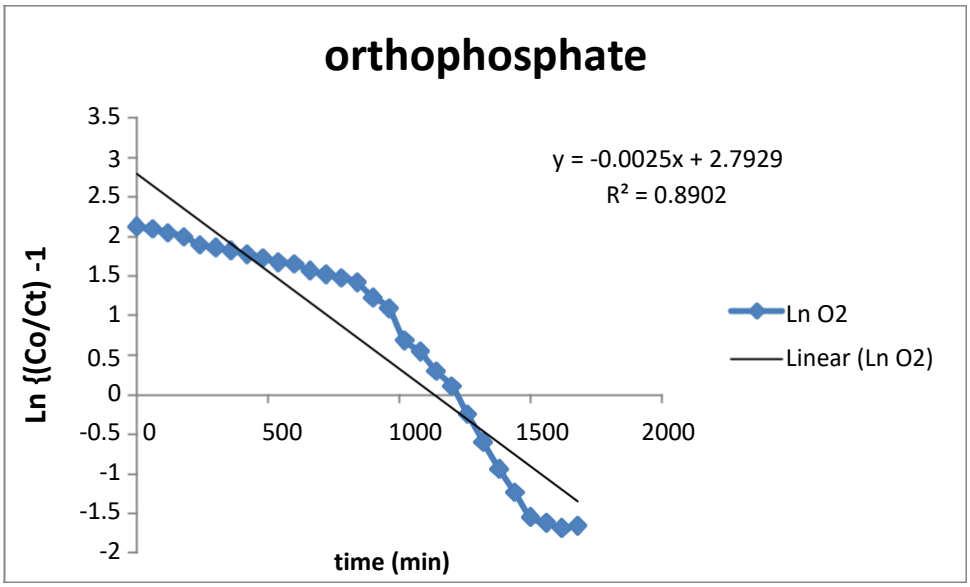

Figure 6.49: Thomas model showing the R^2 value at constant bed height and flow rate at a concentration of 4.8 mg/L

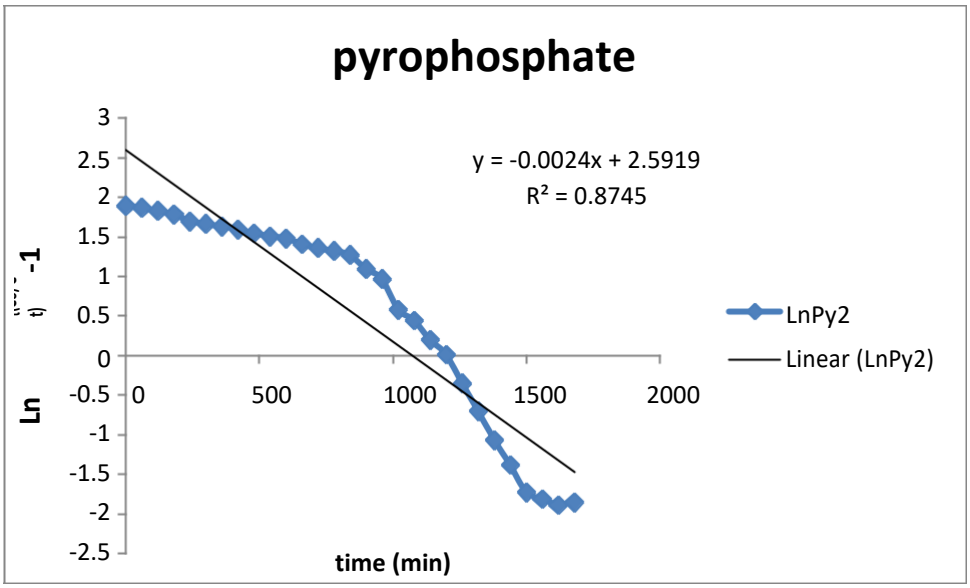

Figure 6.50: Thomas model showing the R^2 value at constant bed height and flow rate at a concentration of 8.9 mg/L

Initial concentration of phosphoric compounds from 1-6 mg/L

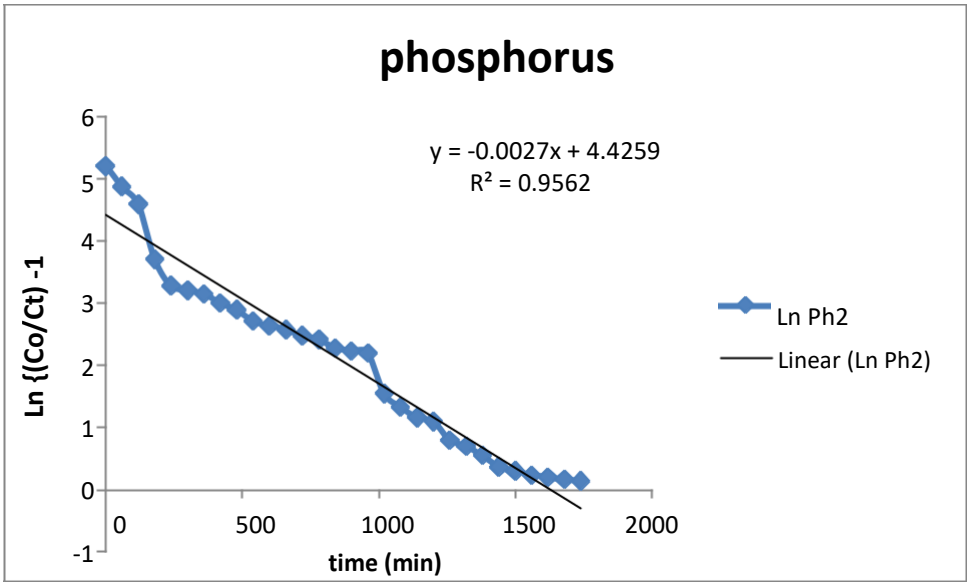

Figure 6.51: Thomas model showing the R^2 value at constant bed height and flow rate at a concentration of 1.0 mg/L

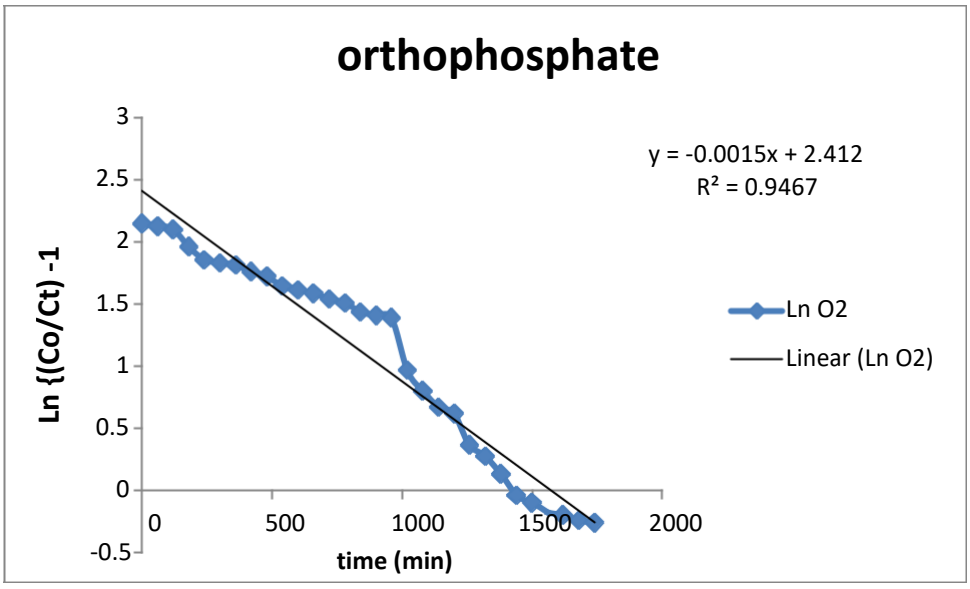

Figure 6.52: Thomas model showing the R^2 value at constant bed height and flow rate at a concentration of 3 mg/L

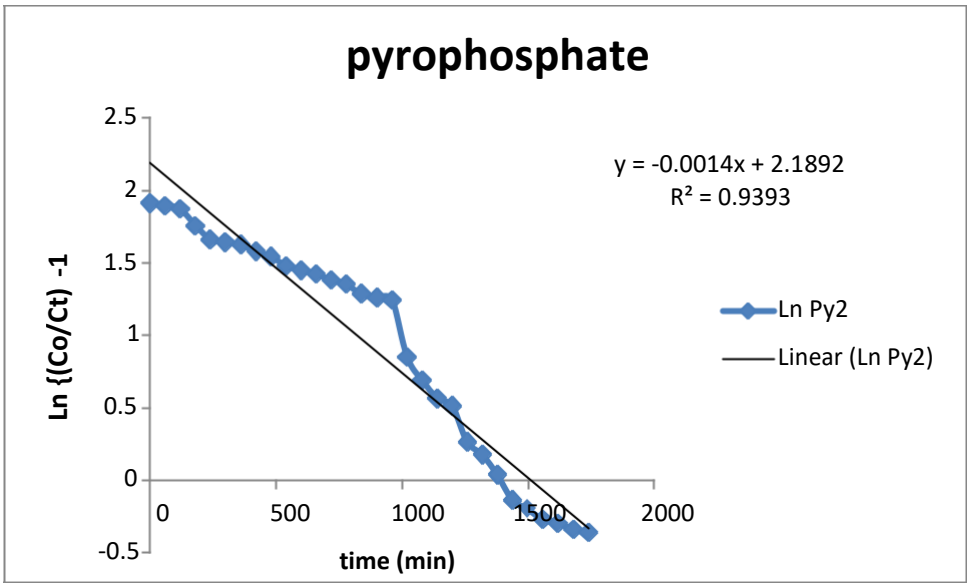

Figure 6.53: Thomas model showing the R^2 value at constant bed height and flow rate at a concentration of 6 mg/L

Table 6.1: Adsorption parameters obtained by the application of the BET model to adsorption isotherms of maize tassel

Surface area data (m^2/g)	
Single point BET	456
Multiple point BET	652.3
Langmuir surface area	2067
BJH method cumulative adsorption surface area	829.9
DH method cumulative adsorption surface area	888.6
t-method external surface area	652.3
DR method micro pore area	748.3
DFT cumulative surface area	180.6

Pore volume data (cc/g)	
BJH method cumulative adsorption pore volume	0.4056
DH method cumulative adsorption pore volume	0.4168
DR method micro pore volume	0.2659
HK method micro pore volume	0.1227
SF method micro pore volume	0.03269
DFT method cumulative pore volume	0.2156
Pore size data (nm)	
BJH method adsorption pore diameter (Mode dv(d))	2.144
DH method adsorption pore diameter (Mode dv(d))	2.144
DR method micro pore width	5.74
DA method pore diameter (Mode)	2.82
HK method pore diameter (Mode)	0.3675
SF method pore diameter (Mode)	0.4523
DFT pore diameter (Mode)	2.647

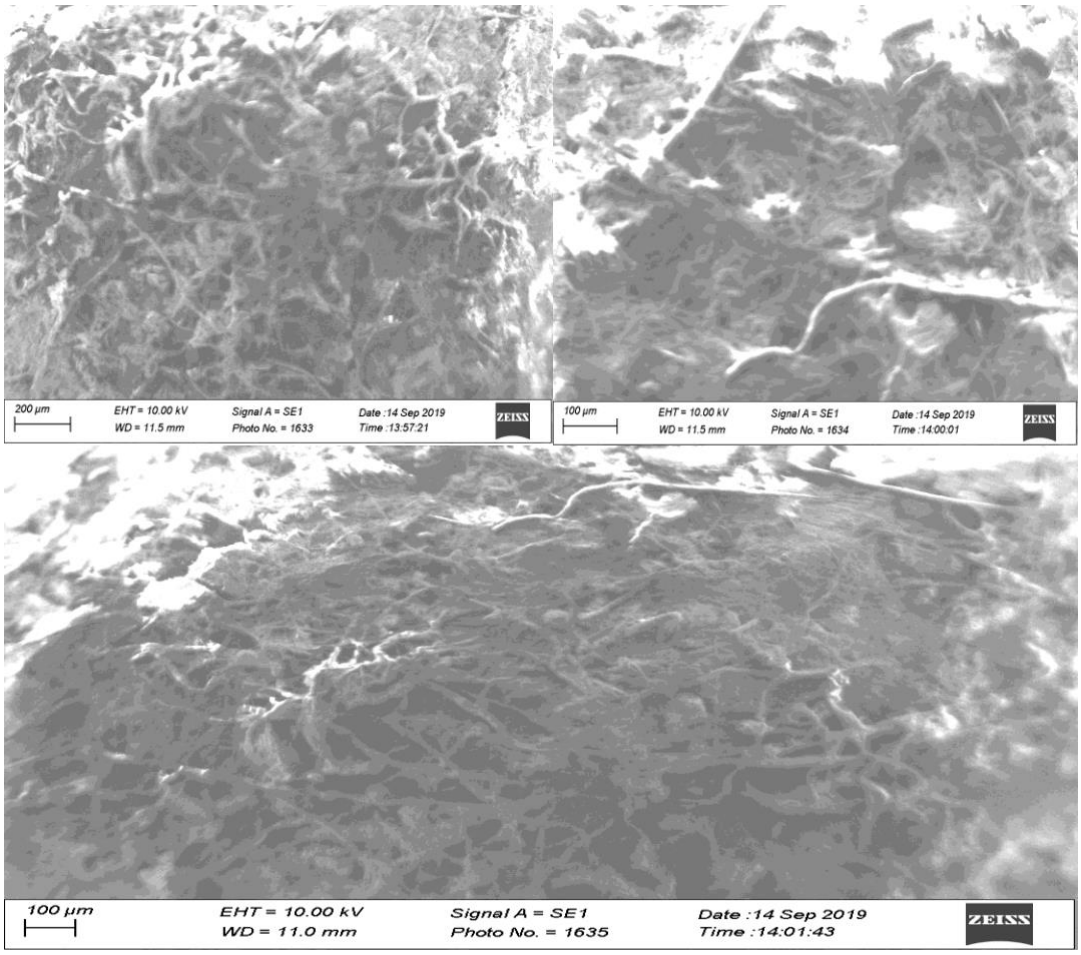

Figure 6.54: SEM Micrograph of maize tassel immobilized in PVA before adsorption

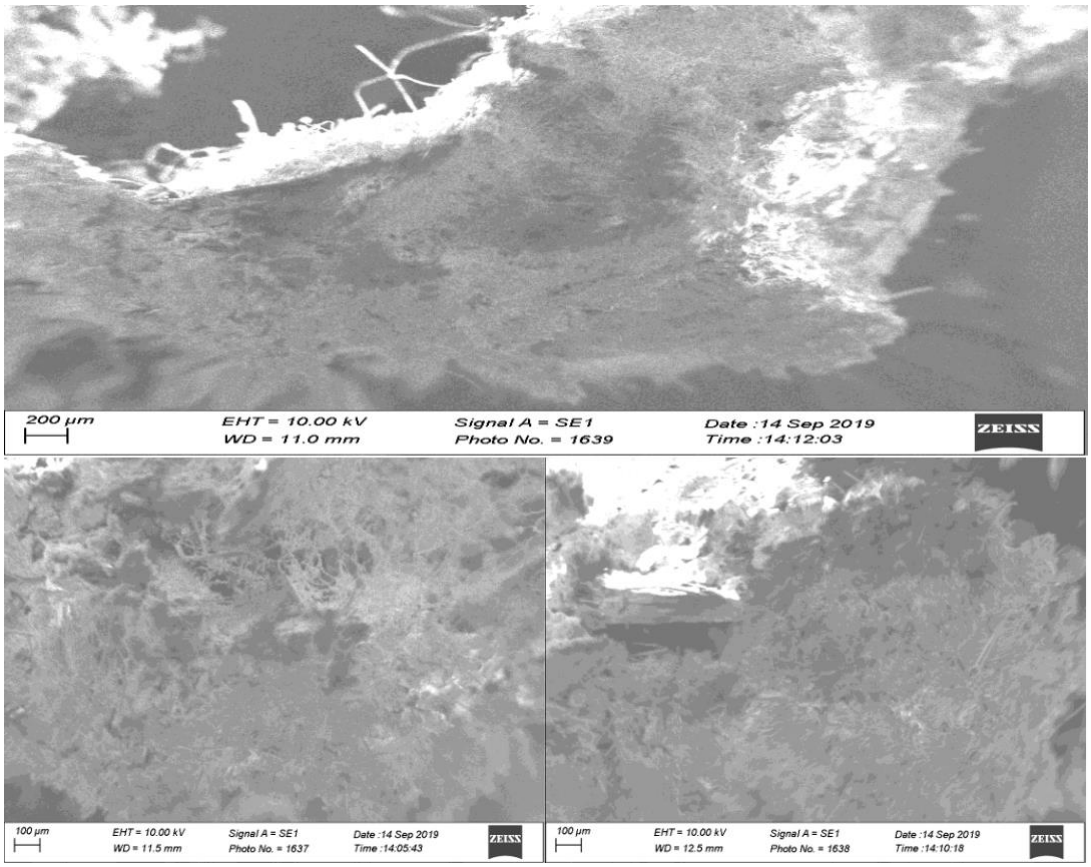

Figure 6.55: SEM Micrograph of maize tassel immobilized in PVA after adsorption